2023-01-25

Development of a Cyanobacterial Biorefinery:Integration of Autofermentation and AnaerobicDigestion for Maximal Value Generation and Reduced Energy Inputs

Demirkaya, Cigdem

UNIVERSITY OF CALGARY

Development of a Cyanobacterial Biorefinery: Integration of Autofermentation and Anaerobic Digestion for Maximal Value Generation and Reduced Energy Inputs

by

Cigdem Demirkaya

A THESIS
SUBMITTED TO THE FACULTY OF GRADUATE STUDIES
IN PARTIAL FULFILMENT OF THE REQUIREMENTS FOR THE
DEGREE OF DOCTOR OF PHILOSOPHY

GRADUATE PROGRAM IN CHEMICAL AND PETROLEUM ENGINEERING

CALGARY, ALBERTA

JANUARY, 2023

ABSTRACT

Cyanobacteria are ideal bio-factories for diverse biotechnological applications owing to their capacity to use solar energy and fix carbon dioxide into valuable bioactive compounds such as proteins and pigments. However, the economic viability of large-scale cyanobacteria cultivation is hindered by low volumetric productivity due to the slow mass transfer rate of CO_2 into the culture media and significant CO_2 losses. High pH (>10) and high alkalinity (>>10000 μEq L^{-1}) can be used to improve CO_2 delivery efficiency, as alkalinity enhances buffering capacity and improves CO_2 mass transfer rates. Another important factor is the high cost associated with harvesting and energy intensive downstream processing methods. Thus, there is a need to develop integrated biorefinery strategies to maximize product recovery and value creation. To develop an economically viable cyanobacterial biorefinery, an alkaline cyanobacterial biomass production system was integrated with an autofermentation step, and a low temperature anaerobic digestion. Integration of these processes increase biomass productivity, trigger the release of valuable products, and enable multiple product recovery, nutrient recycling, and maximum energy production.

Autofermentation was investigated as an energy-efficient and low-cost method to reduce pH to an optimal level (6.8–7.2) for the successful conversion of biomass to biogas and enable the production of hydrogen and organic acids simultaneously. High value-added products, hydrogen, and phycocyanin were also recovered from the process. Maximum total organic acid yield (60 % C mol/ C mol biomass) and hydrogen yield (326.1 μmol/g AFDM) were obtained at the lowest biomass concentration after natural settling with no additional energy requirement.

Three different inocula including digested manure, digested sewage sludge, and soda lake sediment were evaluated for energy efficient anaerobic digestion of cyanobacterial biomass at a

low temperature (21 °C). Low temperature semi-continuous anaerobic digestion of fermented cyanobacterial biomass was carried successfully over 800 days with an average methane yield of 476 ml/ g VS by using soda lake sediment in duplicate 2 L digesters operating at 21 °C. Techno-economic assessment of the integrated process showed that phycocyanin is an important parameter for the economic value of this proposed alkaline cyanobacterial based biorefinery.

Preface

This dissertation is an original work by Cigdem Demirkaya.

Chapter 2 of this thesis has been submitted for publication as Demirkaya C., De la Hoz Siegler, H. Dark fermentation of microalgae and cyanobacteria for hydrogen production. Biotechnological Processes for Green Energy, and High Value Bioproducts by Microalgae, and Cyanobacteria Cultures, 2021.

Chapter 4 of this thesis has been submitted for publication as **Demirkaya C.**, Vadlamani A, Tervahauta T, Strous M, De la Hoz Siegler H. Autofermentation of alkaline cyanobacterial biomass to enable biorefinery approach. Biotechnology for Biofuels and Bioproducts Journal.

Chapter 6 of this thesis has been prepared for submission as **Demirkaya C.**, Strous M, De la Hoz Siegler H, Tervahauta T. Energy Positive Methane Production from Fermented Cyanobacteria in Bioresource Technology Journal.

Acknowledgements

I am thankful to so many special people who supported and guided me along the way to finish my Ph.D. Firstly, I would like to express my sincere gratitude to my supervisor Prof. Hector De la Hoz Siegler, for his patience, the motivation, knowledge, and continuous support that he provided. Dr. De la Hoz Siegler was great advisor and mentor not only for my Ph.D. studies but also for planning my next carrier steps. I sincerely thank Dr. Taina Tervahauta for her supervision and her countless help for planning and design batch and semi continuous anaerobic digestion experiments. Furthermore, Dr. Tervahauta was a great support not only for research but also in my personal life. I would like to thank all the past and present members of the laboratory. Specially, I want to thank to Safina Ujan and Camila Cáceres for their great friendship and their endless support both academically and personally. They were closed to me like my sisters and that was great feeling when I was away from my parents and my sisters. I would like to thank to Md. Mohosin Rana, Alex Paquette, Mohammad Alikarami, and Dr. Jesus Fabricio Sosa for all the help and support. I would like to thank to my summer student Luke Miller for his great support to complete batch anaerobic test and driving to British Columbia to collect soda lake sediments in summer of 2019.

My deepest gratitude goes to my wonderful parents, my sisters and of course loving husband, who have always encouraged me to follow my ambitions and goals. I would like to thank especially my husband Isik Bora Keklik who followed me to everywhere to let me achieve my goals. Without his endless love and support, I would not have been able to complete my Ph.D.

Lastly, I am very grateful for the financial support of the Canada First Research Excellence Fund (CFREF) and the Schulich School of Engineering at the University of Calgary.

Dedicated to my best friend,

My greatest support,

My strongest motivation,

My lovely husband, Isik Bora Keklik.

Contents

List of Figures

List of Tables

List of Abbreviations

acetyl-CoA	Acetyl coenzyme A
AD	Anaerobic digestion
ADP	Adenosine diphosphate
AFDM	Ash free dry mass
ATP	Adenosine triphosphate
BCC	Bacterial community composition
BMP	Biochemical methane potential
CCM	Carbon concentrating mechanism
CEPCI	Chemical Engineering Plant Cost Index
Chl a^{-1}	Chlorophyll a
CHN	Carbon, Hydrogen, Nitrogen
CO_2	Carbon dioxide
COD	Chemical oxygen demand
CWEEDS	Canadian Weather Energy and Engineering Datasets
DAC	Direct air capture
DM	Dry mass
Fd	Ferredoxin
Fe	Iron
FeFe	Iron-iron complex
FID	Flame ionization detector
GC	Gas chromatography
GPP	Gross primary production

H^+	Hydrogen ion
H_2	Hydrogen
H_2O	Water
Ha	Hectare
HCO_3^-	Bicarbonate
HHV	Higher heating value
HPLC	High performance liquid chromatography
HRT	Hydraulic retention time
MgATP	Magnesium adenosine triphosphate
MoFe	Molybdenum – iron complex
N_2	Nitrogen
NAD^+	Nicotinamide adenine dinucleotide
NADH	Nicotinamide adenine dinucleotide
NAHPH	Nicotinamide adenine dinucleotide phosphate
NH_4^+	Ammonium
NiFe	Nickel – iron complex
O_2	Oxygen
OD	Outer diameter
OLR	Organic loading rates
OPA	o-phthaldiadehyde
OPP	Oxidative pentose phosphate
PBR	Photobioreactor
PPM	Parts per million

PSI	Photosystem I
PSII	Photosystem II
PTFE	Polytetrafluoroethylene
SRT	Solid retention time
STR	Stirred tank reactors
TAP	Tris-acetate-phosphate
TCD	Thermal conductivity detector
TS	Total solid
VFA	Volatile fatty acid
VS	Volatile solid

List of Symbols

A	Heat transfer area (m^2)
C	Specific heat capacity (J/g K)
$C_{c,i}$	Carbon content of component i
C_d	Total solid concentration in the digester
C_f	Coefficient of friction
C_{out}	Total solid concentration in effluent
d	Impeller diameter (m)
D	Diameter (m)
dT	Temperature difference across the isolation material (°C)
dx	Thickness of the isolation material (m)
$E_{heating}$	Energy used for heating (MJ)
$E_{methane}$	Energy produced from methane (MJ)
E_{mixing}	Energy used for mixing (MJ)
$E_{pumping}$	Energy used for pumping (MJ)
E_{total}	Total energy (MJ)
F_{feed}	Flow rate of feed (m^3/d)
F_{out}	Flow rate of effluent (m^3/d)
g	Acceleration of gravity (m/s^2)
L	Length (m)
m	Mass of liquid (kg)
m	Number of measured carbon-containing compounds
N	Impeller rotational speed (m/s)

n	Scale-up factor
N_{air}	Air flow rate (m^3/min)
N_p	Power number
P	Power input for mixing (W)
p_0	Atmospheric pressure (kPa)
$P_{air\ friction}$	Power loss due to air friction (W)
$p_{ambient}$	Ambient pressure (kPa)
$P_{electrical}$	Electrical power loss (W)
$P_{electrical,idle}$	Electrical power required while in idle mode (W)
$p_{filtration}$	Pressure in filtration chamber (kPa)
P_{flow}	Power loss due to flow (W)
P_{idle}	Power required while in idle mode (W)
$P_{mechanical}$	Mechanical power loss (W)
P_{total}	Total power (W)
$p_{vacuum\ receiver}$	Pressure of vacuum (kPa)
Q	Flow (m^3/d)
R	Carbon recovery (%)
R	Outer radius of the bowl of the centrifuge (m)
r_c	Minimum radius of the water layer ion the centripetal pump chamber (m)
t	Time
V	Sample volume (m^3)
V_d	Working volume of the digester (L)
$V_{methane}$	Methane volume (L)

V_{PBR}	Volume of PBR (m^3)
$W_{rotation}$	Energy required for rotation of drum (kWh)
W_{total}	Total energy (kWh)
W_{vacuum}	Energy required for vacuum pump (kWh)
$W_{water\ pump}$	Energy required for water pump (kWh)
X_M	Total monosaccharides concentration in the biomass (g/g biomass)
Y_{HB}	Maximum theoretical hydrogen yield (mL H_2/g biomass)
Y_{HM}	Stoichiometric hydrogen yield of monosaccharides (mL H_2/g)
γ	Ratio of the radius of the drum filter to that of the feed tank
Δh	Pump head (m)
Δp	Pressure loss from pump head (kPa)
$\Delta p_{resistance}$	Pressure change due to resistance (kPa)
$\Delta G°$	Gibbs free energy (kj/mol)
ΔQ	Amount of heat transferred to the system (MJ)
ΔT	Temperature difference (°C)
$\eta_{electrical}$	Electrical efficiency (%)
$\eta_{electrical,idle}$	Electrical efficiency in idle mode (%)
$\eta_{electrical,total}$	Total electrical efficiency (%)
η_{motor}	Motor efficiency (%)
λ	Thermal conductivity of the isolation material (W/mK)
ρ	Fluid density (kg/m^3)
ρ_{air}	Density of air (kg/m^3)
Φ	Heat transfer rate (joules/s)

Ω	Operating speed (rpm)

CHAPTER 1

Introduction

The aim of this PhD thesis is to enable the design of a downstream process to produce economically feasible and carbon-neutral biofuels from microalgal biomass. The following sections provide the necessary background to understand the context within which this thesis was conducted. In this chapter, a concise review of literature relevant to the problem, problem statement, and scope of this project together with goals and hypothesized benefits are discussed to provide a clear context for this research.

1.1 Problem statement

Cyanobacteria are microscopic biofactories that produce large varieties of products, which have applications in different industries such as food, pharmaceuticals, and bioenergy (Noreña-Caro & Benton, 2018; Singh et al., 2022). Despite the recent progress that has been done in improving the economic viability of cyanobacterial based products and bioenergy processes, current strategies fail to meet the efficient valorization of biomass as most of them focus on a single product (Gifuni et al., 2019). On the other hand, another bottleneck of the cyanobacterial biorefinery process is downstream strategies, which are difficult to manage economically (Gifuni et al., 2019; Sivaramakrishnan et al., 2022). Thus, there is a need to design newly integrated processes that require less energy, low in cost, and produce minimal waste for an economically viable biorefinery approach.

The anaerobic digestion of cyanobacterial biomass is considered one of the most environmentally feasible options for creating a renewable source to produce multiple bioproducts and bioenergy (Driver et al., 2014). Despite the identified benefits both the sustainability and economic viability of cyanobacterial biorefinery and energy production processes have been under scrutiny, particularly regarding the high costs associated with cultivation, CO_2 supply, and harvesting (Sills et al., 2013; Da Silva et al., 2014; Alam et al., 2017;). A first strategy to address these high costs is to use an alkaline and high pH growth medium that is effective at improving the transfer rate of CO_2 from the atmosphere, and its solubility in the cultivation medium (Vadlamani et al., 2017). The use of a mixed microbial culture dominated by cyanobacteria, which has been obtained from soda lakes having high pH and alkaline conditions, is the second strategy. The use of extremophiles increases culture productivity and prevents the occurrence of culture crashes caused by microbial contamination (Qin et al., 2019). Even though these two strategies improve biomass production,

they introduce additional complexities with respect to the anaerobic digestion of this biomass. High pH and alkalinity, high salinity, and rapid ammonium increase due to low carbon to nitrogen ratio and increased inhibitory effect of ammonium at high pH are the main problems that need to be addressed (Rajagopal et al., 2013; Anwar et al., 2016; Solé-Bundó et al., 2019). Methanogenic bacteria are especially sensitive to this increased ammonia concentration, which causes a rapid inhibition of bacteria and methane production at high pH (Jiang et al., 2019). Correspondingly, inhibition of methane production decreases the efficiency and economic viability of the anaerobic digestion process. A pretreatment step is needed to reduce the pH of alkaline biomass to optimal levels of anaerobic digestion.

Integration of low-cost downstream processes with cyanobacterial biomass cultivation system at high alkalinity and high pH can increase the economic feasibility to a certain extent by allowing simultaneous CO_2 capture and conversion of biomass into valuable products and bioenergy.

1.2 Hypotheses

The underlying hypothesis of this proposal is that the integration of anaerobic digestion with a pre-treatment step such as autofermentation can enhance the bioconversion process of alkaline cyanobacterial biomass, improve anaerobic digestion performance, increase methane production, and reduce the risk of ammonia inhibition by decreasing pH of the highly alkaline algal biomass. In addition, the economic viability of the process can be improved by recovering the high-value products generated by cyanobacterial biomass in the autofermentation step.

1.3 Specific objectives

The proposed research aims to design an economically and ecologically feasible process to convert CO_2 into biogas and high-value products.

Four specific objectives were identified for this goal:

1. Determine if autofermentation is a successful pretreatment step to enable anaerobic digestion of alkaline biomass.
2. Determine the effect of process parameters (temperature, pH, biomass concentration) on autofermentation and anaerobic digestion.
3. Increase biogas productivity and decrease the hydraulic retention time of anaerobic conversion by semi-continuous, integrated autofermentation, and anaerobic digestion system at low temperatures, and
4. Determine the economic viability of integrated biorefinery process at low temperatures by mass and energy balance analysis.

1.4 Thesis overview

In this thesis, an integrated process for the successful conversion of alkaline cyanobacterial biomass into carbon neutral biofuel and bioproducts was developed. The pathway followed for the development of the aforementioned process is summarized in Fig. 1.1.

Chapter 2 provides detailed background information for this thesis. First, CO_2 bio-capture by microalgae utilizing microalgae and cyanobacteria directly from the atmosphere or stationary point sources are discussed. Second, a process overview on integration of CO_2 bio-capture and hydrogen formation in dark anaerobic conditions via indirect biophotolysis, and the factors affecting hydrogen formation rate are provided. Recent developments in dark fermentation hydrogen production from microalgae and cyanobacteria and different strategies to improve hydrogen production efficiency are also presented.

Description of the experimental apparatuses, microalgal cultures, standard analytical method used in this research are presented in **Chapter 3**.

In **Chapter 4**, autofermentation capability of alkaline cyanobacterial biomass was evaluated as a pretreatment step to reduce the pH of alkaline biomass. Autofermentation is a metabolic process in which some microalgae and cyanobacterial strain can convert their own carbon storages (carbohydrate, protein, and lipids) into a wide range of valuable products such as organic acids and hydrogen. The effect of different process parameters such as temperature, oxygen presence, and biomass concentration on the performance of autofermentation was evaluated to find optimum conditions for maximum organic acid and phycocyanin production.

Anaerobic digestion of cyanobacterial biomass fits well with the biorefinery concept because it does not only generate bioenergy in the form of biogas and bio-based products, such as organic acids and biopolymers but also simultaneously remediates the CO_2 emissions and reduces the environmental footprint of the bioenergy production process. **In Chapter 5**, different inoculum sources, digested manure, digested sewage sludge, and soda lake sediment, were chosen to evaluate the anaerobic digestion of autofermented and fresh biomass at different temperatures to determine the suitable inoculum for AD at low temperatures. Reduction in chemical oxygen demand (COD), changes in pH, ammonium accumulation, methane, and CO_2 production were observed to determine process success and optimal conditions for maximum methane production. **In Chapter 6**, a semi-continuous integrated autofermentation and AD process operated at a low temperature (21°C) were successfully carried over 800 days with an average methane yield of 476 ml/ g VS by using soda lake sediment in duplicate 2 L digesters. Initially, a low biomass loading rate was chosen to prevent rapid ammonium accumulation and inhibition of methanogenesis. Recycling of solid digestate was done to prevent digester content and decrease in methane production. Operation at low temperature allowed to obtain an energetically positive energy production from autofermented biomass.

In Chapter 7, a general process evaluation with mass and energy balances was done to determine the economic viability of the integrated biorefinery concept with autofermentation and anaerobic digestion of alkaline cyanobacterial biomass.

Finally, conclusive remarks from the four major objectives were given and future research prospects were discussed in **Chapter 8**.

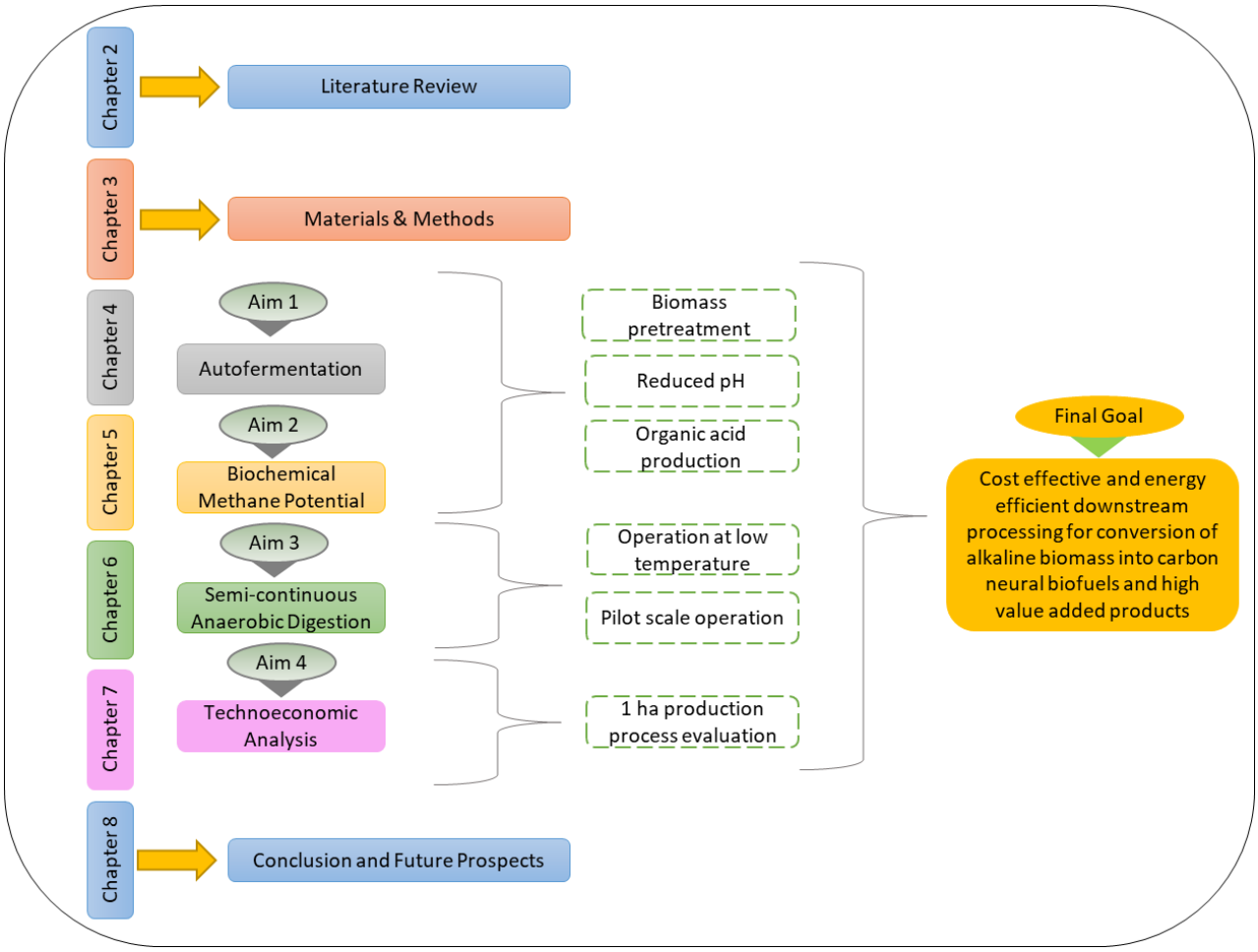

Figure 1.1. Schematic outline of the thesis.

1.5 References

Alam, MA, Wang Z, Yuan, Z. Triphani BN, Kumar D (eds) (2017). In Prospects and Challenges in Algal Biotechnology. Springer Singapore. 89 pp.

Anwar N, Wang W, Zhang J, Li Y, Chen C, Liu G, Zhang R. (2016). Effect of sodium salt on anaerobic digestion of kitchen waste. Water Sci. Technol., 73(8): 1865–1871.

Da Silva TL, Gouveia L, Reis A (2014). Integrated microbial processes for biofuels and high value-added products: The way to improve the cost effectiveness of biofuel production. In Applied Microbiology and Biotechnology. 98 (3): 1043–1053.

Driver T, Bajhaiya A, Pittman JK. (2014). Potential of bioenergy production from microalgae. Curr. Sustain. Energy Reports, 1(3): 94–103.

Gifuni I, Pollio A, Safi C, Marzocchella A, Olivieri G (2019). Current Bottlenecks and Challenges of the Microalgal Biorefinery. Trends Biotechnol. 37(3): 242–252.

Jiang Y, McAdam E, Zhang Y, Heaven S, Banks C, Longhurst P (2019). Ammonia inhibition and toxicity in anaerobic digestion: A critical review. J. Water Process Eng. 32: 100899.

Noreña-Caro D, Benton MG (2018). Cyanobacteria as photoautotrophic biofactories of high-value chemicals. J. CO_2 Util.. 28: 335–366.

Qin L, Wei D, Wang Z, Alam MA (2019). Advantage assessment of mixed culture *of Chlorella vulgaris* and *Yarrowia lipolytica* for treatment of liquid digestate of yeast industry and cogeneration of biofuel feedstock. Appl. Biochem. Biotechnol. 187(3); 856–869.

Rajagopal R, Massé DI, Singh G (2013). A critical review on inhibition of anaerobic digestion process by excess ammonia. Bioresour. Technol. 143: 632–641.

Sills DL, Paramita V, Franke MJ, Johnson MC, Akabas TM, Greene CH, Tester JW (2013). Quantitative uncertainty analysis of life cycle assessment for algal biofuel production. Environ. Sci. Technol. 47(2): 687–694.

Singh G, Ghosh P, Singh D, Kumar J (2022). Cyanobacteria as natural biofactories. Microb. Prod. 35–56.

Sivaramakrishnan R, Suresh S, Kanwal S, Ramadoss G, Ramprakash B, Incharoensakdi A (2022). Microalgal biorefinery concepts developments for biofuel and bioproducts: current perspective and bottlenecks. Int. J. Mol. 23(5): 2623.

Solé-Bundó M., Passos F, Romero-Güiza MS, Ferrer I, Astals S (2019). Co-digestion strategies to enhance microalgae anaerobic digestion: A review. Renew. Sustain. Energy Rev. 112: 471–482.

Vadlamani A, Viamajala S, Pendyala B, Varanasi S (2017). Cultivation of Microalgae at Extreme Alkaline pH Conditions: A Novel Approach for Biofuel Production. ACS Sustain. Chem. Eng. 5(8): 7284–7294.

CHAPTER 2

Microbial Carbon Capture and Hydrogen Production

This chapter provides an overview of the different strategies for utilizing microalgae and cyanobacteria for CO_2 capture directly from the atmosphere or stationary point sources and the formation of hydrogen in dark anaerobic conditions, and the factors affecting hydrogen formation rate. Recent developments in dark fermentation hydrogen production from microalgae and cyanobacteria and different strategies to improve hydrogen production efficiency are also presented.

2.1 Introduction

Due to the role of carbon dioxide (CO_2) in driving global climate change, there is increasing global pressure for limiting CO_2 emissions, particularly at large-emission source points. In 2015, with the signing of the Paris Agreement, nations committed to reduce global emissions annually by 3 % to avoid a global climate catastrophe. However, this hasn't been achieved and the current path, which includes mainly treatment of point sources, such as flue gas, is not enough to meet the target of limiting global average temperature below a 2 °C increase. Thus, there is a rising urgency for innovative methods to mitigate new emissions and to remove the CO_2 already in the atmosphere.

Photosynthetic microbes, including microalgae, cyanobacteria, and diatoms have a great potential for mitigating and abating CO_2 emissions, while producing valuable products (Moreira and Pires, 2016; Vale et al., 2020) and fostering a more sustainable bio-economy. If part of the CO_2 captured in the biomass is used to make products with relatively long-life (i.e., years), or if they are permanently stored, then the cultivation of microalgae and cyanobacteria can become a key carbon negative technology to address the climate change crisis.

Biological carbon capture is an effective and simple approach with potentially much lower energy needs compared to physical and chemical carbon capture methods. For instance, the current standard technology for carbon capture in post-combustion processes is amine scrubbing, using primary or secondary amines. This technology is the basis of several megaton scale carbon capture projects (Feron et al., 2020). The regeneration of the amine, however, is very energy-intensive, introducing a significant energy penalty and reducing the overall mitigation potential of this method (Alesi and Kitchin, 2012; Stern et al., 2013).

Photosynthesis is nature's carbon capture solution. Photosynthetic organisms utilize the energy from light to drive the reaction of CO_2 and water and form biomolecules. In this way, carbon is

removed from the atmosphere and stored into biomass. Gross primary production (GPP) refers to the amount of CO_2 removed from the atmosphere by photosynthesis. This is known to be one of the main fluxes controlling the carbon balance in the atmosphere and has a significant potential to offset anthropogenic carbon emissions (Beer et al., 2010). Terrestrial GPP is estimated at about 120 Pg of Carbon per year (Beer et al., 2010), while marine phytoplankton are estimated to account for an additional 50 Pg of Carbon per year (Yang et al., 2020). Global anthropogenic energy-related CO_2 emissions in 2020 were estimated at 8.6 Pg of Carbon (IEA, 2021), or roughly 5 % of the carbon naturally fixed by photosynthesis. Thus, it is conceivable that technological solutions based on photosynthesis will be able to offset anthropogenic carbon emissions.

Microalgae and cyanobacteria are rapidly growing microorganisms able to fix CO_2 with an efficiency 10 to 50 times higher than that of terrestrial plants (Cheah et al., 2015; Raheem et al., 2018; S. Zhang and Liu, 2021), high areal productivity, and high lipid and/or carbohydrate content. They are able to grow in non-arable land, with minimal nutrient inputs, and in wastewater, saline, brines, or halo-alkaline waters (Moreira and Pires, 2016). Thanks to their high areal productivity and ability to grow in hostile environments, photosynthetic microbes are more suitable for biological carbon capture technologies than terrestrial plants. The use of dedicated crops for industrial purposes has previously resulting in the diversion of arable lands away from traditional food crops, creating unintended impacts on food cost and supply, resulting in the well-known food versus fuel dilemma (Darnoko and Cheryan, 2000; Issariyakul and Dalai, 2012). This dilemma is avoided when using photosynthetic microbes.

In addition to their role fixing CO_2 emissions, microalgae and cyanobacteria can be used to remove nitrogen and phosphorous from agricultural and industrial effluents, reducing eutrophication of receiving water bodies (Fal et al., 2021; Guo et al., 2018; W. Zhang et al., 2020). The microbial

biomass produced can be used for several applications including the production of biofuels, bioplastics, food supplements, animal feed, cosmetic additives, pharmaceuticals products, and building materials (Daneshvar et al., 2022; J. Singh and Dhar, 2019; Venkata Mohan et al., 2016). Thus, biological carbon capture with microalgae and cyanobacteria offers a wide range of opportunities for building sustainable integrated processes to support a bioresource-based circular economy (Hemalatha et al., 2019; Vale et al., 2020; Venkata Mohan et al., 2016).

Microalgae and cyanobacteria are attractive also for their potential to produce biohydrogen (Jiménez-Llanos et al., 2020; Kumari et al., 2017; Nagarajan et al., 2017a) as the higher heating value of hydrogen (HHV) 141.65 MJ kg–1 (All and Basit, 1993), and its clean combustion that results only in the formation of water vapor, make it an excellent energy carrier (Dawood et al., 2020; Goria et al., 2022). Thus, hydrogen has long been identified as a game changing approach for abating carbon dioxide (CO_2) emissions and tackling climate change, as it can replace fossil fuels in different hard to decarbonize areas, including transportation, heating, and metallurgical processes.

This chapter presents an overview of (i) the different strategies for utilizing microalgae and cyanobacteria for CO_2 capture directly from the atmosphere or stationary point sources with minimal environmental impacts; (ii) the metabolic processes that lead to the formation of hydrogen under dark anaerobic conditions, and (iii) the factors affecting hydrogen formation rate. Recent developments in dark fermentation for hydrogen production using cyanobacteria and microalgae, as well as strategies to improve production efficiency, are also presented.

2.2 CO_2 Bio-capture from Different Sources

Microalgae and cyanobacteria can capture CO_2 from stationary point emission sources, such as power plants or other carbon-intensive industrial processes, or directly from the atmosphere. The

CO_2 concentration in the atmosphere is 0.03–0.06 % (v/v), while for stationary point sources the CO_2 concentration can vary between 6–15 % (v/v) (Rahaman et al., 2011). The cost and energy needed for capturing CO_2 is inversely proportional to concentration, the lower the concentration of CO_2 in a given source, the more expensive the capture process is. Thus, capture from large point sources is one of the best and more efficient options to abate CO_2 emissions, as the effluent streams from combustion and industrial processes have higher CO_2 concentrations.

Figure 2-1 shows how different CO_2 sources can be integrated with microalgae and cyanobacteria biomass cultivation for CO_2 bio-capture. In the following sections, we present an overview of technologies for CO_2 bio-capture and a discussion of the efficiency of these bio-capture methods.

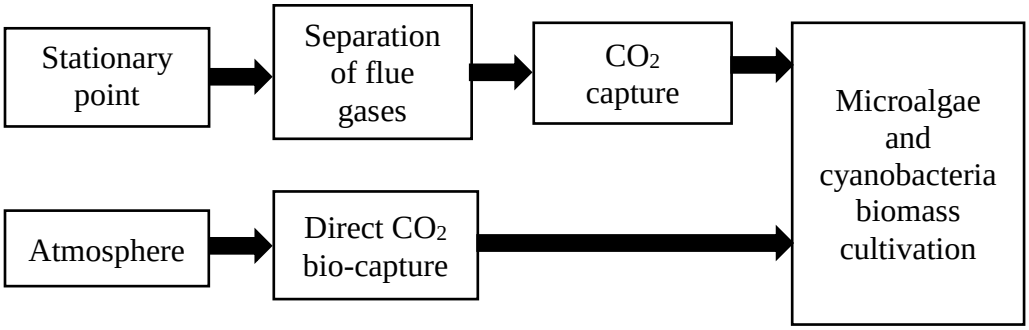

Figure 2.1. CO_2 bio-capture from different sources and utilization into biomass.

2.2.1 Bio-capture of CO_2 from stationary point sources

Flue or stack gases released by various stationary point sources, such as industrial complexes and power plants, have relatively high CO_2 concentrations ranging from 6 to 15 % (v/v) (Thomas et al., 2016). These flue gases can be used to boost the productivity of microalgal and cyanobacteria cultures. The high concentration of CO_2 in the flue gas allows for a faster mass transfer rate, higher photosynthetic efficiency, and support a higher final cell density in the cultures.

Because of the low CO_2 solubility, the flue gas needs to be injected or bubbled directly into the cultivation medium, adding to electricity demands. The energy spent in bubbling and mixing the CO_2 in the media represents up to 27 % of the overall production cost; at the same time, typically between 55 and 90 % of the CO_2 injected in the culture is lost to the atmosphere (Caia et al., 2018; Markou et al., 2014).

Microalgae and cyanobacteria strains with high CO_2 uptake rate and high biomass productivity are desirable to ensure an efficiency CO_2 capture process. Sepulveda et al. (2019) assessed the ability of 11 different microalgae and cyanobacteria strains to capture CO_2 and produce high biomass productivity. They reported that *Scenedesmus almeriensis* and *Neochloris oleoabundans* were the most productive strains when used in CO_2 capture processes compared to the cyanobacteria strains. Park et al. (2021) investigated CO_2 fixation at a CO_2 concentration ranging from 5 to 40 % from biogas in five pure microalgal cultures and a mixed microalgal culture, including *Chlorella sp., Anabaena variabilis, Chlamydomonas iyengarii, Chlorella vulgaris, Chlorella sorokiniana*. The highest CO_2 fixation rate was reported for *Chlorella sp.* at 1.785 g $L^{-1}d^{-1}$ at a CO_2 concentration of 15 %. Additional studies on CO_2 capture and uptake by microalgae and cyanobacteria are summarized in Table 2.1.

Table 2-1. Application of microalgae in CO_2 capture from the atmosphere and CO_2 reach sources.

CO_2 source	Microorganism	CO_2 % (v/v)	CO_2 fixation rate g L^{-1} d^{-1}	Culture Conditions	Reference
Atmospheric CO_2	*Chlorella vulgaris* and *Pseudokirchneriella subcapitata*	-	0.305	OECD medium, temperature 22°C, different dark/light cycles with 126 µmol photons m^{-2} s^{-1}	(Pires et al., 2014)
	Dunaliella tertiolecta	0.04	0.07	Artificial sea water, temperature 26°C, continuous illumination with 350 µmol photons m^{-2} s^{-1}	(Hulatt and Thomas, 2011)
	C. vulgaris	0.09	3.45	Artificial sea water, temperature 25°C, continuous illumination with 48.6µmol photons m^{-2} s^{-1}	(Fan et al., 2008)
Enriched CO_2 supply	*Spirulina* sp. DUT001	2	1.0	Zarrouk medium, pH 9-10, 12 h light/dark photoperiod with 188.7 µmol photons m^{-2} s^{-1}	(Zhu et al., 2020)
	Chlorella vulgaris	15	-	BBM medium, temperature 28°C, µmol photons $m^{-2}s^{-1}$	(Senatore et al., 2021)

Chlorella vulgaris, Synechocystis salina, Microcystis aeruginosa,	5	0.101	OECD test medium, room temperature, μmol photons $m^{-2}s^{-1}$	(Gonçalves et al., 2014)
Scenedesmus obligus	20	-	Soil extract medium, temperature 28°C	(Li et al., 2011)
Chlorella vulgaris	5-25	0.27 – 0.47	ESP-31 medium, temperature 28°C, continuous illumination with 50 μmol photons $m^{-2}s^{-1}$	(Chou et al., 2019)
Microalgae consortia	5.5	-	BBM medium, pH 7.5, temperature 30°C, 12 h light/dark photoperiod with 1650.3 μmol photon $m^{-2}s^{-1}$	(Aslam et al., 2018)
Scenedesmus almeriensis, Neochloris oleoabundans	Flue gas	2.8 – 2.64	Natural water from the River Seine and the artificial Seine river water, temperature 20°C, continuous illumination with 200 μmol photons $m^{-2}s^{-1}$	(Sepulveda et al., 2019)
Spirulina sp.	2	0.81	Modified Zarrouk medium, temperature 20°C, pH 9, continuous illumination with 188.7 μmol photons $m^{-2}s^{-1}$	(Zhu et al., 2020)
Chlorella sp	15	1.785	BG-11 , pH 8.2-8.7, temperature 25°C, 12 h light/dark photoperiod with 171.91 μmol photon $m^{-2}s^{-1}$	(Park et al., 2021)

Although the high CO_2 level in flue gas is beneficial for microalgae and cyanobacteria growth, these gases usually contain substances that can be inhibitory (Lam and Lee, 2012; Vale et al., 2020). In particular, unfiltered flue gas from coal combustion can have high concentration of SO_x and NO_x, microparticles, and heavy metals, such as mercury which can present a challenge for biomass growth (Napan et al., 2015; Thomas et al., 2016). As the concentration of SO_x and NO_x n increases, the acidity of the culture medium increases and this lowers the pH (Vale et al., 2020). Low pH values may inhibit microalgal growth or even result in cell death. Duarte et al. (2016) evaluated the tolerance of microalgae and cyanobacteria to the presence of NO_x and SO_x and found that some strains were able to tolerate those gases at concentration of up to 400 ppm. Aslam et al., (2017) demonstrated the adaptation of mixed microalgal communities to growth in unfiltered flue gas from coal combustion. This microalgal community was dominated by *Desmodesmus* spp. which was the most resilient species. Radmann et al. (2011) evaluated the NO_x and SO_x tolerance of *C. vulgaris, Scenedesmus obliquus,* and *Synechococcus nidulans* by using a simulated gas from coal combustion, containing 12 % (v/v) CO_2, 100 ppm NO_x, and 60 ppm SO_x. They reported that the growth of *C. vulgaris* and *S. obliquus* was not inhibited, but this was not the case for *S. nidulans.*

In short, stationary point sources are excellent for supplying the required CO_2 concentration for carbon capture and biomass production in microalgae and cyanobacteria. However, direct use of flue gas is not in general possible without any separation or treatment. Identifying robust microalgae and cyanobacteria strains capable of high CO_2 bio-capture and adapted to the high concentration of other gases present in flue gas should be further explored to maximize the CO_2 bio-capture potential of microalgae and cyanobacteria culture. Furthermore, despite the large energy requirements for supplying CO_2 to the cultivation medium, a significant amount of the CO_2

provided is released into the atmosphere, decreasing net capture, and incurring in inefficient energy use. Thus, additional research efforts must be directed at improving CO_2 diffusion rates and integrating different CO_2 capture techniques with microalgae and cyanobacteria cultures.

2.2.2 Biological Direct Air Capture with Microalgae and Cyanobacteria

Although capture from concentrated large point sources of CO_2 is the most desirable and efficient option, about half of CO_2 emissions are from diffuse sources (Moreira and Pires, 2016). Moreover, the CO_2 already accumulated in the atmosphere will continue to negatively contribute to climate change (Keith, 2009). Thus, capture of atmospheric CO_2 using negative emissions technologies is needed to address emissions from diffuse sources and to restore the carbon balance in the atmosphere. Direct air capture (DAC) refers to technologies that directly removes CO_2 from the atmosphere. These technologies also offer the advantage of deployment in any location, independent of a specific source and without added costs for CO_2 transportation.

In the case of microalgal and cyanobacterial cultures, to capture 1 million ton of CO_2 per year, between 70 and 86 km^2 are needed assuming an average productivity of 20 g $m^{-2}day^{-1}$ of dry weight biomass and considering that between 1.6 to 2 grams of CO_2 are captured for every gram of biomass (Sayre, 2010). Given the large land requirements for cultivation, it is more likely to find suitable land for deployment of large-scale cultures far away from industrial areas or population centers, where land may be scarce or expensive.

The low concentration of CO_2 in the atmosphere, however, is a major drawback as it limits CO_2 solubility and mass transfer rate into the cultivation media (Kumar et al., 2010). Carbon utilization has been shown to be more efficient when the supply rate of CO_2 matches closely with the demand of the growing biomass (Sobczuk et al., 2000; Vale et al., 2020). For direct air capture, active bubbling is not desirable as it requires a high energy input and will increase water evaporation.

For a cost and energy effective carbon capture process, the CO_2 supply to the cultivation needs to be improved by passive means.

To compensate for the low solubility of CO_2 in natural waters, several microalgae and cyanobacteria strains rely on the Carbon Concentrating Mechanism (CCM) to increase the intracellular concentration of bicarbonate ions and use CA to convert the HCO_3^- back to CO_2 to be used in photosynthesis. The ability of some microalgae and cyanobacteria to utilize HCO_3^- have prompted several researchers to explore the use of alkaline culture conditions to enhance CO_2 mass transfer rate and total inorganic carbon concentration in the culture media (Canon-Rubio et al., 2016; Chi et al., 2013). Alkalinity is defined as the sum of the concentration of hydroxyl ions, bicarbonate ions, and carbonates ions, times the corresponding ion charge. As alkalinity increases, so does the concentration of dissolved inorganic carbon. High alkalinity also improves CO_2 mass transfer rate from the gas phase to the cultivation medium, as there is an increased driving force (Vadlamani et al., 2019). In addition, it provides a higher buffering capacity enabling the uncoupling of CO_2 absorption from biomass growth (Chi et al., 2013), as illustrated in Figure 2.2. Because alkalinity can inhibit cell grow, it is necessary to operate at relatively low alkalinity or use alkali-tolerant or alkaliphilic microalgae or cyanobacteria strains. Extreme alkaline conditions together with alkaliphilic microalgae and cyanobacteria have been suggested for large-scale cultivation (Piiparinen et al., 2018; Song et al., 2019; Zhu et al., 2020). In soda lakes, at pH > 10, high concentrations of bicarbonate are present supporting a high growth rate of CO_2 fixation by photosynthetic microbes, while the consumed CO_2 is spontaneously replenished by passive diffusion from the air above the lakes (Sharp et al., 2017).

Vadlamani et al., (2017) demonstrated high biomass productivity by cultivating *C. sorokiniana* (>16 g $m^{-2} \cdot d^{-1}$) in a 4.2 m^2 raceway pond using an alkaline cultivation medium and atmospheric

CO_2 alone. In another study, Zhu et al., (2020) used extreme alkaline conditions with pH ranging between 10.0 and 12.5 for direct air capture using *Spirulina* sp. DUT001. Effective CO_2 bio-capture was reported with maximum biomass productivity about 1.00 g $L^{-1}d^{-1}$ and carbon-capture rate of 0.81 g L^{-1} d^{-1}.

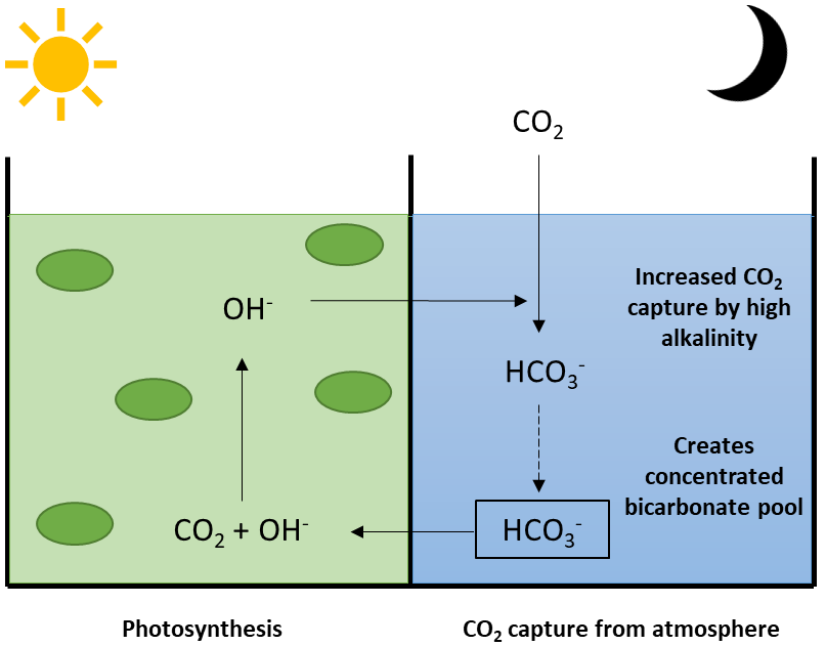

Figure 2.2. Mechanism of the bicarbonate pool's role in the efficient capture of CO_2 from the air and rapid carbon supply for photosynthesis (adapted from Zhu et al., 2020).

2.3 Integration of CO_2 bio-capture and dark fermentation for hydrogen production

To foster the development of an integrated, sustainable, and robust biological CO_2 capture process, circular economy principles must be applied to ensure the efficient processing and conversion of the generated biomass, while designing out or minimizing waste, maximizing the reutilization of resources, and regenerating natural systems. The production of hydrogen from microalgae and

cyanobacterial biomass has gained attention due to its sustainable and renewable nature, low energy requirement, high efficiency, and lack of competition with food or crops (Buitrón et al., 2017). Therefore, coupling microalgae and cyanobacterial culture growth with hydrogen production can be a promising way to enable efficient CO_2 capture and conversion into a carbon neutral energy product.

Microalgae and cyanobacteria can produce hydrogen through four different mechanisms: direct biophotolyis, indirect biophotolysis, photofermentation, and dark fermentation, as well as combinations of these processes (Show et al., 2019). Biophotolysis is the process of splitting water into hydrogen and oxygen by the action of a living organism using light as the energy source (Acar and Dincer, 2018). Water splitting is a two-step process: water oxidation, and hydrogen reduction. In direct biophotolysis these two steps occur simultaneously, driven by the energy of the absorbed photons. Although, direct biophotolysis offers the highest theoretical efficiency, the hydrogen reducing enzymes (i.e., hydrogenases) are quickly inhibited by oxygen. Therefore, there is a need to consume or remove the oxygen as soon as it is produced. Alternatively, the enzymes could be engineered to reduce or eliminate oxygen sensitivity.

Indirect biophotolysis involves the spatial and/or temporal decoupling of the two water splitting reactions. In this case, H_2 does not directly evolve from water but from the autofermentation of endogenously stored carbohydrates (Buitrón et al., 2017; Hallenbeck and Benemann, 2002; Sivaramakrishnan et al., 2021). This process normally occurs in nitrogen-fixing cyanobacteria, where H_2 is a byproduct of nitrogen fixation. In the absence of nitrogen, H_2 is the only reaction product.

Anaerobic fermentation can result in the formation of hydrogen gas. Purple bacteria use light to drive the conversion of organic carbon (usually low-energy organic acids) into biomass with CO_2

and hydrogen as by-products. The process of photofermentation requires the availability of an organic carbon source, but it can be used as a method of carbon recycling as it can start with low-value (in terms of free-energy content) molecules, such as acetate, butyrate, and lactate (N. Singh and Sarma, 2022).

Dark fermentation takes place in the absence of light and results in the production of CO_2. In dark fermentation, the substrate is typically a carbohydrate that is degraded to produce hydrogen and other metabolites (Kamran, 2021). It could potentially be used to convert high-energy organic carbon (e.g., cellulose and lignocellulose) into bioproducts and H_2, offering higher conversion efficiency than other fermentation technologies, such as ethanolic or lactic acid fermentation.

In Table 2.2, a summary of the four biological processes for hydrogen production and the key reactions involved is presented.

2.4. Indirect Biophotolysis – A Process Overview

Indirect biophotolysis can be understood as the combination of photosynthesis and fermentation to produce H_2 (see Figure 2.3). During photosynthesis, cells capture energetic photons with different chromophores, mainly chlorophyll, and use the light energy to drive the reduction of CO_2 into carbohydrates and ultimately to produce biomass. Water is consumed by the photosynthesis reaction, as shown in Table 1. In a second stage, during dark conditions, reserve energy storage polymers like carbohydrates are consumed to fuel the cells' metabolism. Any oxygen present at

Table 2-2. Biological processes for hydrogen production. Adapted from Brentner et al., (2010).

Mechanism	**Reactions**	**Advantages**	**Disadvantages**
Direct biophotolysis	$2H_2O \rightarrow O_2 + 4H^+ + 4e^-$ $4H^+ + 4e^- \rightarrow H_2$ $2H_2O \rightarrow O_2 + 2H_2$	High energy conversion efficiency	O_2 sensitivity; translucent H_2 impermeable material required
Indirect biophotolysis	$H_2O + 6CO_2 \rightarrow C_6H_{12}O_6 + 6O_2$ $C_6H_{12}O_6 + 6H_2O \rightarrow 12H_2 + 6CO_2$ $12H_2O \rightarrow 6O_2 + 12H_2$ $N_2 + 8H^+ + 8e^- + 16\ ATP \rightarrow$ $2NH_3 + H_2 + 16\ ADP + 16Pi$	Separation of H_2 production from O_2 evolution	Translucent H_2 impermeable material may be required
Photofermentation	$C_xH_yO_z + (2x-z)\ H_2O \rightarrow$ $(y/2+2x-2)\ H_2 + xCO_2$ $N_2 + 8H^+ + 8e^- + 16\ ATP \rightarrow$ $2NH_3 + H_2 + 16\ ADP + 16Pi$	No organic byproducts	Translucent H_2 impermeable material required; Organic acids or waste organic material needed as substrate; produces CO_2
Dark fermentation	$C_6H_{12}O_6 + 2H_2O \rightarrow$ $2CH_3COOH + 4H_2 + 2CO_2$	High H_2 production rates	Organic carbon substrate required; many by-products; low H_2 yield; produces CO_2

the start of the dark phase is quickly consumed and if no additional oxygen is provided then an anoxic environment is formed. In the absence of oxygen, excess NADH and NADPH are created using fermentative pathways. The excess NAD(P)H is used to convert H^+ to H_2, thus restoring the redox balance in the cells.

The uncoupling between photosynthesis and fermentation can be achieved temporally by alternating periods of light and darkness in the same culture vessel, or spatially by transferring the biomass produced in the first stage from a photobioreactor or open pond system into an enclosed dark fermenter. Indirect biophotolysis can be realized with microorganisms that are naturally capable of performing both photosynthesis and dark fermentation, or by engineering these metabolic capabilities either by genetic manipulation or by building a consortium of phototrophs and fermentative heterotrophs.

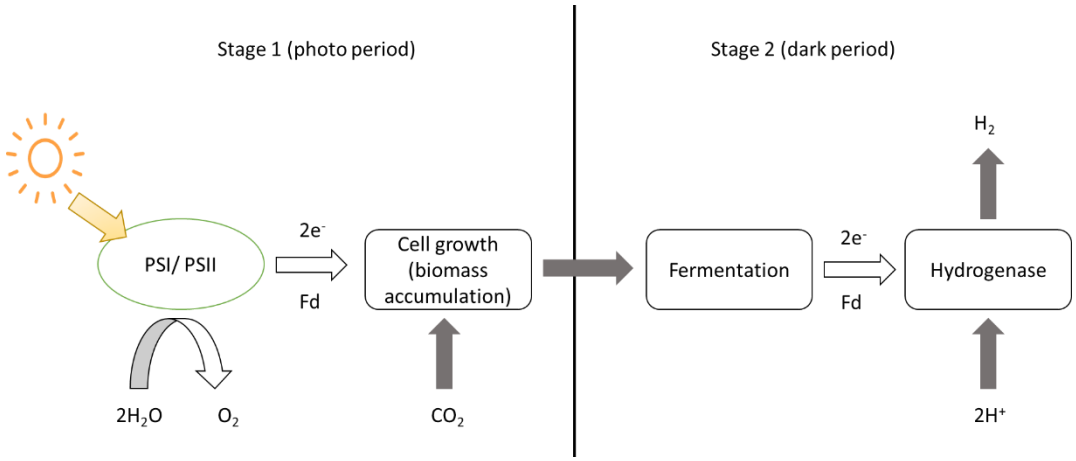

Figure 2.3. Indirect biophotolysis processes of microalgae and cyanobacteria (adapted from Hallenbeck and Benemann, 2002).

H_2 production via indirect biophotolysis is affected by the culture conditions and the type of bioreactor used in each stage (Akhlaghi and Najafpour-Darzi, 2020). In the photosynthetic stage,

light intensity and photoperiod, temperature, pH, nutrient supply, and carbon source type and concentration are known to affect biomass productivity and composition (Gatamaneni et al., 2018). As hydrogen production in the second stage mostly relies on carbohydrate content, culture conditions in the photosynthetic stage need to be optimized to maximize carbohydrate content (Aikawa et al., 2012). Similarly, in the dark fermentation stage, culture conditions play a critical role activating, promoting, or suppressing different metabolic pathways, and ultimately controlling net hydrogen production rate and yield (Chandrasekhar et al., 2015). As the carbohydrate storages are consumed by the different cell metabolic processes, the activation of pathways that do not result in hydrogen formation reduces the yield of hydrogen (Razu et al., 2019).

Hydrogen production by fermentation have been shown to be a process operating close to thermodynamic equilibrium under biologically relevant conditions (Ananyev et al., 2012). Thus, operating conditions or setups that promote a quick removal of evolved hydrogen will result in a higher production rate and yield. Hydraulic retention time is of particular importance in the dark fermentation stage, as a prolonged fermentation time may trigger a shift to unfavourable metabolic pathways (Chandrasekhar et al., 2015). In mixed cultures, a longer fermentation time might favour the activity of methanogenic organisms over that of acidogenic, hydrogen producing ones.

2.5 Key enzymes in hydrogen production

The biological production of hydrogen is dependent upon the presence of a hydrogen-producing enzyme. The enzymes known to catalyze hydrogen evolution are all metalloenzymes, containing a transition metal at the catalytic active site (Hallenbeck and Benemann, 2002). In microalgae and cyanobacteria, there are two major family of enzymes able to drive the production of hydrogen: nitrogenases and reversible or classical hydrogenases. A third family of enzymes, membrane-

bound hydrogenases have not been found to produce any significant or measurable hydrogen (Das and Veziroğlu, 2001a).

2.5.1 Nitrogenases

Many cyanobacteria, both filamentous and unicellular, can convert atmospheric nitrogen into ammonia by the action of nitrogenase, providing these cyanobacteria access to the largest nitrogen pool available on earth (Compaoré and Stal, 2010). Nitrogenases are two-component protein complexes with a dinitrogenase (MoFe) protein and a dinitrogenase reductase (Fe) protein (Anwar et al., 2019). They use magnesium adenosine triphosphate (MgATP) and low-potential electrons to reduce a variety of substrates, including protons into H_2 (Hallenbeck and Benemann, 2002). The expression of nitrogenase is regulated by nitrogen deficiency and oxygen presence, as the assembly and operation of nitrogenase is costly to the cells, and nitrogenases are highly sensitive to the presence of oxygen (Pratte and Thiel, 2014). To protect these oxygen sensitive enzymes, nitrogenase activity is either only present inside the heterocysts, which are specialized cells in filamentous cyanobacteria that lack a functional photosystem, or are only activated in the dark, when no photosynthesis takes place and the intracellular environment becomes micro-aerobic (Compaoré and Stal, 2010).

In N_2 fixation by nitrogenase, 8 mol of ferredoxin are oxidized consuming 16 mol of ATP and producing 2 mol of ammonia and 1 mol of hydrogen. If N_2 is not available, protons become the exclusive substrate and the action of nitrogenase will generate 1 mol of H_2 for every 4 mol of ATP and 2 mol of ferredoxin consumed (Huesemann et al., 2010). Due to this high energy demand, the action of nitrogenase needs to be coupled with photosynthesis or the respiratory electron transport chain (Hatano et al., 2022). Glycolysis alone is not able to provide sufficient ATP for either N_2 fixation or H_2 production under dark anaerobic conditions (Hallenbeck and Benemann, 2002).

2.5.2 Hydrogenases

Hydrogenases are electron transporters in many cellular reactions. They carry electrons from NADH, oxidize ferredoxin, and generate H_2 under anoxic conditions (Eq1) (Buitrón et al., 2017; Hallenbeck and Benemann, 2002; Sivaramakrishnan et al., 2021).

(Eq. 2.1) $$2H^{+}+2Fd^{-} \rightarrow H_2+2Fd$$

Hydrogenases are widely found in microalgae, cyanobacteria, and fermentative bacteria and are broadly classified in three main categories depending on the metals present in the active catalytic site: (i) [FeFe] hydrogenase, (ii) [NiFe] hydrogenase, and (iii) [Fe] only hydrogenase (Lubitz et al., 2014). [FeFe] and [NiFe] hydrogenase have been reported in microalgae and cyanobacteria (Khetkorn et al., 2017). The hydrogen production rate of [FeFe] and [NiFe] hydrogenases is higher than nitrogenase, with turnover rates being 15 times higher in hydrogenases (Srirangan et al., 2011).

[FeFe] hydrogenases contain two irons with a dithionate cofactor (Wittkamp et al., 2018) and they are extremely sensitive to oxygen, getting easily inhibited in the presence of even trace amounts of oxygen. Consequently, synthesis of [FeFe] hydrogenases occur only under anoxic conditions (Posewitz et al., 2009). [NiFe] hydrogenase contains two subunits, with a large subunit of [NiFe] as the active site and a small subunit containing Fe-S bonds (Peters et al., 2015; Volbeda et al., 1996). [NiFe] hydrogenase is more oxygen tolerant than [FeFe] hydrogenase and can work in the presence of oxygen (Goris et al., 2011). The more oxygen tolerant [NiFe] hydrogenases have a modified [NiFe] active site with two cysteines, located at opposite ends, instead of glycine. The replacement of glycine in both locations increases oxygen tolerance. Oxygen tolerance decreases to just 1% oxygen concentration even if just one of the cysteines is replaced with glycine (Lukey et al., 2011).

2.5.3 Hydrogenase activity in microalgae

In green microalgae, hydrogenase enzymes play an important role in both indirect biophotolysis and fermentative hydrogen production pathways. *Chlamydomonas reinhardtii* is the most widely studied model microalgae, and consequently most of the knowledge we have regarding the activity and functioning of hydrogenases is based on this microalga (Hemschemeier et al., 2008; M. S. Kim et al., 2006; Tsygankov et al., 2006).

In most green microalgae, [FeFe] hydrogenases are the only hydrogen producing enzymes. The biggest challenge for producing H_2 in microalgae is consequently the extremely high oxygen sensitivity of these hydrogenases, as H_2 yield is hindered if anoxic conditions are not continuously maintained. Therefore, [FeFe] hydrogenases are typically not active during photosynthetic activity (Bingham et al., 2012), and H_2 production in green microalgae typically does not occur under direct light. It has been shown, however, that hydrogen formation can take place under light if anoxic conditions are created by continuously removing oxygen (Mus et al., 2007). Induction of H_2 production in *C. reinhardtii* has also been achieved by creating sulfur deprivation, thus inhibiting the repair of PSII proteins that get damaged by light (Kosourov et al., 2007; Laurinavichene et al., 2004; Pollock et al., 2005). Inhibition of PSII results in reduced photosynthetic activity, and lower oxygen evolution rate. As cells use the oxygen for respiration to produce energy for cell maintenance, this quickly creates an anoxic environment that facilitates H_2 formation.

Some studies have attempted to identify oxygen tolerant [FeFe] hydrogenases or obtaining oxygen tolerant [FeFe] hydrogenases by genetic modification (Bhagat et al., 2020). Optimization of photoperiod can also help to minimize oxygen accumulation, thus preventing hydrogenase inhibition. Kosourov et al. (2018) achieved sustained efficient H_2 production by transferring the

growing *C. reinhardtii* cultures from continuous light to a train of strong light pulses superimposed on darkness or low background illumination. This method redirected the photosynthetic electron flow to the hydrogenase rather than towards CO_2 fixation and biomass formation, thus increasing the overall H_2 photoproduction yield.

The capability of fermentation under dark anoxia helps *C. reinhardtii* to survive by allowing it to produce ATP from reserves accumulated during photosynthesis (Catalanotti et al., 2013). During light periods, photosynthesis generates excess anabolic activity leading to the accumulation of polysaccharides and/or lipids. Then, during dark periods these reserve molecules are converted to pyruvate to fuel cell metabolism. Pyruvate acts as substrate for several fermentative pathways that lead to the production of organic acids, acetyl-CoA, alcohols, CO_2, and H_2 (Catalanotti et al., 2013). Hydrogenases play an important role in the fermentative pathways that produce hydrogen (Das and Veziroğlu, 2001). The enzyme pyruvate ferredoxin oxidoreductase oxidizes pyruvate to acetyl-CoA and CO_2, generating reduced ferredoxin. Hydrogenases use the reduced ferredoxin to generate H2 (Catalanotti et al., 2013; Melis et al., 2000). As there are several competing fermentative pathways that consume pyruvate, hydrogen yield is typically low under dark fermentation conditions.

2.5.4 Hydrogenase activity in cyanobacteria

Cyanobacteria have multiple enzymes involved in H_2 metabolism including [FeFe] and [NiFe] hydrogenases, as well as nitrogenases (Madamwar et al., 2000; Schütz et al., 2004) Several cyanobacteria strains have evolved different strategies to protect these oxygen sensitive enzymes. Furthermore, most cyanobacteria have [NiFe] hydrogenase or bidirectional [NiFe] hydrogenase, which are more tolerant to oxygen.

Cournac et al., (2004) showed that the bidirectional [NiFe] hydrogenase in *Synechocystis* sp. (PCC 6803) was insensitive to light but was reversibly inactivated by O_2. Reactivation of the enzyme was shown to occur quickly in the presence of NADH or NADPH. Interestingly, the analysis of this enzyme showed that the enzyme was constitutively expressed in the presence of oxygen during the light period but was activated under dark anoxic conditions, which is different from the *C. reinhardtii* hydrogenase enzyme that is produced and activated only under anoxic conditions. Biohydrogen production in microalgae and cyanobacteria under various environmental conditions is given in Table 2.3.

2.5.5 Hydrogenase activity in heterotrophic bacteria

Hydrogen production can be achieved under heterotrophic conditions using hydrogen producing bacteria cultures. Hydrogenases are found in many heterotrophic fermentative bacteria. *Clostridium* has been widely studied as model organism for hydrogen production. From the three main type of hydrogenases, only [FeFe] and [NiFe] hydrogenases have been identified in most *Clostridium* strains (Calusinska et al., 2010). Although most of the hydrogen producing bacteria are known as anaerobic, some facultative anaerobes (Escherichia coli, Enterobacter, Citrobacter), and some aerobes (Alcaligenes, Bacillus) can produce hydrogen via hydrogenase activity (Kothari et al., 2012). Other than pure bacteria cultures, fermentative bacterial communities such as anaerobic inoculum obtained from biogas production plant and wastewater treatment plants also have gained attention as they are robust, cheap, and readily available (Wainaina et al., 2019).

Using heterotrophic hydrogen producing bacteria provides flexibility for using different substrate including microalgal biomass for hydrogen production. Combination of microalgae cultivation and dark fermentation has been shown to be a promising pathway to produce hydrogen (Ren et al., 2015).

2.6 Factors affecting hydrogen production

The growth rate of microalgae and cyanobacteria cultures are affected by many different environmental factors such as the photoperiod, light intensity, nutrient availability, and temperature. Furthermore, H_2 production from microalgae and cyanobacteria is also affected by the same factors and causes some limitations and challenges. The effect of those factors and limitations will be discussed in this section.

2.6.1 Photoperiod and light intensity

Light intensity and light/dark cycle play a big role in photosynthesis, cell growth rate, and cell composition (Laurinavichene et al., 2004; Vítová et al., 2011). High cell density and carbohydrate rich composition is important to increase H_2 yield the during dark fermentation stage as carbohydrate storage serves as feedstock for dark fermentation. Higher initial carbohydrate storage can result in a longer fermentation process thus increasing total H_2 production. To achieve higher cell density and increased carbohydrate composition improved photosynthetic efficiency is crucial. This can be achieved by the manipulation of light intensity and light/dark cycle (Iasimone et al., 2018).

Cheng et al. (2017) reported increased biomass production and carbohydrate accumulation when the light intensity raised from 500 to 1800 μmol $m^{-2}s^{-1}$. In another study, a significant increase in carbohydrate content was reported with an increase of light intensity under continuous illumination. The increase continued until the photo saturation of the photosynthetic system. When the light intensity was above saturation, a decrease in photosynthesis and cell growth occurred due to photoinhibition (Ho et al., 2012).

Table 2-3. Biohydrogen production by microalgae and cyanobacteria under various environmental conditions and responsible enzymes.

Enzyme	Type	Microalgae/ cyanobacteria	Conditions	Hydrogen yield	Ref
Hydrogenase	[NiFe]	*Synechocystis sp*	Medium A+, Temp 35°C, nitrogen starvation, dark, anoxic	30 mol/10^{17} cells	(McNeely et al., 2014)
	[NiFe]	*Synechocystis*	BG-11 medium, pH 8, Temp 28°C, dark, anoxic	600 nmol mg of Chl a^{-1}min^{-1}	(Gutekunst et al., 2018)
	[FeFe]	*Chlamydomonas reinhardtii*	TAP medium, pH 8, Temp 25°C, two stage (light and dark), anoxic	6 ml L^{-1}	(Saleem et al., 2012)
	[FeFe]	*Chlorella vulgaris*	BCC medium, pH 8, Temp 22°C, dark, anoxic	0.35 ml / h	(Alalayah et al., 2017)
	[NiFe]	*Synechococcus*	Medium A+, Temp 38°C, dark, anoxic	15 nmol/10 cells ml^{-1}	(Kumaraswamy et al., 2013)
	[Fe]	*Chlorella fusca*	Temp 20°C, dark, anoxic	20 µmol mg of Chl a^{-1}	(Winkler et al., 2002)
Nitrogenase		*Cyanothece* sp. *Miami* BG 043511 Anabena	Artificial wastewater, pH 8, Temp 30°C, two stage (light and dark), anoxic	16.4 µmol g^{-1}	(Skizim et al., 2012)
		Anabena siamensis	BG-11 medium, Temp 21°C, dark, anoxic	3.092-2.426 µmol mg of Chl a^{-1}	(Andrić et al., 2017)
		Synechococcus sp.	BG-11 medium, Temp 25°C, dark, anoxic	4.44 µmol mg of Chl a^{-1}	(Kossalbayev et al., 2020)

2.6.2 Nutrient availability

Microalgae growth rate and cell composition are highly dependent on available nutrients. Selection of appropriate medium is important to achieve the desired cell composition, and activation of metabolic pathways to start the accumulation of desired metabolites. It is critical to adjust the media components to maximize H_2 synthesis from microalgae and cyanobacteria via indirect photolysis. Jo et al. (2006) adjusted the concentration of media components and observed improved H_2 generation by increasing nitrogen, phosphate, and changing the pH to 7 using *C. reinhardtii* under sulfur deficient conditions.

Accumulation of different cell components (carbohydrates, lipids, and proteins) can be achieved by applying creating nutrient deficiencies (Paliwal et al., 2017). Furthermore, stress conditions can directly activate or deactivate the H_2 production mechanism and change in the cell composition alters H_2 production yield.

Nitrogen is required for cell growth and plays a key function in protein and lipid synthesis. (Arumugam et al., 2013; Yaakob et al., 2021). Nitrogen depletion reduces photosynthetic activity and results in an anoxic environment that activates the H_2 production mechanism (Azwar et al., 2014). H_2 production can be stimulated by nitrogen depletion using nitrogen fixing cyanobacteria. The presence of nitrogen in some heterocysts cyanobacteria such as *Anabaena* inhibits the nitrogenase activity. H_2 synthesis is catalyzed by the bidirectional [NiFe] hydrogenase in some non-nitrogen fixing cyanobacteria like Synechocystis, which is unaffected by nitrogen present. (De Rosa et al., 2015). Like nitrogenase, bi-directional hydrogenase is also regulated and activated under nitrogen depletion.

Sulfur is another macronutrient that has an important role in photosynthesis. Sulfur deprivation results in decreased chlorophyll content and inhibits photosynthetic activity reversibly (Eroglu and

Melis, 2011). In the absence of sulfur, O_2 evolution will be reduced, and further stopped. When there is no photosynthetic activity to produce energy, microalgae cells become anaerobic and induce the Fe-hydrogenase pathway of electron transport and photosynthetically produce H_2. Different species can show different hydrogenase activity level and H_2 production yield. For example, cyanobacteria, *Synechocystis* sp. strain PCC 6803 performs well under sulfur depletion while another cyanobacterium, *Aphanothece halophytica* performs well under nitrogen depletion as sulfur depletion reduces cell growth and hydrogenase activity (Cournac et al., 2002; Taikhao et al., 2013).

The effect of phosphorus depletion on hydrogenase activation, although the mechanism is still not clear, has been shown on microalgae *Chlorella* sp. (Batyrova et al., 2015). Phosphorous depletion slowed down the photosynthetic activity, which then result in a transition to anaerobic conditions, activation of hydrogenase enzyme, and H_2 production consequently. H_2 evolution by phosphorus-deprived marine *Chlorella* sp. was almost similar to sulfur deprived freshwater *C. reinhardtii* (Batyrova et al., 2015). In addition, H_2 production can be increased under magnesium deprivation. Lack of magnesium results in decreased chlorophyll and photosynthesis rate which creates anoxic conditions and activates hydrogenase activity.

2.6.3 Temperature

Temperature is another important factor that can directly affect the microalgae growth rate and H_2 production capacity (Cui et al., 2021; Gonçalves et al., 2021) Temperature can change the metabolic pathways and increase H_2 production in different cyanobacteria and microalgae (Jabri et al., 2021). The optimal temperature has also been reported to vary between 15–60°C depend on the type of strain (Patel et al., 2019; Varshney et al., 2015). Mesophilic temperatures between 20-30 °C were used in many studies to evaluate and further increase H_2 production (Bernard and

Rémond, 2012; Ras et al., 2013). Temperatures above and below inhibit the metabolism, cell growth rate, and consequently H_2 production.

2.7 Strategies to improve hydrogen production via indirect biophotolysis

2.7.1 Bioreactor Design

Bioreactor design and configuration is another important factor to reach desired H_2 yield using microalgae and cyanobacteria cultures via indirect biophotolysis. Reactor configuration and design can be done to optimize the light intensity and orientation, photoperiod, CO_2 transfer, mixing, and temperature which have been shown to affect H_2 production (Nagarajan et al., 2017b) CO_2 capture and fixation by microalgae is the first and most important step of H_2 production from microalgae, as it significantly affects biomass growth (Nagarajan et al., 2021).

Photobioreactors (PBRs) are cultivation systems to grow microalgae and cyanobacteria biomass. They provide many advantages such as protection from contamination by unwanted microorganisms and a more controlled environment (Markou, 2020). Their design parameters are mostly based on surface area and light usage to efficiently deliver enough light to promote cell growth (Legrand et al., 2021; Ranganathan et al., 2022). Therefore, a large surface to volume ratio is beneficial for increased cell growth and biomass accumulation (Deprá et al., 2019). Control of photoperiod and dark conditions, and removal of oxygen or nitrogen, however, are needed to activate hydrogenase or nitrogenase enzymes (González-Camejo et al., 2019; Vélez-Landa et al., 2021). Closed reactor systems such as vertical or horizontal tubular, flat-plate, or helical-tubular reactors can be useful and efficient to create oxygen and/or nitrogen free systems (Giannelli and Torzillo, 2012; Tamburic et al., 2011; Torzillo and Chini Zittelli, 2015).

Stirred tank reactors (STRs) ensure effective homogeneous mixing, pH, high mass transfer, and better control of most of the process parameters (Brindhadevi et al., 2021). SRTs can be used for

both microalgae growth in aerobic environment and H_2 production under dark and anoxic environment (Krishnan et al., 2019). STRs can be efficient in inducing and controlling anoxic and dark conditions to initiate fermentative pathways in microalgae or cyanobacteria.

A two-stage process that involves the integration of PBRs and STRs can be beneficial to increase H_2 production. In the first stage, microalgae and cyanobacteria biomass grow in phototrophic conditions, and then it is transferred to the second reactor where dark and anoxic conditions are applied to induce hydrogenase activity for H_2 production. Moreover, cells can be recycled back to the first stage for regrowth. Fedorov et al., (2005) demonstrated a two-stage H_2 production system with a maximum of 0.58 ml $H_2\,L^{-1}$ for more than 4000 h. In the research *C. reinhardtii* was grown in aerobic environment then the cells were delivered to a tank reactor for H_2 production under hypoxia.

2.7.2 Genetic modification

Inhibition of hydrogenase and nitrogenase by oxygen and activity of bidirectional hydrogenase limit the successful application of indirect biophotolysis. Furthermore, sustainable large scale H_2 production from this pathway is hampered due to low yields under dark conditions. Genetic manipulation or modification of microalgal and cyanobacterial strains can be vital to achieving H_2 production under oxic conditions for sustainable H_2 production (Anwar et al., 2019).

According to the literature, it can be said that genetic manipulations target to eliminate the following main problems: 1) Oxygen sensitivity of H_2 producing enzymes, 2) the presence and activity of uptake hydrogenase, 3) elimination of other competing pathways for electron 4) lower heterocyst formation frequently for H_2 production from cyanobacteria (Kruse and Hankamer, 2010; J. Li et al., 2020).

To achieve increased H_2 production under oxic conditions, oxygen sensitivity of the hydrogenase enzyme is required. The major reason for H_2 production under sulfur deprived conditions is the inactivity of PSII. Thus, it can be suggested that complete or partial inactivation of the PSII system with genetic modification can prevent oxygen inhibition and lead to increased H_2 production. Lin et al., (2013) reported partial inactivation of PSII in *Chlorella* sp. DT by knocking down the PSBO subunit, which is related to low photosynthetic activity. They reported that photobiological H_2 production increased by as much as tenfold compared to its WT.

The activity of uptake hydrogenase is another limiting factor on H_2 production due to the consumption of H_2. This usually happens in cyanobacteria. Therefore, to increase H_2 production, inactivation of uptake hydrogenase is one way of preventing H_2 consumption. 4.7-fold increased H_2 production was obtained by knocking down the gene regulating the uptake of hydrogen in cyanobacterium *Anabaena* sp. PCC 7120 with 101.33 μmol H2 mg chl a^{-1} h^{-1}, compared to wild type under the same condition (Khetkorn et al., 2012; Shahkouhi and Motamedian, 2020).

Another genetic engineering strategy for enhanced H_2 production is eliminating other metabolic pathways that are competing for electrons (Yacoby et al., 2011). Electrons are mainly transferred to other assimilatory or competing pathways, namely the respiratory electron transport system, oxidative pentose pathway (OPP), nitrate assimilation, and carbon fixation via the Calvin-Benson cycle. During indirect biophotolysis, the intermediate compounds may enter either the oxidative pentose phosphate pathway or the glycolysis pathway (Stincone et al., 2015) To produce more H_2 during indirect biophotolysis, it is beneficial to redirect the electron to the OPP pathway as a substrate is all the way degraded into H_2 and carbon dioxide while a big portion of electrons goes to organic acid production pathways in the glycolysis pathway (Y. M. Kim et al., 2011). This difference between the two pathways results in three times higher H_2 production from the OPP

pathway. Therefore, it has been proposed that enhancing the flux through the OPP pathway may help enhance H_2 production (Skizim et al., 2012). McNeely et al., (2014) reported increased NADPH production and therefore increased H_2 production by partially redirecting the electrons to the OPP pathway in *Synechococcus* 7002. In another study, Khetkorn et al., (2012) investigated the inhibition of competitive metabolic pathways by various inhibitors to redirect electron flow towards nitrogenase and bidirectional Hox-hydrogenase in *Anabaena siamensis* TISTR 8012. They reported a threefold increase in H_2 production with 22 μmol H_2 mg chl a^{-1} h^{-1}. Also increased H_2 production was reported after inhibition of the respiratory terminal oxidases (ΔctaI, ΔctaII, and Δcyd) in *Synechocystis* PCC 6803, which induced higher activity of bidirectional Hox-hydrogenase by (Gutthann et al., 2007). In another study interruption of the nitrate assimilation pathway of *Synechocystis* PCC 6803 resulted in higher H_2 production than wild type strain (Baebprasert et al., 2011). Accordingly, an engineering approach by eliminating competitive electron pathways can be a very effective and promising method to maximize H_2 production using cyanobacteria. This genetic modification deserves more attention for future microalgal and cyanobacterial H_2 production.

2.7.3 Process integration

H_2 synthesis via indirect biophotolysis using microalgae and cyanobacteria appears to face many difficulties. There are primarily two bottlenecks, which restrict long-term H_2 generation through indirect biophotolysis. These bottlenecks are (1) low H_2 yield in the dark and (2) high energy cost of microalgae and cyanobacteria biomass cultivation. Integration of different bioprocesses can enhance H_2 production while reducing the cost of an operation via the recovery of different bio products other than H_2.

The indirect biophotolysis process yields only 4 mol of H_2 per mole of glucose, whereas photo-fermentation produces 12 mol of hydrogen per mole of glucose. A two-stage process that combines direct biophotolysis with indirect biophotolysis was suggested to increase the total yield of H_2 produced from the same biomass (Goria et al., 2022). Furthermore, light/dark cycling can be done to maximize the H_2 production under both conditions. This process allows cells to grow under phototrophic conditions, then H_2 production can be initiated with the removal of oxygen, and later cells can be transferred to dark conditions to induce indirect biophotolysis for further production of H_2. Moreover, cells can be recycled for phototrophic growth and used again for H_2 production for a longer period. Kosourov et al., (2018) achieved sustained H_2 production using *C. reinhardtii* by combined direct and indirect biophotolysis. *C. reinhardtii* cultures were subjected to short strong white light pulses followed by longer dark phases. Through this process, they were able to recycle the electrons to the hydrogenase instead of CO_2 fixation and achieved increased H_2 yield. Although this integration can increase H_2 production, the photosynthetic efficiency of microalgae cells is still too low (3%) to make the process viable for H_2 production. To make this process comparable with other biological production methods, photosynthetic efficiency needs to be increased to 10-15%.

To achieve sustainable H_2 production from microalgae and cyanobacteria, indirect biophotolysis can be integrated with other biological H_2 production methods. Furthermore, integration with wastewater treatment systems can simultaneously result in the valorization of waste, reduce the cost of nutrients for microalgae and cyanobacteria cultivation, and the production of hydrogen together with other high value-added products (Chandrasekhar et al., 2015). Hwang et al. (2018) evaluated the presence of acetic acid obtained from wastewater to eliminate the oxygen evolution

in PSII, for sustainable biohydrogen production using *Chlorella vulgaris*. Acetic acid presence resulted in continuous microalgal H_2 production with a maximum H_2 yield of 65.4 ± 0.3 μmoL L^{-1}. Dark fermentation is a similar process to indirect biophotolysis. It occurs under dark and anoxic conditions via fermentative bacteria and archaea (Lee et al., 2011). Indirect biophotolysis can be coupled with dark fermentation further utilizing the microalgal biomass to increase H_2 yield. Furthermore, it can be coupled with other carbon sources to improve efficiency. Other valuable by-products such as organic acids, can be further used to improve the economic viability of the process. Chandra and Venkata Mohan (2011) studied the integration of microalgal photo fermentation and dark fermentation using synthetic wastewater and food waste to achieve higher H_2 productivity.

Another approach is combining indirect biophotolysis with anaerobic digestion. After H_2 production, the residual biomass can be used as feedstock for methane production via anaerobic digestion (Nagarajan et al., 2017). Furthermore, other by-products such as organic acids and pigments can be extracted before anaerobic digestion (Chia et al., 2018; Nobre et al., 2013; Passos et al., 2014). In Chapter 4 of this these, simultaneous organic acid and H_2 production via indirect biophotolysis under dark anoxic conditions is reported. Fufthermore, the integration of indirect biophotolysis with anaerobic digestion to improve organic acid and hydrogen productivities under high alkaline conditions further utilization of biomass into methane has been discussed in Chapter 4, 5, and 6.

2.8 Conclusion

Hydrogen production from cyanobacteria via indirect biophotolysis is a feasible and promising pathway to produce an efficient, carbon neutral energy carrier and reduce greenhouse gas emissions. Although this method is promising for low carbon and energy efficient hydrogen

production, low photon conversion efficiency and oxygen sensitivity of hydrogenases are important drawbacks that reduces the efficiency and sustainability of hydrogen production. Application of genetic and metabolic engineering can address the main problems such as hydrogenase inhibition due to oxygen, low photochemical efficiency, and competition for reducing agents. Although application of genetic and metabolic engineering can improve productivity, integration of indirect biophotolysis with other processes such as direct biophotolysis, dark fermentation and anaerobic digestion, is needed to increase hydrogen production efficiency and reduce cost for sustainable hydrogen production. Future studies in this area may lead the transition to a carbon-free hydrogen economy from fossil fuels.

2.9 References

Acar C, Dincer I (2018) Hydrogen Production. In: Dincer I (ed) Comprehensive Energy Systems. Elsevier, Amsterdam pp 1–40.

Aikawa S, Izumi Y, Matsuda F, Hasunuma T, Chang JS, Kondo A (2012) Synergistic enhancement of glycogen production in *Arthrospira platensis* by optimization of light intensity and nitrate supply. Bioresour Technol 108: 211–215.

Akhlaghi N, Najafpour-Darzi G (2020) A comprehensive review on biological hydrogen production. Int J Hydrogen Energ 45(43): 22492–22512.

Alalayah WM, Al-Zahrani A, Edris G, Demirbas A (2017) Kinetics of biological hydrogen production from green microalgae *Chlorella vulgaris* using glucose as initial substrate. Energy Sources A: Recovery Util. Environ. Eff 39(12): 1210–1215.

Alesi, WR, Jr Kitchin JR (2012) Evaluation of a primary amine-functionalized ion-exchange resin for CO2 capture Ind. Eng. Chem. Res 51 (19): 6907

All I, Basit MA (1993) Significance Of Hydrogen Content In Fuel Combustion. Int J Hydrogen

Energ 18(12):1009–1011.

Ananyev GM, Skizim NJ, Dismukes GC (2012) Enhancing biological hydrogen production from cyanobacteria by removal of excreted products. J. Biotechnol 162(1): 97–104.

Andrić I, Pina A, Ferrão P, Fournier J, Lacarrière B, Le Corre O, Taikhao S, Phunpruch S (2017) Increasing Hydrogen Production Efficiency of N_2-Fixing Cyanobacterium *Anabaena siamensis* TISTR 8012 by Cell Immobilization. Energy Procedia 138: 366–371.

Anwar M, Lou S, Chen L, Li H, Hu Z (2019) Recent advancement and strategy on bio-hydrogen production from photosynthetic microalgae. Bioresour Technol 292: 121972.

Arumugam M, Agarwal A, Arya MC, Ahmed Z (2013) Influence of nitrogen sources on biomass productivity of microalgae *Scenedesmus bijugatus*. Bioresour Technol 131: 246–249.

Aslam A, Thomas-Hall SR, Mughal TA, Schenk PM (2017) Selection and adaptation of microalgae to growth in 100% unfiltered coal-fired flue gas. Bioresour. Technol 233: 271–283.

Aslam A, Thomas-Hall SR, Manzoor M, Jabeen F, Iqbal M, uz Zaman Q, Schenk PM, Asif Tahir M (2018) Mixed microalgae consortia growth under higher concentration of CO_2 from unfiltered coal fired flue gas: Fatty acid profiling and biodiesel production. J. Photochem. Photobiol. B Biol 179: 126–133.

Azwar MY, Hussain MA, Abdul-Wahab AK (2014) Development of biohydrogen production by photobiological, fermentation and electrochemical processes: A review. Renew Sustain Energy Rev 31: 158–173.

Baebprasert W, Jantaro S, Khetkorn W, Lindblad P, Incharoensakdi A (2011) Increased H_2 production in the cyanobacterium *Synechocystis* sp. strain PCC 6803 by redirecting the electron supply via genetic engineering of the nitrate assimilation pathway. *Metab Eng*, 13(5):610–616.

Batyrova K, Gavrisheva A, Ivanova E, Liu J, Tsygankov A (2015) Sustainable hydrogen photoproduction by phosphorus-deprived marine green microalgae *Chlorella* sp. Int J Mol Sci 16(2): 2705–2716.

Beer C, Reichstein M, Tomelleri E, Ciais P, Jung M, Carvalhais N, Rödenbeck C, Arain MA, Baldocchi D, Bonan GB, Bondeau A, Cescatti A, Lasslop G, Lindroth A, Lomas M, Luyssaert S, Margolis H, Oleson KW, Roupsard O, Veenendall E, Viovy N, Williams C, Woodward FI, Papale D (2010) Terrestrial gross carbon dioxide uptake: Global distribution and covariation with climate. Science 329(5993): 834–838.

Bernard O, Rémond B (2012) Validation of a simple model accounting for light and temperature effect on microalgal growth. Bioresour Technol 123: 520–527.

Bhagat AK, Buium H, Shmul G, Alfonta L (2020) Genetically Expanded Reactive-Oxygen-Tolerant Alcohol Dehydrogenase II. ACS Catal 10(5): 3094–3102.

Brentner LB, Jordan PA, Zimmerman JB (2010) Challenges in developing biohydrogen as a sustainable energy source: implications for a research agenda. Environ Sci Technol 44(7): 2243–2254.

Brindhadevi K, Shanmuganathan R, Pugazhendhi A, Gunasekar P, Manigandan S (2021) Biohydrogen production using horizontal and vertical continuous stirred tank reactor- a numerical optimization. Int J Hydrogen Energ 46(20): 11305–11312.

Buitrón G, Carrillo-Reyes J, Morales M, Faraloni C, Torzillo G (2017) Biohydrogen production from microalgae. In: Gonzalez-Fernandez C, and Muñoz R (eds) Microalgae-based biofuels and bioproducts from feedstock cultivation to end-products. Elsevier, Duxford, pp 209-234.

Caia M, Bernard O, Béchet Q (2018) Optimizing CO_2 transfer in algal open ponds. Algal Res 35: 530–538.

Calusinska M, Happe T, Joris B, Wilmotte A (2010) The surprising diversity of clostridial hydrogenases: a comparative genomic perspective. Microbiology 156: 1575-1588.

Canon-Rubio, KA, Sharp CE, Bergerson J, Strous M, De la Hoz Siegler H (2016) Use of highly alkaline conditions to improve cost-effectiveness of algal biotechnology. Applied Microbiology and Biotechnology. 100 (4):, 611–1622.

Catalanotti C, Yang W, Posewitz MC, Grossman AR (2013) Fermentation metabolism and its evolution in algae. Front. Plant Sci 4: 1-17

Chandra R, Venkata Mohan S (2011) Microalgal community and their growth conditions influence biohydrogen production during integration of dark-fermentation and photo-fermentation processes. Int J Hydrogen Energ 36(19): 12211–12219.

Chandrasekhar K, Lee YJ, Lee DW (2015) Biohydrogen Production: Strategies to Improve Process Efficiency through Microbial Routes. Int. J. Mol. Sci 16(4): 8266.

Cheah WY, Show PL, Chang JS, Ling TC, Juan JC (2015) Biosequestration of atmospheric CO_2 and flue gas-containing CO_2 by microalgae. Bioresour. Technol 184: 190–201.

Cheng D, Li D, Yuan Y, Zhou L, Li X, Wu T, Wang L, Zhao Q, Wei W, Sun Y (2017) Improving carbohydrate and starch accumulation in *Chlorella* sp. AE10 by a novel two-stage process with cell dilution. Biotechnol. Biofuels 10(1): 75.

Chi Z, Xie Y, Elloy F, Zheng Y, Hu Y, Shulin C, (2013) Bicarbonate-based integrated carbon capture and algae production system with alkalihalophilic cyanobacterium. Bioresour. Technol 133: 513–521.

Chia SR, Chew KW, Show PL, Yap YJ, Ong HC, Ling TC, Chang JS (2018) Analysis of Economic and Environmental Aspects of Microalgae Biorefinery for Biofuels Production: A Review. Biotechnol. J 13(6): 1700618.

Chou HH, Su HY, Song XDi, Chow TJ, Chen CY, Chang JS, Lee TM (2019) Isolation and characterization of *Chlorella* sp. mutants with enhanced thermo- and CO_2 tolerances for CO_2 sequestration and utilization of flue gases. Biotechnol. Biofuels 12(1): 1–14.

Compaoré J, Stal LJ (2010) Oxygen and the light–dark cycle of nitrogenase activity in two unicellular cyanobacteria. Environmental Microbiology 12: 54-62.

Cournac L, Guedeney G, Peltier G, Vignais PM (2004) Sustained Photoevolution of Molecular Hydrogen in a Mutant of *Synechocystis* sp. Strain PCC 6803 Deficient in the Type I NADPH-Dehydrogenase Complex. J. Bacteriol 186(6): 1737.

Cournac L, Mus F, Bernard L, Guedeney G, Vignais P, Peltier G (2002) Limiting steps of hydrogen production in *Chlamydomonas reinhardtii* and *Synechocystis* PCC 6803 as analysed by light-induced gas exchange transients. Int J Hydrogen Energ 27(11–12): 1229–1237.

Cui X, Yang J, Cui M, Zhang W, Zhao J (2021) Comparative experiments of two novel tubular photobioreactors with an inner aerated tube for microalgal cultivation: Enhanced mass transfer and improved biomass yield. Algal Res 58: 102364.

Daneshvar E, Wicker RJ, Show PL, Bhatnagar A (2022) Biologically-mediated carbon capture and utilization by microalgae towards sustainable CO_2 biofixation and biomass valorization – A review. Chem. Eng. J 427: 130884.

Darnoko D, Cheryan M (2000) Kinetics of palm oil transesterification in a batch reactor. J. Am. Oil Chem. Soc., 77(12): 1263–1267.

Das D, Veziroglu N (2001) Hydrogen production by biological processes: a survey of literature. Int J Hydrogen Energ 26(1): 13-28.

Dawood F, Anda M, Shafiullah GM (2020) Hydrogen production for energy: An overview. Int J Hydrogen Energ 45(7): 3847–3869.

De Rosa E, Checchetto V, Franchin C, Bergantino E, Berto P, Szabò I, Giacometti GM, Arrigoni G, Costantini P (2015) [NiFe]-hydrogenase is essential for cyanobacterium *Synechocystis* sp. PCC 6803 aerobic growth in the dark. Sci. Reports 5(1): 1–12.

Deprá MC, Mérida L GR, de Menezes CR, Zepka LQ, Jacob-Lopes E (2019) A new hybrid photobioreactor design for microalgae culture. Chem. Eng. Res. Des 144: 1–10.

Duarte JH, Fanka LS, Costa JAV (2016) Utilization of simulated flue gas containing CO_2, SO2, NO and ash for Chlorella fusca cultivation. Bioresour. Technol 214: 159–165.

Eroglu E, Melis A (2011) Photobiological hydrogen production: Recent advances and state of the art. Bioresour. Technol 102(18): 8403–8413.

Fal S, Benhima R, El Mernissi N, Kasmi Y, Smouni A, El Arroussi H (2021) Microalgae as promising source for integrated wastewater treatment and biodiesel production. Int. J. Phytoremediation 24(1): 34–46.

Fan LH, Zhang YT, Zhang L, Chen HL (2008) Evaluation of a membrane-sparged helical tubular photobioreactor for carbon dioxide biofixation by *Chlorella vulgaris*. J. Memb. Sci 325(1): 336–345.

Fedorov AS, Kosourov S, Ghirardi ML, Seibert M (2005) Continuous hydrogen photoproduction by *Chlamydomonas reinhardtii*. Appl. Biochem. Biotechnol 121(1): 403–412.

Feron P, Cousins A, Jiang K, Zhai R, Garcia M (2020) An update of the benchmark post-combustion CO_2-capture technology. Fuel 273(1): 117776.

Gatamaneni BL, Orsat V, Lefsrud M (2018) Factors affecting growth of various microalgal species. Environ. Eng. Sci. 35(10), 1037–1048.

Giannelli L, Torzillo G (2012) Hydrogen production with the microalga *Chlamydomonas reinhardtii* grown in a compact tubular photobioreactor immersed in a scattering light

nanoparticle suspension. Int J Hydrogen Energ 37(22): 16951–16961.

IEA (2021), Global Energy Review 2021, International Enery Agency, Paris, France. https://www.iea.org/reports/global-energy-review-2021.

Gonçalves AL, Simões M, Pires JCM (2014) The effect of light supply on microalgal growth, CO2 uptake and nutrient removal from wastewater. Energy Convers. Manag 85: 530–536.

Gonçalves AL, Almeida F, Rocha FA, and Ferreira A (2021) Improving CO_2 mass transfer in microalgal cultures using an oscillatory flow reactor with smooth periodic constrictions. J. Environ. Chem. Eng 9(6): 106505.

González-Camejo J, Viruela A, Ruano MV, Barat R, Seco A, Ferrer J (2019) Effect of light intensity, light duration and photoperiods in the performance of an outdoor photobioreactor for urban wastewater treatment. Algal Res 40: 101511.

Goria K, Kothari R, Singh HM, Singh A, Tyagi VV (2022) Biohydrogen: potential applications, approaches, and hurdles to overcome. In: Sahay S (ed) Handbook of Biofuels. Elsevier, London, pp 399–418.

Goris T, Wait AF, Saggu M, Fritsch J, Heidary N, Stein M, Zebger I, Lendzian F, Armstrong FA, Friedrich B, Lenz O (2011) A unique iron-sulfur cluster is crucial for oxygen tolerance of a [NiFe]-hydrogenase. Nat. Chem. Biol. 7(5): 310–318.

Guo P, Zhang Y, Zhao Y (2018) Biocapture of CO_2 by different microalgal-based technologies for biogas upgrading and simultaneous biogas slurry purification under various light intensities and photoperiods. Int. J. Environ. Res. Public Health. 15(3): 528

Gutekunst K, Hoffmann D, Westernströer U, Schulz R, Garbe-Schönberg D, Appel J (2018) In-vivo turnover frequency of the cyanobacterial NiFe-hydrogenase during photohydrogen production outperforms in-vitro systems. Sci. Reports 8(1): 1–10.

Gutthann F, Egert M, Marques A, Appel J (2007) Inhibition of respiration and nitrate assimilation enhances photohydrogen evolution under low oxygen concentrations in Synechocystis sp. PCC 6803. Biochim. Biophys. Acta - Bioenerg 1767(2): 161–169.

Hallenbeck PC, Benemann JR (2002) Biological hydrogen production; fundamentals and limiting processes. Int. J. Hydrogen Energ 27(11–12): 1185–1193.

Hatano J, Kusama S, Tanaka K, Kohara A, Miyake C, Nakanishi S, Shimakawa G (2022) NADPH production in dark stages is critical for cyanobacterial photocurrent generation: a study using mutants deficient in oxidative pentose phosphate pathway. Photosynth. Res 1: 1–8.

Hemalatha M, Sravan JS, Min B, Venkata Mohan, S (2019) Microalgae-biorefinery with cascading resource recovery design associated to dairy wastewater treatment. Bioresour. Technol 284: 424–429.

Hemschemeier A, Fouchard S, Cournac L, Peltier G, Happe T (2008) Hydrogen production by *Chlamydomonas reinhardtii*: An elaborate interplay of electron sources and sinks. Planta 227(2): 397–407.

Ho SH, Chen CY, Chang JS (2012) Effect of light intensity and nitrogen starvation on CO2 fixation and lipid/carbohydrate production of an indigenous microalga Scenedesmus obliquus CNW-N. Bioresour. Technol 113: 244–252.

Huesemann MH, Hausmann TS, Carter BM, Gerschler JJ, Benemann JR (2010) Hydrogen Generation through Indirect Biophotolysis in Batch Cultures of the Nonheterocystous Nitrogen-Fixing Cyanobacterium Plectonema boryanum. Appl Biochem Biotechnol 162: 208–220.

Hulatt CJ, Thomas DN (2011) Productivity, carbon dioxide uptake and net energy return of microalgal bubble column photobioreactors. Bioresour. Technol 102(10): 5775–5787.

Hwang JH, Church J, Lim J, Lee WH (2018) Photosynthetic biohydrogen production in a wastewater environment and its potential as renewable energy. Energy 149: 222–229.

Iasimone F, Panico A, De Felice V, Fantasma F, Iorizzi M, Pirozzi F (2018) Effect of light intensity and nutrients supply on microalgae cultivated in urban wastewater: Biomass production, lipids accumulation and settleability characteristics. J. Environ. Manage 223: 1078–1085.

Issariyakul T, Dalai AK (2012) Comparative kinetics of transesterification for biodiesel production from palm oil and mustard oil. Can. J. Chem. Eng 90: 342–350.

Jabri Hal, Taleb A, Touchard R, Saadaoui I, Goetz V, Pruvost J (2021) Cultivating microalgae in desert conditions: Evaluation of the effect of light-temperature summer conditions on the growth and metabolism of *Nannochloropsis* QU130. Appl. Sci 11(9): 3799.

Jiménez-Llanos J, Ramírez-Carmona M, Rendón-Castrillón L, Ocampo-López C (2020) Sustainable biohydrogen production by *Chlorella* sp. microalgae: A review. Int. J. Hydrogen Energy 45(15): 8310–8328.

Jo JH, Lee DS, Park JM (2006) Modeling and Optimization of photosynthetic hydrogen gas production by green alga *Chlamydomonas reinhardtii* in sulfur-deprived circumstance. Biotechnol. Prog 22(2): 431–437.

Kamran M (2021). Bioenergy. In: Kamran M, Rayyan M (eds) Renewable Energy Conversion Systems. Elsevier, London, pp 243–264.

Keith DW (2009) Why capture CO_2 from the atmosphere?. Science 325(5948), 1654–1655.

Khetkorn W, Lindblad P, Incharoensakdi A (2012) Inactivation of uptake hydrogenase leads to enhanced and sustained hydrogen production with high nitrogenase activity under high light exposure in the cyanobacterium *Anabaena siamensis* TISTR 8012. J. Biol. Eng 6(1): 1.

Khetkorn W, Rastogi R P, Incharoensakdi A, Lindblad P, Madamwar D, Pandey A, Larroche C

(2017) Microalgal hydrogen production – A review. Bioresour. Technol 243: 1194–1206.

Kim MS, Baek JS, Yun YS, Jun Sim S, Park S, Kim SC (2006) Hydrogen production from Chlamydomonas reinhardtii biomass using a two-step conversion process: Anaerobic conversion and photosynthetic fermentation. Int. J. Hydrogen Energy 31(6): 812–816.

Kim YM, Cho HS, Jung GY, Park JM (2011) Engineering the pentose phosphate pathway to improve hydrogen yield in recombinant *Escherichia coli*. Biotechnol. Bioeng 108(12): 2941–2946.

Kosourov S, Patrusheva E, Ghirardi ML, Seibert M, Tsygankov A (2007) A comparison of hydrogen photoproduction by sulfur-deprived *Chlamydomonas reinhardti*i under different growth conditions. J. Biotechnol 128(4): 776–787.

Kosourov S, Jokel M, Aro EM, Allahverdiyeva Y (2018) A new approach for sustained and efficient H_2 photoproduction by *Chlamydomonas reinhardtii*. Energy Environ. Sci 11(6): 1431–1436.

Kossalbayev BD, Tomo T, Zayadan BK, Sadvakasova AK, Bolatkhan K, Alwasel S, Allakhverdiev SI (2020) Determination of the potential of cyanobacterial strains for hydrogen production. Int. J. Hydrogen Energy 45(4): 2627–2639.

Kothari R, Singh D P, Tyagi VV, Tyagi SK (2012) Fermentative hydrogen production – An alternative clean energy source. Renew. Sustain. Energy Rev 16(4): 2337–2346.

Krishnan S, Md Din MF, Taib SM, Nasrullah M, Sakinah M, Wahid ZA, Kamyab H, Chelliapan S, Rezania S, Singh L (2019) Accelerated two-stage bioprocess for hydrogen and methane production from palm oil mill effluent using continuous stirred tank reactor and microbial electrolysis cell. J. Clean. Prod 229: 84–93.

Kruse O, Hankamer B (2010) Microalgal hydrogen production. Curr. Opin. Biotechnol 21(3):

238–243.

Kumar A, Ergas S, Yuan X, Sahu A, Zhang Q, Dewulf J, Malcata F X, van Langenhove H (2010) Enhanced CO_2 fixation and biofuel production via microalgae: recent developments and future directions. Trends Biotechnol 28(7): 371–380.

Kumaraswamy GK, Guerra T, Qian X, Zhang S, Bryant DA, Dismukes GC (2013) Reprogramming the glycolytic pathway for increased hydrogen production in cyanobacteria: metabolic engineering of NAD+-dependent GAPDH. Energy Environ. Sci 6(12): 3722–3731.

Kumari S, Nasr M, Kumar S (2017) Technological Advances in Biohydrogen Production from Microalgae. In: Gupta SK, Malik A, Bux F (eds) Algal Biofuels: Recent Advances and Future Prospects. Springer, Singapore, pp 347–360.

Lam MK, Lee KT, Mohamed AR (2012) Current status and challenges on microalgae-based carbon capture. Int. J. Greenh. Gas Control 10: 456–469.

Laurinavichene T, Tolstygina I, Tsygankov A (2004) The effect of light intensity on hydrogen production by sulfur-deprived *Chlamydomonas reinhardtii*. J. Biotechnol 114(1–2): 143–151.

Lee DJ, Show KY, Su A (2011) Dark fermentation on biohydrogen production: Pure culture. Bioresour. Technol 102(18): 8393–8402.

Legrand J, Artu A, Pruvost J (2021) A review on photobioreactor design and modelling for microalgae production. React. Chem. Eng 6(7): 1134–1151.

Li FF, Yang ZH, Zeng R, Yang G, Chang X, Yan JB, Hou YL (2011) Microalgae capture of CO_2 from actual flue gas discharged from a combustion chamber. Ind. Eng. Chem. Res 50: 6496–6502.

Li S, Li F, Zhu X, Liao Q, Chang JS, and Ho SH (2022). Biohydrogen production from microalgae

for environmental sustainability. Chemosphere 291: 132717.

Lin HDi, Liu BH, Kuo TT, Tsai HC, Feng TY, Huang CC, Chien LF (2013) Knockdown of PsbO leads to induction of HydA and production of photobiological H_2 in the green alga *Chlorella* sp. DT. Bioresour. Technol 143: 154–162.

Lubitz W, Ogata H, Rüdiger O, Reijerse E (2014) Hydrogenases. Chem. Rev 114(8): 4081–4148.

Lukey MJ, Roessler MM, Parkin A, Evans RM, Davies RA, Lenz O, Friedrich B, Sargent F, Armstrong FA (2011) Oxygen-tolerant [NiFe]-hydrogenases: The individual and collective importance of supernumerary cysteines at the proximal Fe-S cluster. J. Am. Chem. Soc 133(42): 16881–16892.

Madamwar D, Garg N, Shah V (2000) Cyanobacterial hydrogen production. World J. Microbiol. Biotechnol 16(8): 757–767.

Markou G, Vandamme D, Muylaert K (2014) Microalgal and cyanobacterial cultivation: the supply of nutrients. Water Res 65: 186–202.

Markou G (2020) Overview of microalgal cultivation, biomass processing and application. In: Konur O (ed) Hand Book of Algal Science, Technology and Medicine. Elsevier, London, pp 343–352.

McNeely K, Kumaraswamy GK, Guerra T, Bennette N, Ananyev G, Dismukes GC (2014) Metabolic switching of central carbon metabolism in response to nitrate: Application to autofermentative hydrogen production in cyanobacteria. J. Biotechnol 182–183(1): 83–91.

Melis A, Zhang L, Forestier M, Ghirardi ML, Seibert M (2000) Sustained photobiological hydrogen gas production upon reversible inactivation of oxygen evolution in the green alga Chlamydomonas reinhardtii. Plant Physiol 122: 127–136.

Moreira D, Pires JCM. (2016) Atmospheric CO_2 capture by algae: Negative carbon dioxide

emission path. Bioresour. Technol 215: 371–379.

Mus F, Dubini A, Seibert M, Posewitz MC, Grossman AR (2007) Anaerobic acclimation in *Chlamydomonas reinhardtii*: anoxic gene expression, hydrogenase induction, and metabolic pathways. J. Biol. Chem 282(35): 25475–25486.

Nagarajan D, Lee DJ, Kondo A, Chang JS (2017) Recent insights into biohydrogen production by microalgae – From biophotolysis to dark fermentation. Bioresour. Technol 227: 373–387.

Nagarajan D, Dong CDi, Chen CY, Lee DJ, Chang JS (2021) Biohydrogen production from microalgae—Major bottlenecks and future research perspectives. Biotechnol. J 16(5): 2000124.

Napan K, Teng L, Quinn JC, Wood BD (2015) Impact of heavy metals from flue gas integration with microalgae production. Algal Res 8: 83–88.

Nobre BP, Villalobos F, Barragán BE, Oliveira AC, Batista AP, Marques PASS, Mendes RL, Sovová H, Palavra AF, Gouveia L (2013) A biorefinery from *Nannochloropsis* sp. microalga – Extraction of oils and pigments. Production of biohydrogen from the leftover biomass. Bioresour. Technol 135: 128–136.

Park J, Kumar G, Bakonyi P, Peter J, Nemestóthy N, Koter S, Kujawski W, Bélafi-Bakó K, Pientka Z, Muñoz R, Kim SH (2021) Comparative evaluation of CO_2 fixation of microalgae strains at various CO_2 aeration conditions. Waste Biomass Valorization 12(6): 2999–3007.

Passos F, Uggetti E, Carrère H, Ferrer I (2014) Pretreatment of microalgae to improve biogas production: A review. Bioresour. Technol. 172: 403–412.

Patel A, Matsakas L, Rova U, Christakopoulos P (2019) A perspective on biotechnological applications of thermophilic microalgae and cyanobacteria. Bioresour. Technol 278: 424–434.

Peters JW, Schut GJ, Boyd ES, Mulder DW, Shepard EM, Broderick JB, King PW, Adams MWW (2015) [FeFe]- and [NiFe]-hydrogenase diversity, mechanism, and maturation. Biochim. Biophys. Acta - Mol. Cell Res 1853(6): 1350–1369.

Piiparinen J, Barth D, Eriksen NT, Teir S, Spilling K, Wiebe MG (2018) Microalgal CO_2 capture at extreme pH values. Algal Res 32: 321–328.

Pires JCM, Gonçalves AL, Martins FG, Alvim-Ferraz MCM, Simões M (2014) Effect of light supply on CO_2 capture from atmosphere by *Chlorella vulgaris* and *Pseudokirchneriella subcapitata*. Mitig. Adapt. Strateg. Glob. Chang 19(7): 1109–1117.

Pollock SV, Pootakham W, Shibagaki N, Moseley JL, Grossman AR (2005) Insights into the acclimation of Chlamydomonas reinhardtii to sulfur deprivation. Photosynth. Res 86(3): 475–489.

Pratte BS, Thiel T (2014) Regulation of nitrogenase gene expression by transcript stability in the cyanobacterium *Anabaena variabilis*. J Bacteriology 196(20): 3609-3621.

Radmann EM, Camerini FV, Santos TD, Costa JAV (2011) Isolation and application of SO_x and NO_x resistant microalgae in biofixation of CO_2 from thermoelectricity plants. Energy Convers. Manag 52(10): 3132–3136.

Rahaman MSA, Cheng LH, Xu XH, Zhang L, Chen HL (2011) A review of carbon dioxide capture and utilization by membrane integrated microalgal cultivation processes. Renew. Sustain. Energy Rev 15(8): 4002–4012.

Raheem A, Prinsen P, Vuppaladadiyam AK, Zhao M, Luque R (2018) A review on sustainable microalgae based biofuel and bioenergy production: Recent developments. J. Clean. Prod 181: 42–59.

Ranganathan P, Pandey AK, Sirohi R, Tuan Hoang A, Kim SH (2022) Recent advances in

computational fluid dynamics (CFD) modelling of photobioreactors: Design and applications. Bioresour. Technol 350: 126920.

Ras M, Steyer JP, Bernard O (2013) Temperature effect on microalgae: A crucial factor for outdoor production. Rev. Environ. Sci. Biotechnol 12(2): 153–164.

Razu MH, Hossain F, Khan M (2019) Advancement of bio-hydrogen production from microalgae. In: Alam MdA, Wang Z (eds) Microalgae Biotechnolgy for Development of Biofuel and Wastewater Treatment. Springer, Singapore, pp 423–462.

Ren HY, Liu BF, Kong F, Zhao L, Ren NQ (2015) Sequential generation of hydrogen and lipids from starch by combination of dark fermentation and microalgal cultivation. RSC Adv 5(94): 76779–76782.

Saleem M, Chakrabarti MH, Abdul Raman AA, Hasan DB, Ashri Wan Daud WM, Mustafa A (2012) Hydrogen production by *Chlamydomonas reinhardtii* in a two-stage process with and without illumination at alkaline pH. Int. J. Hydrogen Energy 37(6): 4930–4934.

Sayre R (2010) Microalgae: The Potential for Carbon Capture, BioSci 60(9): 722–727,

Schütz K, Happe T, Troshina O, Lindblad P, Leitão E, Oliveira P, Tamagnini P (2004) Cyanobacterial H_2 production - A comparative analysis. Planta 218(3): 350–359.

Senatore V, Buonerba A, Zarra T, Oliva G, Belgiorno V, Boguniewicz-Zablocka J, Naddeo V (2021) Innovative membrane photobioreactor for sustainable CO2 capture and utilization. Chemosphere 273: 129682.

Sepulveda C, Gómez C, El Bahraoui N, Acién G (2019) Comparative evaluation of microalgae strains for CO_2 capture purposes. J. CO2 Util 30: 158–167.

Shahkouhi AM, Motamedian E (2020) Reconstruction of a regulated two-cell metabolic model to study biohydrogen production in a diazotrophic cyanobacterium *Anabaena variabilis* ATCC

29413. Plos One 15(1): 1-18.

Sharp CE, Urschel S, Dong X, Brady AL, Slater GF, Strous M (2017) Robust, high-productivity phototrophic carbon capture at high pH and alkalinity using natural microbial communities. Biotechnol. Biofuels 10(1): 1–13.

Show KY, Yan Y, Zong C, Guo N, Chang JS, Lee DJ (2019) State of the art and challenges of biohydrogen from microalgae. Bioresour. Technol 289: 121747.

Singh J, Dhar DW (2019) Overview of carbon capture technology: Microalgal biorefinery concept and state-of-the-art. Front. Mar. Sci. 29.

Singh N, Sarma S (2022) Biological routes of hydrogen production: a critical assessment. In: Sahay S (ed) Handbook Biofuels. Elsevier, London, pp 419–434.

Sivaramakrishnan R, Shanmugam S, Sekar M, Mathimani T, Incharoensakdi A, Kim SH, Parthiban A, Edwin Geo V, Brindhadevi K, Pugazhendhi A (2021) Insights on biological hydrogen production routes and potential microorganisms for high hydrogen yield. Fuel 291: 120136.

Skizim NJ, Ananyev GM, Krishnan A, Dismukes GC (2012) Metabolic pathways for photobiological hydrogen production by nitrogenase- and hydrogenase-containing unicellular cyanobacteria Cyanothece. J. Biol. Chem 287(4): 2777–2786.

Sobczuk TM, Camacho FG, Camacho Rubio F, Acié N Ferná Ndez FG, Molina Grima E (2000) Carbon dioxide uptake efficiency by outdoor microalgal cultures in tubular airlift photobioreactors. Biotechnol. Bioeng. 67(4): 45-475.

Song C, Liu Q, Qi Y, Chen G, Song Y, Kansha Y, Kitamura Y (2019) Absorption-microalgae hybrid CO2 capture and biotransformation strategy—A review. Int. J. Greenh. Gas Control 88: 109–117.

Srirangan K, Pyne ME, Perry Chou C (2011) Biochemical and genetic engineering strategies to enhance hydrogen production in photosynthetic algae and cyanobacteria. Bioresour. Technol. 102(18): 8589-8604.

Stern MC, Simeon F, Herzog H, Hatton TA (2013) Post- combustion carbon dioxide capture using electrochemically mediated amine regeneration. Energy Environ. Sci 6(8): 2505–2517.

Stincone A, Prigione A, Cramer T, Wamelink MMC, Campbell K, Cheung E, Olin-Sandoval V, Grüning NM, Krüger A, Tauqeer Alam M, Keller MA, Breitenbach M, Brindle KM, Rabinowitz, JD, Ralser M (2015) The return of metabolism: biochemistry and physiology of the pentose phosphate pathway. Biol. Rev 90(3): 927–963.

Taikhao S, Junyapoon S, Incharoensakdi A, Phunpruch S (2013) Factors affecting biohydrogen production by unicellular halotolerant cyanobacterium *Aphanothece halophytica*. J. Appl. Phycol 25(2): 575–585.

Tamburic B, Zemichael FW, Crudge P, Maitland GC, Hellgardt K (2011) Design of a novel flat-plate photobioreactor system for green algal hydrogen production. Int. J. Hydrogen Energy 36(11): 6578–6591.

Thomas DM, Mechery J, Paulose SV (2016).\ Carbon dioxide capture strategies from flue gas using microalgae: a review. Environ. Sci. Pollut. Res 23(17): 16926–16940.

Torzillo G, Chini Zittelli G (2015) Tubular photobioreactors. In: Prokop A, Bajpai RK, and Zappi ME (eds) Algal Biorefineries Volume 2: Prododuct and Refinery Desing. Springer, Heidelberg, pp 187–212.

Tsygankov AA, Kosourov S N, Tolstygina IV, Ghirardi ML, Seibert M (2006) Hydrogen production by sulfur-deprived *Chlamydomonas reinhardtii* under photoautotrophic conditions. Int. J. Hydrogen Energy 31(11): 1574–1584.

Vadlamani A, Viamajala S, Pendyala B, Varanasi S (2017) Cultivation of microalgae at extreme alkaline ph conditions: A novel approach for biofuel production. ACS Sustain. Chem. Eng 5(8): 7284–7294.

Vadlamani A, Pendyala B, Viamajala S, Varanasi S (2019) High productivity cultivation of microalgae without concentrated CO_2 input. ACS Sustain. Chem. Eng 7(2): 1933–1943.

Vale MA, Ferreira A, Pires JCM, and Gonçalves AL (2020) CO_2 capture using microalgae. In: Rahimpour MR, Farsi M, Makerem MA (eds) Advances in Carbon Capture. Elsevier, Duxfor, pp 381–405.

Varshney P, Mikulic P, Vonshak A, Beardall J, Wangikar PP (2015) Extremophilic micro-algae and their potential contribution in biotechnology. Bioresour. Technol 184: 363–372.

Vélez-Landa L, Hernández-De León HR, Pérez-Luna YDC, Velázquez-Trujillo S, Moreira-Acosta J, Berrones-Hernández R, Sánchez-Roque Y (2021) Influence of light intensity and photoperiod on the photoautotrophic growth and lipid content of the microalgae *Verrucodesmus verrucosus* in a photobioreactor. Sustain 13(12): 6606.

Venkata Mohan S, Modestra JA, Amulya K, Butti SK, Velvizhi G (2016) A circular bioeconomy with biobased products from CO_2 sequestration. Trends Biotechnol 34(6): 506–519.

Vítová M, Bišová K, Umysová D, Hlavová M, Kawano S, Zachleder V, Čížková M (2011) *Chlamydomonas reinhardtii*: Duration of its cell cycle and phases at growth rates affected by light intensity. Planta 233(1): 75–86.

Volbeda A, Garcin E, Piras C, De Lacey AL, Fernandez VM, Hatchikian EC, Frey M, Fontecilla-Camps JC (1996) Structure of the [NiFe] Hydrogenase active site: Evidence for biologically uncommon Fe ligands⊥. J. Am. Chem. Soc 118(51): 12989–12996.

Wainaina S, Lukitawesa, Kumar Awasthi M, Taherzadeh MJ (2019) Bioengineering of anaerobic

digestion for volatile fatty acids, hydrogen or methane production: A critical review. Bioengineered 10(1): 437–458.

Winkler M, Heil B, Heil B, Happe T (2002) Isolation and molecular characterization of the [Fe]-hydrogenase from the unicellular green alga *Chlorella fusca*. Biochim. Biophys. Acta - Gene Struct. Expr 1576(3): 330–334.

Wittkamp F, Senger M, Stripp ST, Apfel UP (2018) [FeFe]-Hydrogenases: recent developments and future perspectives. Chem. Commun 54(47): 5934–5942.

Yaakob MA, Mohamed RMSR, Al-Gheethi A, Ravishankar GA, Ambati RR (2021) Influence of nitrogen and phosphorus on microalgal growth, biomass, lipid, and fatty acid production: An overview. Cells 10(2): 393.

Yacoby I, Pochekailov S, Toporik H, Ghirardi ML, King PW, Zhang S (2011) Photosynthetic electron partitioning between [FeFe]-hydrogenase and ferredoxin:NADP+-oxidoreductase (FNR) enzymes in vitro. Proc. Natl. Acad. Sci. U. S. A 108(23): 9396–9401.

Yang X, Liu L, Yin Z, Wang X, Wang S, Ye Z (2020) Quantifying photosynthetic performance of phytoplankton based on photosynthesis - Irradiance response models. Environ. Sci. Eur. 32, 24.

Zhang S, Liu Z (2021) Advances in the biological fixation of carbon dioxide by microalgae. J. Chem. Technol. Biotechnol 96(6): 1475–1495.

Zhang W, Zhao C, Cao W, Sun S, Hu C, Liu J, Zhao Y (2020) Removal of pollutants from biogas slurry and CO_2 capture in biogas by microalgae-based technology: a systematic review. Environ. Sci. Pollut. Res 27(23): 28749–28767.

Zhu C, Zhai X, Xi Y, Wang J, Kong F, Zhao Y, Chi Z (2020) Efficient CO_2 capture from the air for high microalgal biomass production by a bicarbonate Pool. J. CO2 Util 37: 320–327.

CHAPTER 3

Methodology

This chapter describes the experimental set-up used to conduct the experiments, the analytical methods used to quantify important process variables, as well as the methodology for mass balance and energy balance calculations.

3.1. Biomass production

The cyanobacterial culture used here consisted of a consortium dominated by *Candidatus* "Phormidium alkaliphilum", an alkaliphilic and halotolerant cyanobacterium (Ataeian et al., 2021, 2022). This culture was derived by enrichment of microbial mats collected from several soda lakes located in British Columbia, Canada, as described by Sharp et al., (2017). Biomass was grown in cyclic batch mode using 10 L glass bottles under a photon flux of 900 µmol $m^{-2}s^{-1}$ using full spectrum LED lamps (Hyperikon, HyperT5-4C-50). At the end of each batch, lasting 7 days, 95 % of the culture medium was removed and replenished with fresh medium. The alkaline medium was prepared to a final pH of 10 and 0.5 mol L^{-1}total alkalinity. Composition of the alkaline cultivation media is given in Table 3.1.

Table 3-1. Composition of alkaline culture media.

Chemicals	Concentration	Unit
Macronutrients		
Na_2CO_3	22.36	g L^{-1}
$NaHCO_3$	6.54	g L^{-1}
$NaNO_3$	340	mg L^{-1}
$MgSO_4 \cdot 7H_2O$	120	mg L^{-1}
$CaCl_2$	19	mg L^{-1}
NaCl	250	mg L^{-1}
K_2HPO_4	216	mg L^{-1}
KCl	122	mg L^{-1}
$FeCl_2$	5	mg L^{-1}
Micronutrients		
$ZnCl_2$	20	µg L^{-1}
$MnCl_2 \cdot 4H_2O$	250	µg L^{-1}
H_3BO_3	600	µg L^{-1}
$CoCl_2 \cdot 6H_2O$	15	µg L^{-1}
$CuCl_2 \cdot 2H_2O$	15	µg L^{-1}
$NiCl_2 \cdot 6H_2O$	10	µg L^{-1}
$Na_2MoO_4 \cdot 2H_2O$	15	µg L^{-1}
KBr	10	µg L^{-1}

3.2. Biomass Harvesting

At the end of each batch, biomass was harvested by either natural settling or centrifugation. Harvesting by natural settling was done by stopping mixing and allowing the culture to settle for up to 6 hours. Samples were taken in triplicates at 1, 2, 3, and 6 hours to monitor biomass concentration, settling efficiency, and used media removal. Centrifugation was carried at varying relative centrifugal force, applied for 15 min, for further dewatering of the harvested biomass. Harvested alkaline and high pH biomass before any pretreatment is referred as fresh biomass. Total solids and volatile solid concentrations were determined after each harvesting procedure. The biomass paste harvested by centrifugation is referred as solid-state condition as there was no free water, but it was moist enough to allow the fermentation process to happen.

3.3. Fermentation

Approximately 2.0 g of the harvested biomass, either as a paste or slurry, were placed in sterile serum bottles. Serum bottles of varying volumes (20 mL, 100 mL, and 200 mL) were used for the different concentration experiments and sealed with rubber septa. The headspace in each bottle was vacuumed to 50 mbar and filled with argon gas up to atmospheric pressure to create anoxic conditions. Hypoxic conditions were created by sealing with a rubber septum without gas exchange. Incubation was performed under dark conditions to start respiration and eventually fermentation. The bottles were incubated at 21 ± 0.5 °C for up to 16 days. Every two days, three bottles were removed from the incubation chamber and analyzed as described in Sections 3.8 (liquid and solid phases) and 3.10 (gas phase).

3.4 Batch anaerobic digestion of cyanobacteria

Batch anaerobic digestion of fermented and freshly harvested cyanobacterial biomass was done using three different inocula (digested manure, digested sewage sludge, and soda lake sediment)

at two different temperatures (21 °C and 35 °C). 200 mL serum bottles were used with a 120 mL working volume. The cyanobacteria: inoculum ratio was set at 1:2 based on chemical oxygen demand (COD). Volume was adjusted to 120 mL using a media micronutrient solution as described in Nolla-Ardevol et al., (2015). The headspace in each bottle was vacuumed to 0.050 bar and filled with argon gas up to atmospheric pressure (around 0.950 bar) to create anoxic conditions. Bottles were sealed with rubber septa and incubated in an orbital shaker at 120 rpm for 30 days.

3.5 Ammonium inhibition test

To determine the effect of the NH_4^+concentration on methane production, the soda lake sediment was fed with the micronutrient solution described by Nolla-Ardèvol et al. (2015), supplemented with ammonia (at 0, 20, 40 and 60 mM) and acetate (20 mM). The acetate concentration range was selected to mimic the main organic acid concentration in the fermented cyanobacterial biomass. The headspace in each bottle was vacuumed to 0.050 bar and filled with argon gas up to atmospheric pressure (around 0.950 bar) to create anoxic conditions. Bottles were sealed with rubber septa and incubated on an orbital shaker at 120 rpm for 30 days at two different temperatures (21°C and 35°C).

3.6 Semi-continuous anaerobic digestion of fermented cyanobacteria

Semi-continuous anaerobic digestion was carried out in two 3 L glass, autoclavable Applikon bioreactors (ez2-Control) with 2.5 L working volume. Initially, one of the digesters was inoculated with 1.5 L of alkaline soda lake sediment obtained from four different soda lakes located in Cariboo Plateau in British Columbia (Zorz et al., 2019). The digester was fed with media containing micronutrient solution (Nolla-Ardèvol et al., 2015) and 20 mM acetate to acclimate the micro-organisms in the sediment and to reduce the pH to optimal conditions for anaerobic digestion. Afterwards, half of the first digester content was used to inoculate the second digester.

A flow chart of the digester set up is presented in Figure 3.1. The digesters were operated with different organic loading rates (OLR) at different phases of AD and a hydraulic retention time (HRT) of 44 days at ambient temperature (21 ± 1 °C). Digesters were mixed at 120 rpm with a marine impeller. Fermented cyanobacterial biomass stock was diluted to a concentration using the media given in Table 3.2. Feeding was done twice a week.

Table 3-2. Composition of media used for dilution of fermented biomass.

Chemicals	Concentration	Unit
$FeSO_4 \cdot 7H_2O$	0.2	g L^{-1}
$MnCl2 \cdot 4H_2O$	0.5	g L^{-1}
H_3BO_3	0.3	g L^{-1}
$CoCl_2 \cdot 6H_2O$	0.2	g L^{-1}
$NiCl_2 \cdot 6H_2O$	0.092	g L^{-1}
$ZnSO_4 \cdot 7H_2O$	0.1	g L^{-1}
$AlCL_3 \cdot 8H_2O$	0.09	g L^{-1}
$CuCl_2 \cdot 2H_2O$	0.038	g L^{-1}
$NaCH_3COO.$	1.64	g L^{-1}
RPMI-1640 Vitamin Solution 100X (Sigma Aldrich, R7256)	1	mL

3.7 Semi-continuous anaerobic digestion of fermented cyanobacteria with recycling

After 222 days of continuous biogas production, biomass recycling was established to prevent biomass loss and improve solid retention time, thus eliminating the risk of wash out. Biomass recycling was conducted by settling the digester effluent for 4 hours; after which the clarified effluent was removed, and the settled slurry mixed into the feeding tank to the digesters. The solid retention time (SRT) was calculated using Equation 1:

(Eq.3.1) $$Solid\ retention\ time = \frac{V_d \times C_d}{F_{out} \times C_{out}}$$

where V_d is the working volume of the digester, C_d is total solid concentration in the digester, F_{out} is flow rate of effluent, and C_{out} is total solid concentration in effluent. C_d *and* C_{out} were measured by total solid analysis as described in section 3.8.2.

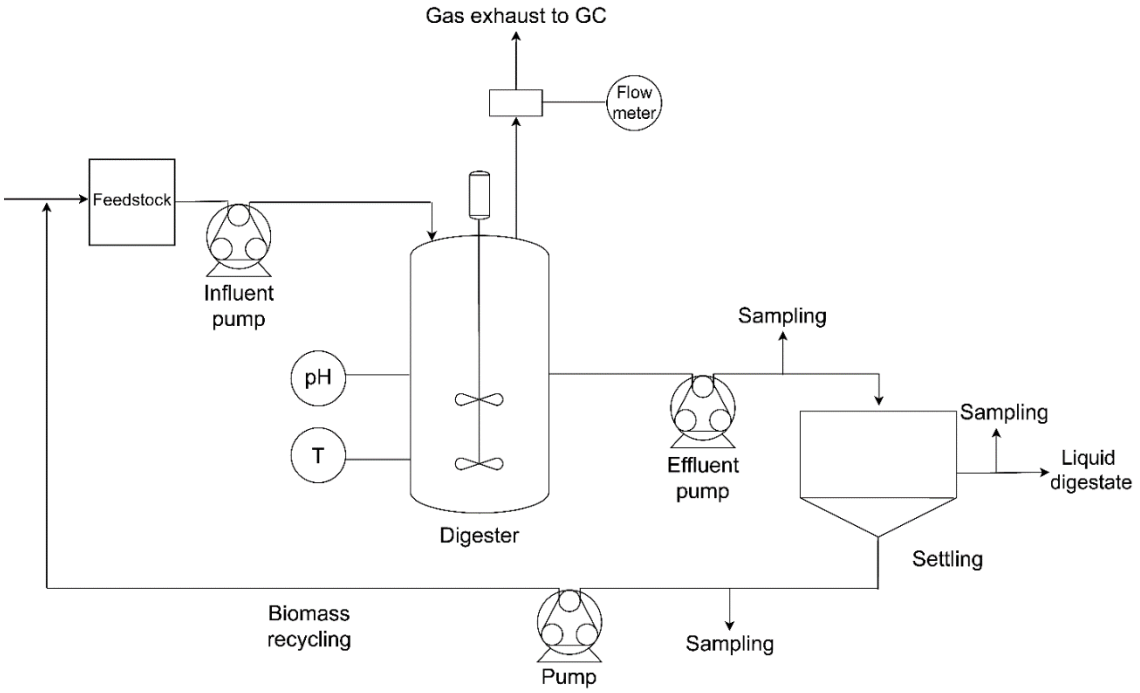

Figure 3.1. Schematic of the semi-continuous anaerobic digestion system.

3.8. Analysis of fermentation products and semi-continuous anaerobic digestion samples

The pH of the fermented biomass was measured using a micro-pH probe (InLab, Mettler Toledo). The fermented biomass was either a slurry or a paste. In the latter case, the whole paste was resuspended in 5 mL of deionized water to extract organic acids and other soluble organic materials. In both cases, centrifugation for 15 min at 3894 × g was used to separate the solid fraction containing cells and cell debris from the liquid phase. The supernatant was recovered and stored at – 80 °C, while the solid pellet was freeze dried and stored at – 20 °C for elemental analysis.

3.8.1 Liquid phase analysis

Organic acid analysis

The liquid samples recovered from the fermentation stage were filtered through a 0.2 µm PES sterile filter (Basix) and were diluted 5 to 15 times with deionized water (Type I, 18.2 MOh·cm) to get the concentrations of organic acids in the calibration range of 0.34 mM to 50 mM. Samples were analyzed by HPLC (Dionex ICS 3000, Thermo Fisher) using an Aminex HPX-87H (Bio-Rad) organic acid column (9 µm; 7.8 × 300 mm) and a UV-Vis detector. The HPLC was operated using 5 mM H_2SO_4 as mobile phase at a flow rate of 0.5 mL/min at a temperature of 35 °C. Standard calibration curves were prepared using acetic acid (Alfa Aesar, 99.7+%), propionic acid (Acros Organics, 99%), formic acid (Acros Organics, 99%), butyric acid (Acros Organics, 99%), lactic acid (Acros Organics, 90%), and succinic acid (Alfa Aesar, 99.7+%) as analytical standards. Known concentrations of aqueous solutions of succinic acid, lactic acid, formic acid, acetic acid, propionic acid, and butyric acid were used to build a calibration curve as shown in Figure 3.2.

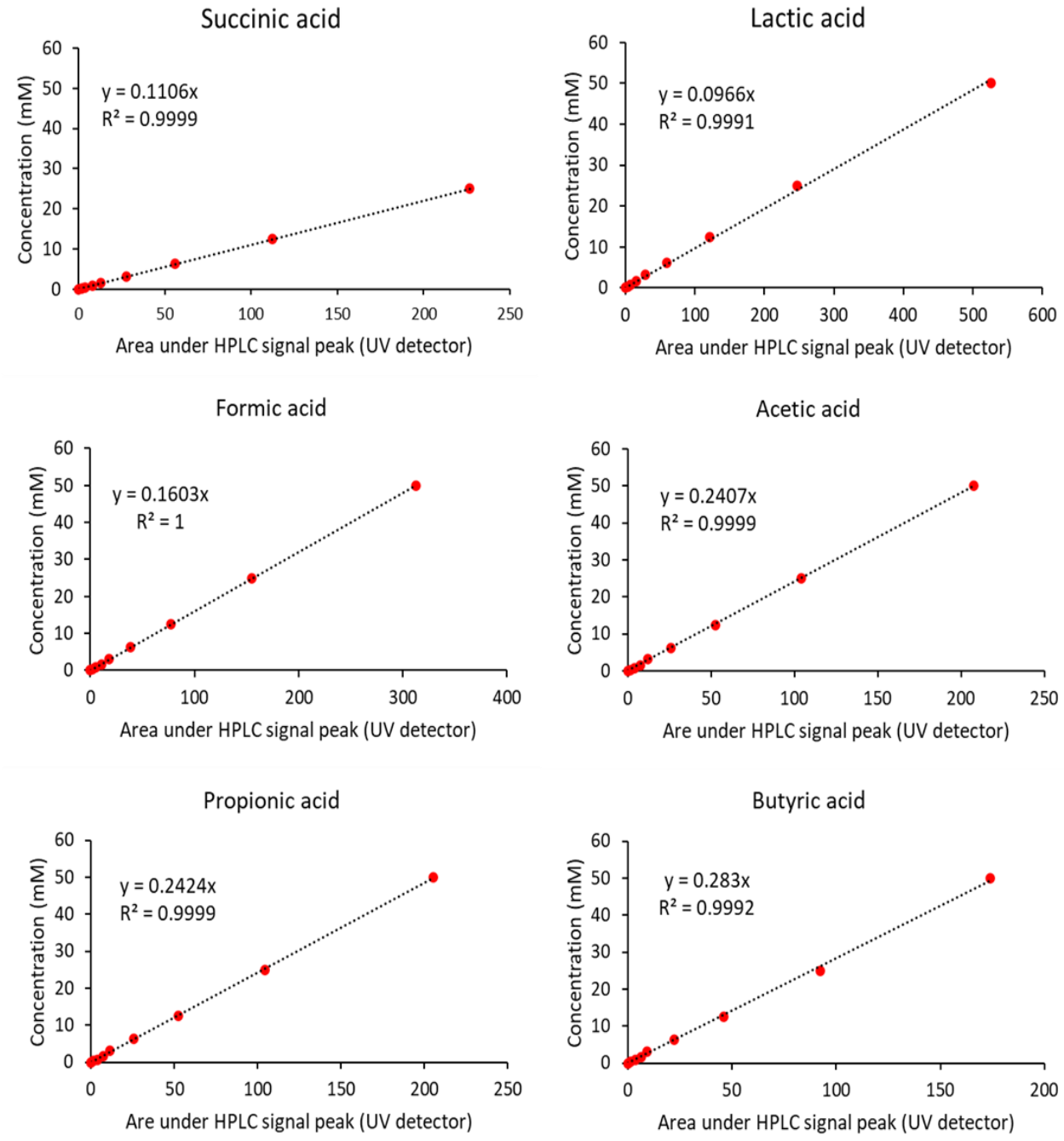

Figure 3.2. Calibration curve for organic acids in aqueous solutions with respect to high performance liquid chromatograph (HPLC) measurements, using UV detector.

Soluble sugar analysis

Soluble sugar was analyzed by the sulfuric acid-phenol method; briefly, 50 µl of the sample were mixed with 150 µl of 98 % sulfuric acid followed immediately by the addition of 30 µl of 5 % phenol in water. After incubating for 5 min at 90 °C in a static water bath, the samples were cooled to room temperature for 5 min and absorbance at 490 nm was recorder with a SpectraMax ID3 microplate reader (Masuko et al., 2005). Glucose was used as standard for calibration curve. Aqueous solutions of glucose of known concentration were used to build a calibration curve as shown in Figure 3.3.

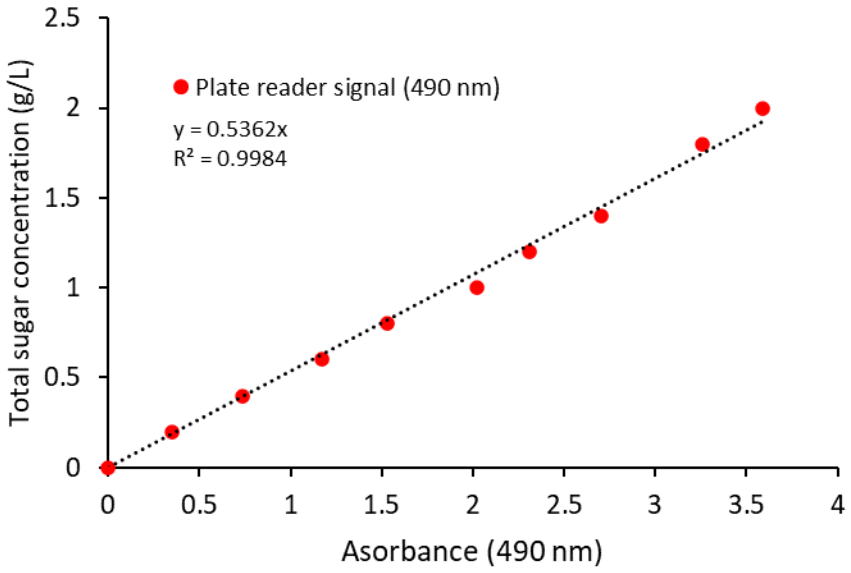

Figure 3.3. Calibration curve for glucose in aqueous solutions with respect to plate reader measurements.

Soluble protein analysis

For soluble protein content analysis, 600 µL of the sample were mixed with 950 µL of the Lowry Reagent D and 0.1 mL of diluted Folin-Ciocalteu's phenol reagent, then incubated for 30 min at room temperature. Absorbance was measured at 600 nm and protein concentration was obtained using a calibration curve prepared with bovine serum albumin (VWR Life Science, 30 % solution) (Slocombe et al., 2013). Aqueous solutions of fetal bovine serum of known concentration were used to build a calibration curve as shown in Figure 3.4.

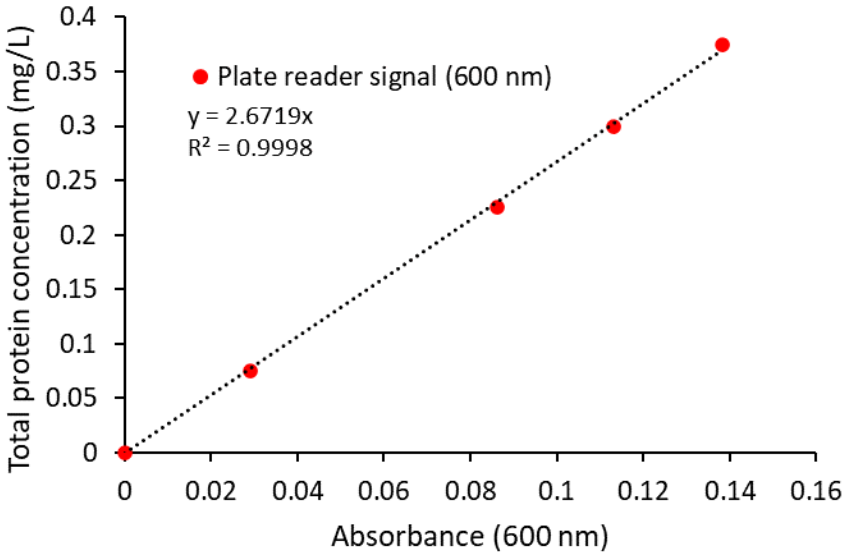

Figure 3.4. Calibration curve for fetal bovine albumin in aqueous solutions with respect to plate reader measurements.

Chemical oxygen demand

Chemical oxygen demand (COD) was determined using CHEMetrics COD vials (K-7355) with a range of 0-1500 ppm. Required dilution (2-5 times) were done to different to reduce the COD level to the measurement range. 5 ml of sample was added into COD vial and vortexed for 1 min. Vials were incubated at 150°C for 2 hours. Absorbance of the samples were measured by VWR brand UV/Visible spectrophotometer (UV-3100PC). Potassium hydrogen phthalate solution (100 – 900 mg/L) was used as standard for calibration curve (Blaird et al., 2017). Aqueous solutions of potassium hydrogen phthalate of known concentration were used to build a calibration curve as shown in Figure 3.5.

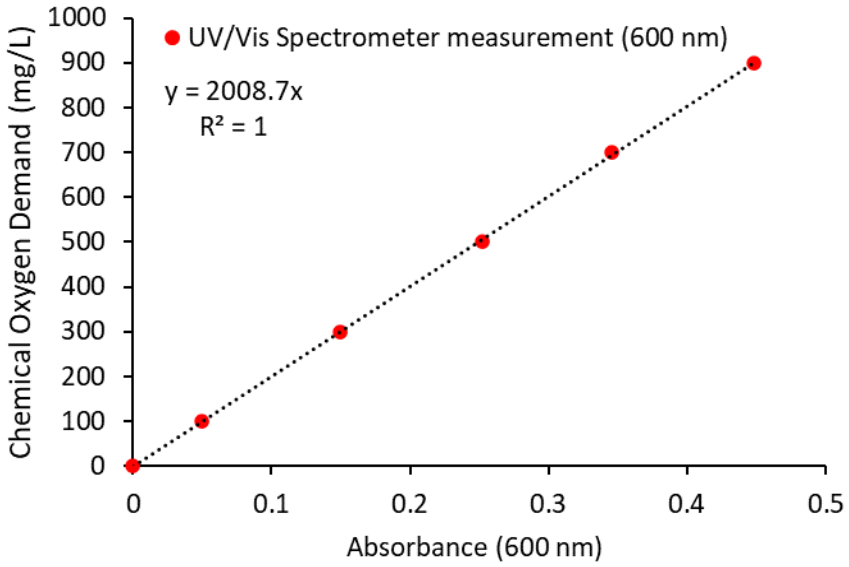

Figure 3.5. Calibration curve for potassium hydrogen phthalate solution in aqueous solutions with respect to plate reader measurements

Ammonium Analysis

Ammonium concentrations were determined using the OPA (*o*-phthaldiadehyde, Sigma P-1378) colorimetric assay as described by Holmes et al., (1999). Samples were diluted between 40 and 200 times to get into the range of standard 0 -5 mM ammonium concentration. 40 µl of sample was transferred to 96 well plate and 160 µl OPA reagent was added. 96 well plate was shaken on orbital shaker for 3 hours and absorbance of samples were measured at 600 nm with a SpectraMax ID3 microplate reader. Aqueous solutions of ammonium sulfate of known concentration were used to build a calibration curve as shown in Figure 3.6.

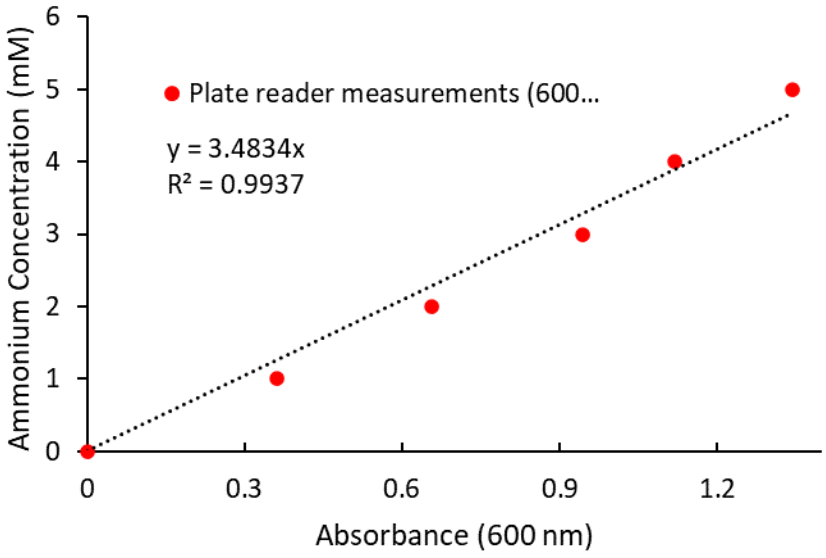

Figure 3.6. Calibration curve curve for ammonium sulfate in aqueous solutions with respect to plate reader measurements.

3.8.2 Solid phase analysis

Total solids and Volatile Solid Analysis

Total solids and volatile solid concentration at every sampling point were determined using the method outlined by Wychen and Laurens, (2016). 100 ± 5mg of wet biomass samples were transferred into a pre-weighed crucible. Samples were placed into a convection drying oven at 60°C ± 1°C under vacuum and dried for 24 hours. Samples were placed into desiccator for cooling after removing form oven. The weight of crucible and oven-dried samples were record for total solid content calculation. For volatile solid determination, 100 ± 5mg of dry biomass samples were transferred into a pre-weighed crucible. Samples were placed into a muffle furnace at 575°C for 24 hours. The weight of crucible and ash samples were record for volatile solid content calculation.

Analysis of Protein Content in Biomass Analysis

Protein content of the initial biomass was extracted and determined by the method described by Slocombe et al., (2013). 5 mg ± 10% dry biomass samples were placed in PTFE capped glass tubes. 200 µL of 24% trichloroacetic acid solution was added into each tube and vortexed. Tubes were placed in 90 °C dry bath for 15 min incubation. Samples were cooled down after removing from dry bath and 600 µL of deionized water (Type I, 18.2 MOh·cm) was added into each tube and samples were centrifuged at 15000 g for 20 min at 4 °C to separate liquid phase and solid phase. After centrifugation, solid phase was recovered and 500 µL of Lowry Reagent D was added to resuspend. Tubes were placed in 55 °C dry bath for 3 hours of incubation. At the end of 3 hours, tubes were removed and centrifuged at 15000 g for 20 min at room temperature. Supernatant recovered and stored at -20 °C for further protein analysis.

CHN Analysis

Elemental composition of the harvested biomass was determined using a CHN analyzer (2400 Series II, Perkin Elmer), for determination of carbon, hydrogen, and nitrogen content. 3 mg of samples in duplicate for each sampling point were used for more accurate analysis. The method is based on the combustion of the sample in an oxygen atmosphere at 925°C.

3.9. Carbon Recovery and Hydrogen Yield

The carbon recovery, *R*, was calculated based on:

(Eq.3.2) $$R = \frac{\sum_{i=1}^{m} C_{c,i} \times V}{C_{c,biomass,t=0}}$$

where C_c is the carbon content of component *i* at time *t*, *V* is the sample volume, and *m* is the number of measured carbon-containing compounds.

The maximum theoretical hydrogen yield (Y_{HB}, in mL H_2/g biomass) was calculated as:

(Eq.3.3) $$Y_{HB} = Y_{HM} \times X_M$$

where Y_{HM} is the stoichiometric hydrogen yield of monosaccharides (497.8 mL H_2/g monosaccharides), and X_M is the total monosaccharides concentration in the biomass (Xia et al., 2015).

3.10. Biogas and hydrogen measurements by gas chromatography

Biogas Analysis

Biogas production was continuously measured using a gas flow meter (Ritter, model MiliGasCounter). Biogas samples were taken from the headspace of the digesters with a Hamilton brand air-tight syringe (Model 1001 LTN CTC SYR) and analyzed with a gas chromatographer (Agilent Technologies, 7890B) equipped with Hayesep N (1.83 m x 3.17 mm) and Molsieve 5A (2.44 m x 3.17 mm) columns in series. The columns temperature was kept at 100 °C and the analysis was conducted using a thermal conductivity detector (TCD) and a flame ionization

detection (FID, 250°C). Helium was used as carrier gas at a flow rate of 21 mL min^{-1}. A custom-made gas mixture, supplied by Air Liquide and containing 25.39 % hydrogen, 4963 ppm oxygen, 1 % nitrogen, 4977 ppm methane, 495 ppm nitrous oxide, 9985 ppm carbon dioxide and an argon balance, was used for calibration.

Hydrogen Analysis

An air-tight syringe (Hamilton Company) was used to collect gas samples from the incubation vials' headspace. Samples were injected into a Varian GC to determine hydrogen and methane concentration. The instrument was equipped with a porous polymer column (10'x1/8" OD SS, 80/100 Mesh), a Molecular Sieve column (10'x1/8" OD SS, 80/100 Mesh), and a thermal conductivity detector. Argon (99.999 %, Air Liquide) was used as the carrier gas, running at 30 mL/min with column oven temperature at 100 °C and the TCD operating at 120 °C.

3.11 Energy balance calculations

The net energy production by the microalgae digestion system was calculated from the energy balance shown in Equation 3.4.

(Eq.3.4) $$E_{total} = E_{methane} - E_{heating} - E_{pumping} - E_{mixing}$$

The energy produced from methane ($E_{methane}$) was determined using Equation 5, where the lower calorific value of methane (35.8 MJ/m^3) under standard pressure and temperature was used as a reference for the available thermal energy produced from combustion:

(Eq.3.5) $$E_{methane} = V_{methane}(m^3) \times 35.8 \left(\frac{MJ}{m^3}\right)$$

The energy required for heating the digesters ($E_{heating}$) was calculated as the sum of the energy used to heat up the feed to the operational temperature of the digester and the energy used to compensate the heat losses through the digester walls. The energy used to heat up the feed, ΔQ, was calculated using Equation 3.6, where *m* is the mass of liquid (g) being heated, *C* is the specific heat capacity

of water (4.2 J/g K) and ΔT is the temperature difference between the feed temperature and the operational temperature of the digester. The mass of liquid is the feed flow calculated by assuming a microalgae feed of 1 kg VS/d, VS/TS ratio of 0.9, and a dry weight of 4 %. The energy used for dewatering the microalgae was not included. The feed temperature was the ambient temperature of 21°C assumed in this study.

(Eq.3.6) $$\Delta Q = m\ C\ \Delta T$$

The energy used to compensate the heat losses through the digester walls was calculated according to Fourier's law as presented in Equation 3.7, where Φ is the heat transfer rate (W), λ is the thermal conductivity of the isolation material (W/m K), A is the heat transfer area (m^2), dT is the temperature difference across the isolation material (K), and dx is the thickness of the isolation material (m). Fiberglass with thermal conductivity of 0.04 W/m K and thickness of 0.05 m was assumed as the isolation material for the digester. The area of heat transfer was the surface area of the digester, calculated using the digester volume, and by assuming a height to diameter ratio of 1.5. The digester volume was calculated with the OLR (kg VS/m^3d) specific to each digester, and the assumed microalgae feed of 1 kg VS/d. The temperature difference was the difference between ambient temperature (21°C) and the operational temperature of the digester.

(Eq.3.7) $$\Phi = \frac{-\lambda\ A\ dT}{dx}$$

The heating energy required for the pre-treatment systems was calculated using Equations 3.6 and 3.7, similarly to the energy use for the digesters, except for the operating time of the pre-treatment systems. While the digesters were assumed to be operating continuously, the pre-treatment systems typically only operate from 15 minutes to 10 hours per day, depending on the study, and were included accordingly in the calculation of the heat loss in kWh.

The energy required for pumping ($E_{pumping}$) was calculated using Equation 3.8, where Δp is the pressure loss from pump head (Pa), ρ is the fluid density (1000 kg/m^3), g is the acceleration of gravity (9.81 m/s^2), and Δh is the pump head (m). Power usage for pumping (MJ/d) was calculated from the pressure loss (Pa) and the influent flow (m^3/d). Pressure loss from dynamic head was considered negligible.

(Eq.3.8) $$\Delta p = \rho\, g\, \Delta h$$

The energy required for mixing (E_{mixing}) was calculated using Equation 3.9, with P the power input for mixing (W), N_p the power number (0.75), ρ the fluid density (1000 kg/m^3), N the impeller rotational speed (rps), and d the impeller diameter (m). The impeller rotational speed and the impeller diameter were assumed to be 50 rpm and 0.09 m, respectively, based on mixing conditions for optimal biogas production at lab scale (6 L digester) (Mary Carliell-Marquet Severn Trent et al., 2013) and were then extrapolated to large scale specific to each digester size, while keeping the mixing speed constant.

(Eq.3.9) $$P = N_P\, \rho\, N^3\, d^5$$

The unit used in the energy balance was MJ/kg VS and was calculated using OLR (kg VS/m^{3}d), digester volume (m^3), and methane yield (L/kg VS) specific to each digester. The methane yield presented was calculated as the average of the two digesters.

Heat of reaction is energy production due to conversion of organic acids into acetate and methane. Heat of reaction was calculated based on the Table 3.3.

Table 3-3. Reactions occur in conversion of organic acids into acetate and methane.

Reactions	ΔG° (kj/mol)
$Butyrate^- + 2H_2O \rightarrow 2\ Acetate^- + 2H_2 + H^+$	48.1
$Propionate^- + 2HCO_3^- \rightarrow 2\ Acetate^- + 2\ Formate^- + H^+$	45.5
$Formate^- + ¼\ H_2O + ¼\ H^+ \rightarrow ¼\ CH_4 + ¾\ HCO_3^-$	-32.6
$Acetate^- + H_2O \rightarrow CH_4 + HCO_3^-$	-31

3.12 References

Ataeian M, Liu Y, Kouris A, Hawley AK, Strous M (2022) Ecological interactions of cyanobacteria and heterotrophs enhances the robustness of cyanobacterial consortium for carbon sequestration. Front. Microbiol. 13: 1-16.

Ataeian M, Vadlamani A, Haines M, Mosier D, Dong X, Kleiner M, Strous M, Hawley AK (2021) Proteome and strain analysis of cyanobacterium *Candidatus* "Phormidium alkaliphilum" reveals traits for success in biotechnology. IScience. 24(12): 103405.

Blaird RB, Eaton AD, Rice EW (2017) Standard methods for the examination of water and wastewater, chemical oxygen demand (COD) 5220, American Public Health Association, American Water Works Association, Water Environment Federation, Washington, USA. p. 5-17–5-21.

Carliell-Marquet C, Sindall R, Bridgeman J (2013) Effect of mixing speed on lab-scale anaerobic digester stability and biogas production (short paper and poster), In: 13th World Congress on Anaerobic Digestion (IWA Specialist Conference).

Holmes RM, Aminot A, Kérouel R, Hooker BA, Peterson BJ (1999) A simple and precise method for measuring ammonium in marine and freshwater ecosystems. Can. J. Fish. Aquat. Sci., 56(10), 1801–1808.

Masuko T, Minami A, Iwasaki N, Majima T, Nishimura SI, Lee YC (2005) Carbohydrate analysis by a phenol-sulfuric acid method in microplate format. Anal. Biochem. 339(1): 69–72.

Nolla-Ardevol V, Strous M, Tegetmeyer H (2015) Anaerobic digestion of the microalga Spirulina at extreme alkaline conditions: biogas production, metagenome, and metatranscriptome. Front. Microbiol., 6, 597.

Sharp CE, Urschel S, Dong X, Brady AL, Slater GF, Strous M. (2017) Robust, high-productivity phototrophic carbon capture at high pH and alkalinity using natural microbial communities. Biotechnol. Biofuels 10(1): 1–13.

Slocombe SP, Ross M, Thomas N, McNeill S, Stanley MS (2013) A rapid and general method for measurement of protein in micro-algal biomass. Bioresour. Technol. 129: 51–57.

Van Wychen S, Laurens LML (2016) Determination of total solids and ash in algal biomass: laboratory analytical procedure (LAP). United States. https://doi.org/10.2172/1118077.

Xia A, Cheng J, Song W, Su H, Ding L, Lin R, Lu H, Liu J, Zhou J, Cen K (2015) Fermentative hydrogen production using algal biomass as feedstock. Renew. Sustain. Energy Rev. 51: 209–230.

CHAPTER 4

Autofermentation of alkaline cyanobacterial biomass to enable biorefinery approach

This chapter has been submitted as **Demirkaya C**, Vadlamani A, Tervahauta T, Strous M, De la Hoz Siegler H, (2022) Autofermentation of alkaline cyanobacterial biomass to enable biorefinery approach. Biotechnology for Biofuels and Bioproducts.

Authors' contributions: Here, I designed and carried out all the experimentation, methodology, data analysis, visualization and writing the original draft. Dr. Vadlamani contributed to the methodology and experimentation of autofermentation. Dr. Tervahauta contributed to the methodology and experimentation of anaerobic digestion. Prof De la Hoz Siegler and Prof Strous supervised the project, contributed to the methodology, conceptualization, reviewed and edited the manuscript. All authors read and approved the final manuscript.

Abstract

Carbon capture using alkaliphilic cyanobacteria can be an energy-efficient and environmentally friendly process for producing bioenergy and bioproducts. However, the inefficiency of current harvesting and downstream processes hinders large-scale feasibility. The high alkalinity of the biomass also introduces extra challenges such as potential corrosion, inhibitory effects, or contamination of the final products. Thus, identifying low cost and energy efficient downstream processes is critical. In this chapter, autofermentation was investigated as an energy-efficient and low-cost biomass pre-treatment method to reduce pH to levels optimal for downstream processes. Temperature, initial biomass concentration, and oxygen presence were found to affect yield and distribution of organic acids. Autofermentation of alkaline cyanobacterial biomass was found to be a viable approach to produce hydrogen and organic acids simultaneously, while enabling the successful conversion of biomass to biogas. Between 5.8 to 60 % of the initial carbon was converted into organic acids, 8.7-25 % was obtained as soluble protein, and 16-72 % stayed in the biomass. Interestingly, we found that extensive dewatering is not needed to effectively process the alkaline cyanobacterial biomass. Using natural settling as the only harvesting and dewatering method resulted in a slurry with relatively low biomass concentration. Nevertheless, autofermentation of this slurry led to the maximum total organic acid yield (60 % C mol/ C mol biomass) and hydrogen yield (326.1 μmol/g AFDM).

4.1 Introduction

Cyanobacteria are promising biomass feedstocks to produce bioenergy and bioproducts, as they are fast growing organisms with doubling times as low as 1.5 hours (Wendt et al., 2022). A fast-growing cyanobacterial culture, however, can quickly deplete the dissolved inorganic carbon in the medium, leading to growth limitation. Carbon limitation can be addressed by operating at high pH and alkalinity, as under these conditions the CO_2 mass transfer rate between air and the liquid medium is significantly enhanced, while the buffering capacity of the culture medium increases (Cannon-Rubio et al., 2016; Vadlamani et al., 2019). Thus, more inorganic carbon is available to support photosynthesis and biomass growth, resulting in improved productivity (Vadlamani et al., 2017; Kuo et al., 2018). Fresh water has an alkalinity between 100 and 5000 µEq L^{-1} and a pH ranging from 6 to 9. Seawater has an alkalinity of about 2300 µEq L^{-1} and a pH of 8.2 (Mattson et al., 2014). A wide range of alkalinity has been used in prior studies to enhance biomass productivity (Wensel et al., 2014; Kuo et al., 2018; Liu et al., 2021) with alkalinity levels above 10000 µEq L^{-1} (= 0.01 Eq L^{-1}) considered as alkaline conditions. Protection against common competing organisms and predators have additionally been reported at alkalinities higher than 0.1 Eq L^{-1} (Vadlamani et al., 2019). In this report, we are concerned with the processing of cyanobacterial biomass produced at this higher end of the alkalinity gradient.

Alkalinity has a complex effect on the performance of downstream processes. For instance, high alkalinity can improve biomass degradability and biopolymers solubility, facilitating certain biomass conversion and product recovery operations (Cai et al., 2015; Kassim and Bhattacharya, 2016; Solé-Bundó et al., 2017). To the contrary, the alkaline biomass slurry may be corrosive or may contain compounds that could have inhibitory effects or be considered as contaminants in the final products (Passos et al. 2014). As downstream processes have a significant effect on the

economic viability and environmental footprint of the produced biofuels or bioproducts, innovations in downstream processing must aim at minimizing energy inputs and avoiding the addition of chemicals. The harvested biomass can be processed into several bioenergy products, such as biodiesel through the transesterification of neutral lipids, bioethanol through fermentation, biogas through anaerobic digestion, or bio-crude through thermochemical conversion (Enamala et al., 2018). Among these potential downstream processes, anaerobic digestion (AD) is attractive due to its low energy requirements and its ability to handle wet biomass, which eliminates the need for drying (Saratale et al., 2018). AD can also play a more general role within a biorefinery platform, as it can be used as a final step to convert any residual biomass into bioenergy (i.e., methane) at low cost and with high energy efficiency.

AD is a complex process involving four different stages: hydrolysis and acidogenesis, followed by acetogenesis and methanogenesis. The microorganisms more active in each stage differ in terms of their nutrient and pH requirements, physiology, growth, and tolerance to environmental stresses (Manyi-Loh et al., 2013). Although high pH and high alkalinity are beneficial for biomass cultivation, they are undesirable in all stages of AD due to their inhibitory effect (Jiang et al., 2019). Jiunn-Jyi et al. (1997) investigated the effect of pH on the AD of activated sludge by changing the initial pH from 5.0 to 10.0. A significant decrease in methane production was reported when pH was above 8.3. Nolla-Ardevol et al. (2015) proposed using microbial communities obtained from haloalkaline sediments to enable AD under high pH and high alkalinity. They reported that digestion of *Spirulina* under highly alkaline conditions (pH 10, 2.0 M Na^+) into methane-rich (96 %) biogas was possible. However, only 7 % of the initial biomass was converted into methane due to the inhibitory effect of NH_3-N and the accumulation of volatile fatty acids.

To enable the successful conversion of alkaline biomass slurries, a pretreatment method can be implemented to decrease the pH. However, direct neutralization is undesirable as it increases chemical usage and processing costs (Daelman et al., 2016). Dark anaerobic fermentation may be a suitable pretreatment, as it can result in the formation of acidic products and a reduction of pH. Towards this aim, it is relevant the work of Dahiya et al. (2015) who reported acetic acid, butyric acid, and propionic acid production from food waste by dark fermentation under alkaline conditions (pH 10-11) and a subsequent reduction of pH.

Ananyev et al. (2012) and Hasunuma et al. (2015) have shown that *Spirulina platensis* and *Synechocystis* sp. can convert their own carbohydrates to a wide range of end products (*e.g.*, ethanol, formate, acetate, H_2, and CO_2). If this autofermentative metabolic capability is widely distributed among the cyanobacteria, then it may be possible to use it as a pretreatment step to reduce the pH of the cyanobacterial biomass slurry, reducing or eliminating the use of additional energy, catalysts, external organisms (bacteria or yeast), and nutrients (Hasunuma et al., 2015; Hasunuma et al., 2016; Halim et al., 2019). Autofermentation can also become a key processing step within a biorefinery concept, allowing the production and recovery of chemical precursors and other valuable products.

Autofermentation can also become a key processing step within a biorefinery concept, allowing the production and recovery of chemical precursors and other valuable products.

In this report, we explore the feasibility of introducing a dark anaerobic fermentation step to enable the acidification of the highly alkaline biomass slurry harvested from cyanobacterial cultures grown at high alkalinity, while simultaneously performing the first two steps of anaerobic digestion, hydrolysis and acidogenesis. Furthermore, we combine the autofermentation with different harvesting techniques to reduce harvesting cost and evaluate the effect of several process

parameters, such as initial biomass concentration and temperature, on the formation of acidic products, lowering of pH, and hydrogen formation during the autofermentation step. We also assess biogas production after autofermentation for the first time.

4.2 Feasibility of anaerobic digestion for processing alkaline cyanobacterial biomass

Cyanobacterial biomass cultivated at high pH and alkalinity was harvested via centrifugation. The harvested biomass paste, with a pH of 10.48 ± 0.02, was left to auto-ferment statically in the dark for 10 days at 21 °C. Next, activated sludge was added to the autofermented paste and the mixture was incubated anoxically for 40 days to stimulate anaerobic digestion and biogas production.

Harvested biomass paste was used directly as a control in the anaerobic digestion experiments. During digestion, the pressure in the gas head space was monitored to determine biogas production (Fig 4-1). No biogas production was observed in the incubations of untreated alkaline biomass. On the other hand, the dark fermentation pretreatment step decreased the biomass pH from 10.48 to 6.90, due to the accumulation of organic acids. In this case, the pressure in the head space during AD incubations increased to 3.84 ± 0.35 bar, and the headspace consisted of 61.84 ± 0.25 % methane (314.15 ml/g AFDM).

Ammonium concentration increased significantly during AD of both autofermented and untreated biomass. It must be noted that the freshly harvested cyanobacterial biomass was determined to have a protein content of 60.9 %. This high protein content reduces the C:N ratio of the biomass and leads to high ammonia production from amino acids degradation (Milledge et al., 2019). During anaerobic digestion, the ammonium concentration increased steadily from 17 mM to 90 mM and 126 mM in the untreated and autofermented biomass, respectively. Even though the ammonium concentration during digestion of autofermented biomass was higher than during

digestion of untreated biomass, it did not appear to cause inhibition. At high pH, a large part of the ammonium is present as the free base, ammonia (NH_3). Ammonia easily permeates cell membranes and can increase intracellular pH, causing inhibition (Chen et al., 2018).

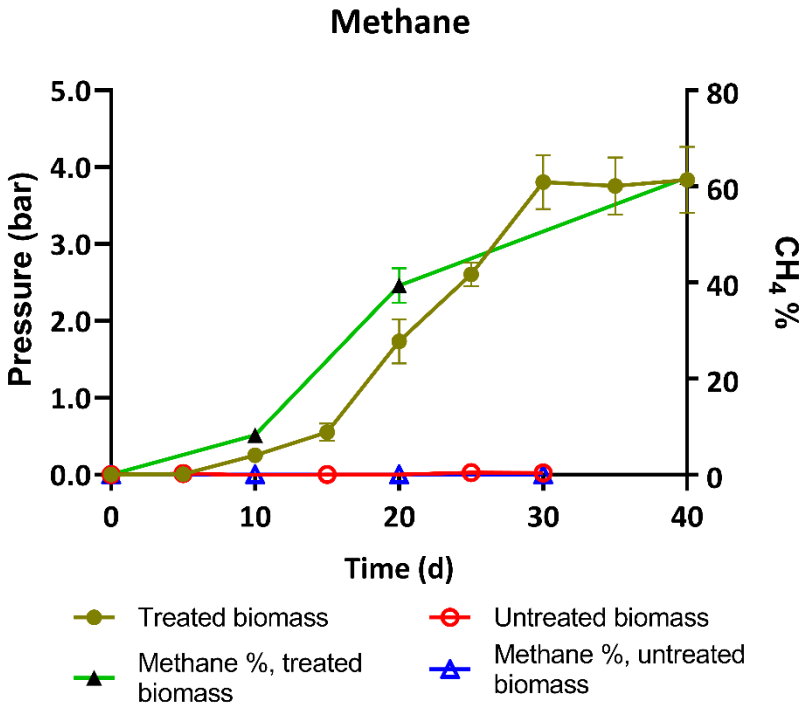

Figure 4.1. Change in pressure and accumulated methane concentration obtained from inoculation of untreated and treated highly alkaline and high pH microalgal biomass with activated sewage sludge inoculum during 30 and 40 days of incubation respectively.

4.3 Optimization of dark fermentation conditions

Based on the previous results, dark autofermentation shows to be a feasible treatment for alkaline cyanobacterial biomass, enabling its successful anaerobic digestion by reducing the pH. During autofermentation, several organic acids accumulated while proteins and other cellular materials were released into the growth medium. To further explore autofermentation as a potential element

of a biorefinery concept, experiments were performed to determine the effect of fermentation conditions on product distribution.

4.3.1 Effect of temperature

Static fermentation of the biomass paste harvested by centrifugation was conducted at different temperatures (21, 30, and 37 °C). Six organic acids: acetate, propionate, butyrate, formate, succinate, and lactate, were detected as fermentation products at 21 °C. Butyrate and formate were not detected at 30 and 37 °C. The organic acid yield and distribution obtained at different temperatures are shown in Figs. 4-2 and 4-3.

The yield of each organic acid increased significantly as the operating temperature increased from 21 °C to 30 °C (Fig. 4-2). For all temperatures, the highest total organic acid yield was obtained between days 6 and 8. The highest total organic acid yield was obtained at 30 °C on day 8. The yields at 21 °C were significantly different from those at higher temperatures for acetate ($P = 0.009$), butyrate ($P = 0.02$), and lactate ($P = 0.0005$). The highest succinate and lactate yields were obtained at 30 °C on day 8; however, the relative abundance of these two acids at 30 °C was lower than at 21 °C. Thus, organic acid recovery may be simpler at the lower fermentation temperature.

The soluble protein increased rapidly at 30 °C and 37 °C, reaching its maximum at day 2 and decreasing afterwards (Fig 4-4). This indicates that higher temperature resulted in an increase in the rate of both protein release and protein degradation. At 21 °C, there was a steady increase in the total soluble protein, reaching the highest concentration at day 6. Thus, low fermentation temperature may be beneficial as it will allow to maximize the recovery of protein.

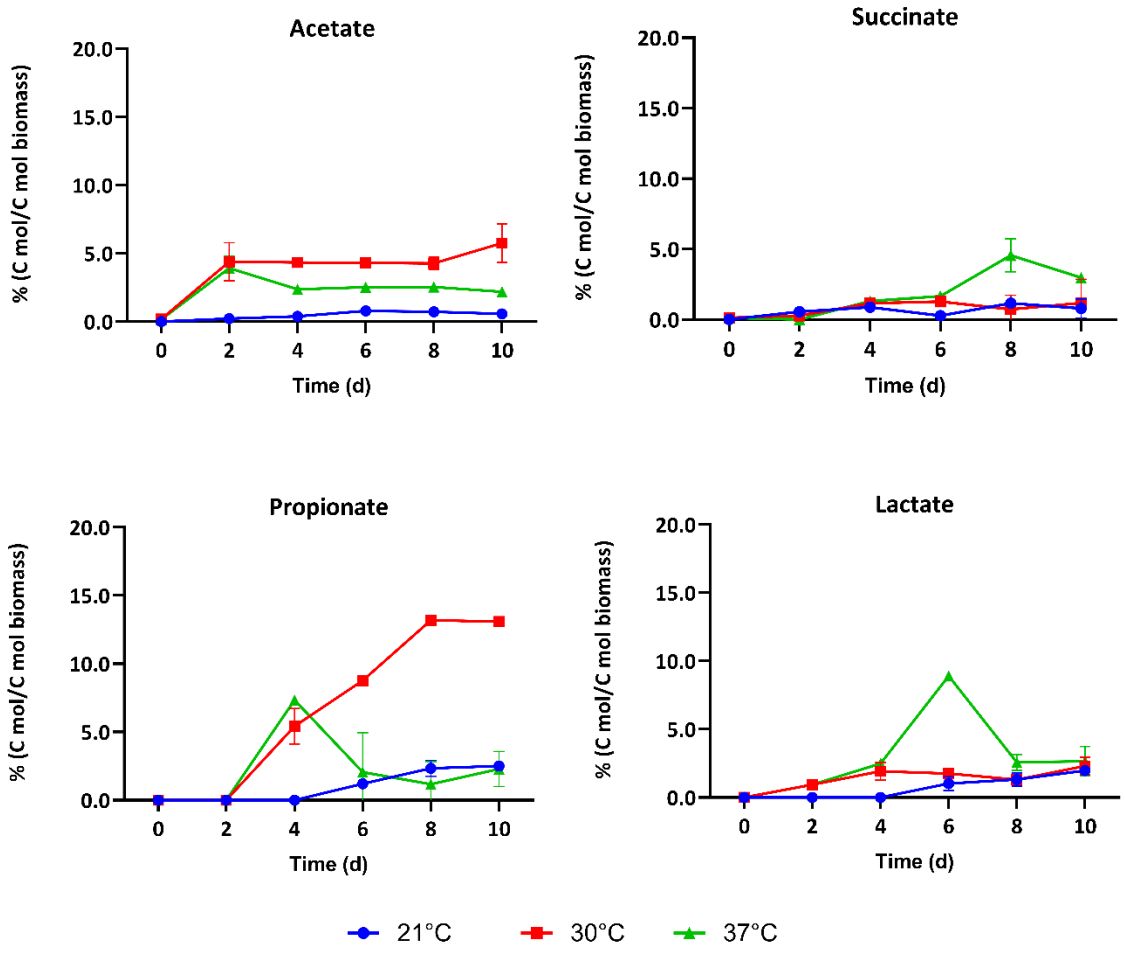

Figure 4.2. The effect of fermentation temperature on organic acid yield during anoxic dark fermentation. Initial pH in all cases was 10.36 ± 0.05. Values reported corresponding to the average of triplicate measurements +/- 95% confidence interval.

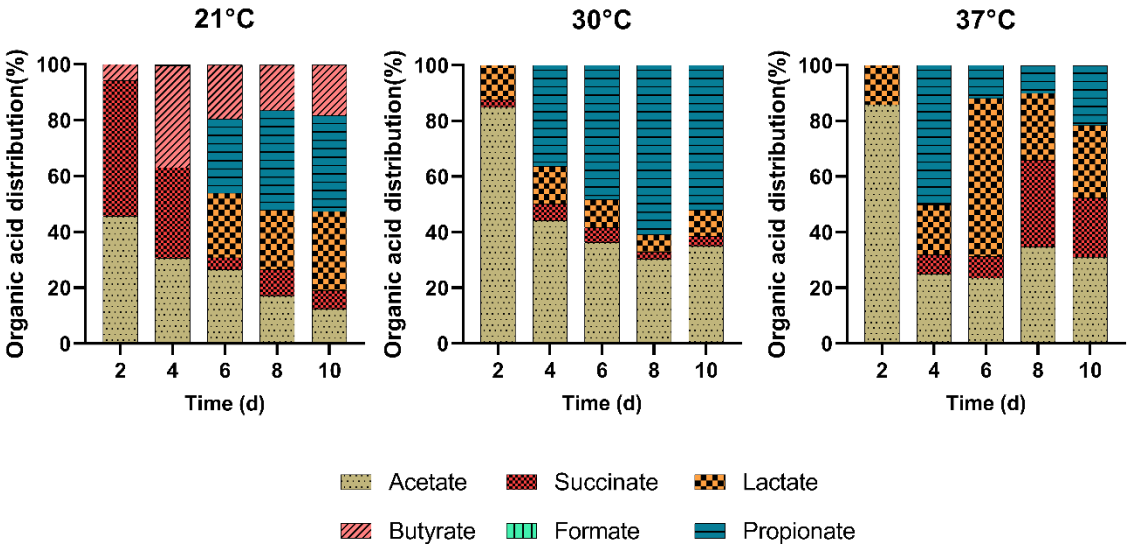

Figure 4.3. Organic acid product distribution at different fermentation temperatures. Initial pH in all cases was 10.36 ± 0.05.

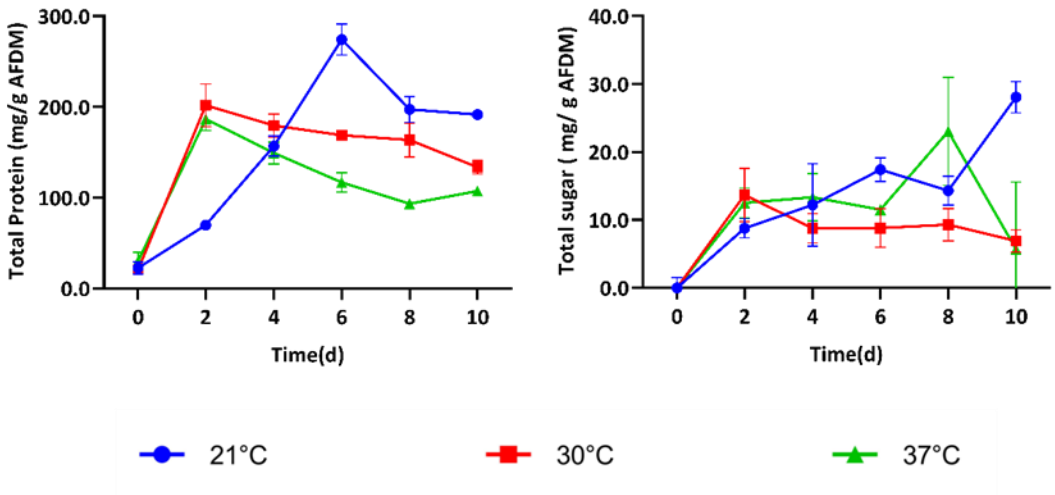

Figure 4.4. The effect of fermentation temperature on soluble protein and sugar (mg per g-initial biomass) during 10 days of anoxic dark fermentation. Initial pH in all cases was 10.36 ± 0.05.

The fractional recovery of carbon in fermentation products provides a measure of the efficiency of the bioconversion. A higher carbon recovery indicates that most of the carbon initially present in

the biomass has been transformed into desired products. Carbon recovery at different temperatures after 8 days of fermentation is shown in Table 4-1.

Table 4-1. Carbon balance for the autofermentation of highly alkaline cyanobacterial biomass at different temperatures.

	Carbon recovery (mg C/g initial AFDM)[a]		
	21°C	30°C	37°C
Initial total carbon in biomass	500.95	507.81	508.27
Final total carbon in biomass	231.01	258.38	251.61
Total carbon in organic acids	35.62	98.99	55.22
Acetate carbon	3.67	21.74	12.95
Succinate carbon	4.54	3.64	23.17
Formate carbon	1.22	n.d.	n.d.
Butyrate carbon	7.83	n.d.	n.d.
Propionate carbon	11.76	66.95	5.99
Lactate carbon	6.60	6.66	13.12
Total sugar carbon	5.73	3.73	9.22
Total protein carbon	98.71	81.79	46.63

[a] Carbon distribution results are reported after 8 days under dark anaerobic conditions.

At 30 °C, the carbon conversion into soluble organic acids was maximized, reaching 19 %. At this same temperature, 87% of the carbon was recovered in the form of organic molecules. The remainder evolved as CO_2 and other non-measured products, including free amino acids. The lowest total carbon recovery was at 37 °C, where only 71.3 % of the carbon was accounted for; while, at 21 °C most of the solubilized carbon was in the form of solubilized proteins (19.7 %) and only about 7.1 % of the carbon was present as organic acids. Depending on the relative value of the different fermentation products, fermentation temperature can be adjusted to maximize the recovery of the most valuable ones. Moreover, as organic acid production reaches its peak at day six, fermentation could be stopped at that time if the goal is to maximize organic acid recovery.

4.3.2 Effect of initial solids concentration

In Section 4.2, we established that static fermentation is a suitable pretreatment to enable the anaerobic digestion of the alkaline cyanobacterial biomass paste. Although this pretreatment offers several advantages compared to suspended cultures, including a reduction in water utilization and easiness for recovering high value by-products, it requires an energy intensive and expensive step for harvesting and dewatering, such as centrifugation or membrane filtration. These steps increase the solid fraction in the harvested biomass up to 27 % at the expense of high energy use of up to 8 kWh m^{-3} (Weschler et al., 2014; Fasaei et al., 2018). The higher energy requirement of centrifugation accounts for up to 40 % of the total operating costs in some algal production systems (Ummalyma et al., 2017; Fasaei et al., 2018). Consequently, it is desirable to replace centrifugation with a low energy harvesting technique.

Several low energy techniques such as flocculation, flotation, filtration, and sedimentation, or a combination of any of these, are used to harvest and concentrate microalgal biomass (Singh and Patidar, 2018). Biomass concentration can be increased from dilute solid concentrations (0.1-0.26%) to 3-10% solid concentration by settling, flocculation, or filtration, which have energy consumption in the range of 0.1-0.4 kWh m^{-3} (Ummalyma et al., 2017).

Flocculation and sedimentation can be used as a primary method to decrease the cost of harvesting (Weschler et al., 2014). Some microbes can form large settleable flocs as a result of co-precipitation with ions at high pH, and cell-cell interactions capable of self-flocculation, forming large settleable colonies, and enabling simple and effective separation by gravity sedimentation.

Water recovery and solid concentration after natural settling and centrifugation are reported in Fig 4-5. The biomass concentration (as ash-free dry mass, AFDM) in the culture medium at harvesting was 0.75 ± 0.09 g/L. Approximately 97.6 % of the water was recovered after settling, reaching a

final biomass concentration of 30.96 ± 2.52 g/L. Biomass concentration could be further increased to 50 g/L by applying low-speed centrifugation at 48 × g for 15 min. To reach a concentrated paste (219 g/L), biomass was centrifuged at 3,894 × g for 15 min.

Next, we evaluated the impact of these harvesting and dewatering methods on the outcomes of the autofermentation. Different harvesting and dewatering methods resulted in changes in the concentration of the harvested biomass, also modifying the total carbonate concentration and buffering capacity of the autofermented slurry. For a fixed biomass load (AFDM basis), the total fermentation volume differs for each harvesting method. Although the carbonate concentration is the same across all harvesting methods, the amount of medium relative to solids differs. Thus, harvesting methods that result in a more concentrated slurry or paste have lower ratio of medium relative to solids, and this results in a lower buffering capacity. In Table 4-2, the maximum total organic acid yield and final pH after 8 days of fermentation at 21 °C is reported for biomass harvested via primary settling ($t_{settling}$ = 1 h), secondary settling ($t_{settling}$ = 2 h), low speed centrifugation (RCF = 48 × g), and high-speed centrifugation (RCF = 3894 × g).

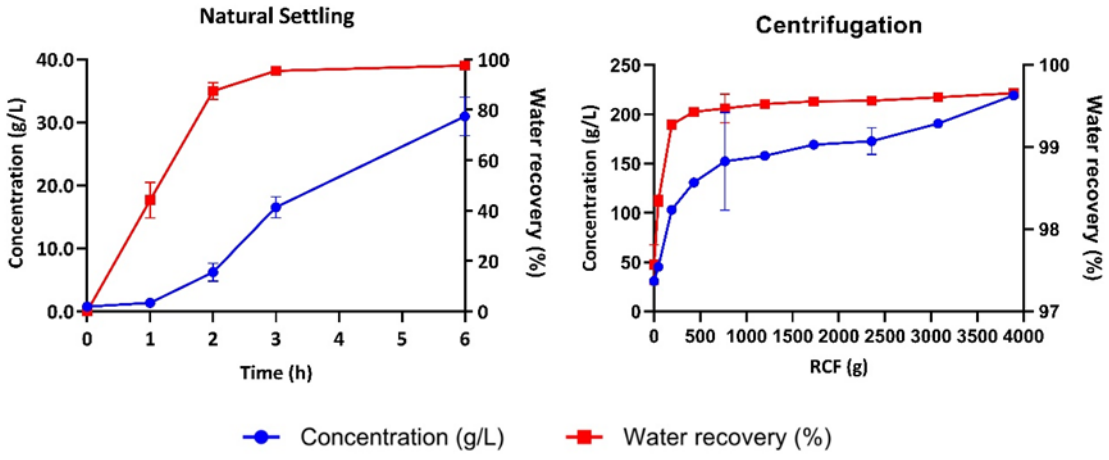

Figure 4.5. Change in biomass concentration by natural settling for 6 hours (a) and centrifugation at different speed for 15 min (b) and water recovery efficiency.

Table 4-2. Effect of harvesting method on the performance of autofermentation of alkaline cyanobacterial biomass.

	High Speed centrifugation	**Low speed centrifugation**	**Secondary Settling**	**Primary settling**
Biomass concentration (g AFDM/L)	219.36 ± 3.94	47.05 ± 3.95	10.21 ± 0.36	3.04 ± 0.16
Volume (mL)	2.00	8.76	43.8	146
Initial pH	10.48 ± 0.02	10.48 ± 0.02	10.48 ± 0.02	10.48 ± 0.02
Final pH	6.87 ± 0.06	8.48 ± 0.06	9.80 ± 0.01	10.25 ± 0.01
Maximum organic acid yield (mmol/g AFDM)	0.91 ± 0.15	1.51 ± 0.22	2.43 ± 0.19	10.28 ± 0.80
Organic acid peak day	10	10	10	8

[a] Results reported correspond to fermentation at 21°C, under anoxic conditions.

Even though the initial pH was the same for all cases, the centrifuged paste had less buffering capacity due to lower total amount of carbonates and resulted in a rapid decrease in pH, reaching neutral values (7.19 ± 0.07) within 2 days. At the lowest biomass concentration obtained by natural settling, the decrease in pH was much smaller. The small pH change was due to the higher total carbonates and corresponding higher buffering capacity. The final pH at the lowest biomass concentration was 10.31 ± 0.01, which may still be inhibitory for methanogenesis as suggested by the results shown in Section 4.2.

The effect of initial biomass concentration on organic acid yields and organic acid composition profile is shown in Figs. 4-6 and 4-7, respectively.

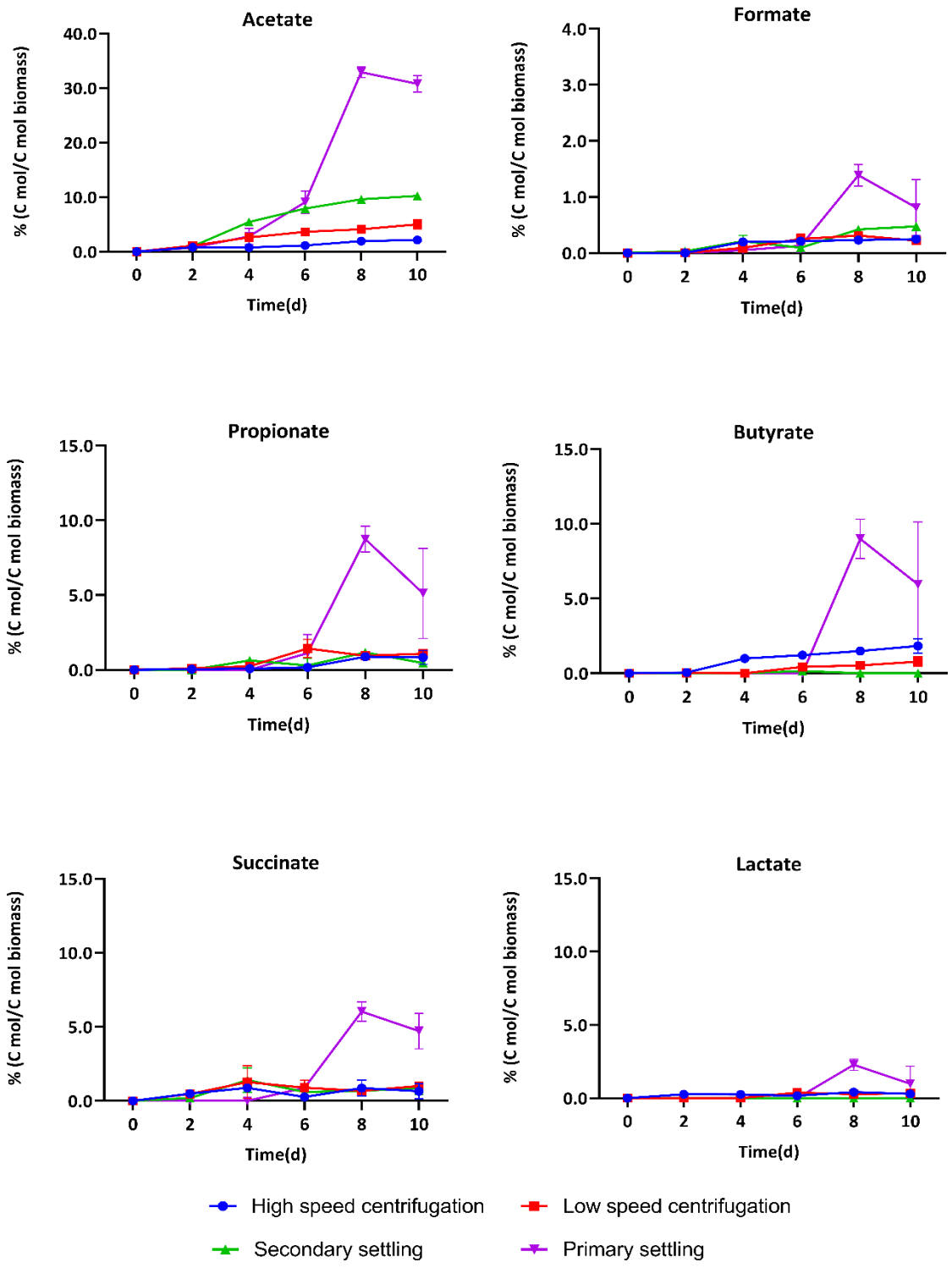

Figure 4.6. The effect of harvesting and dewatering method on organic acid yields (mmol-organic acids produced per g-initial biomass) during 10 days of anoxic dark fermentation. Initial pH in all cases was 10.48 ± 0.02.

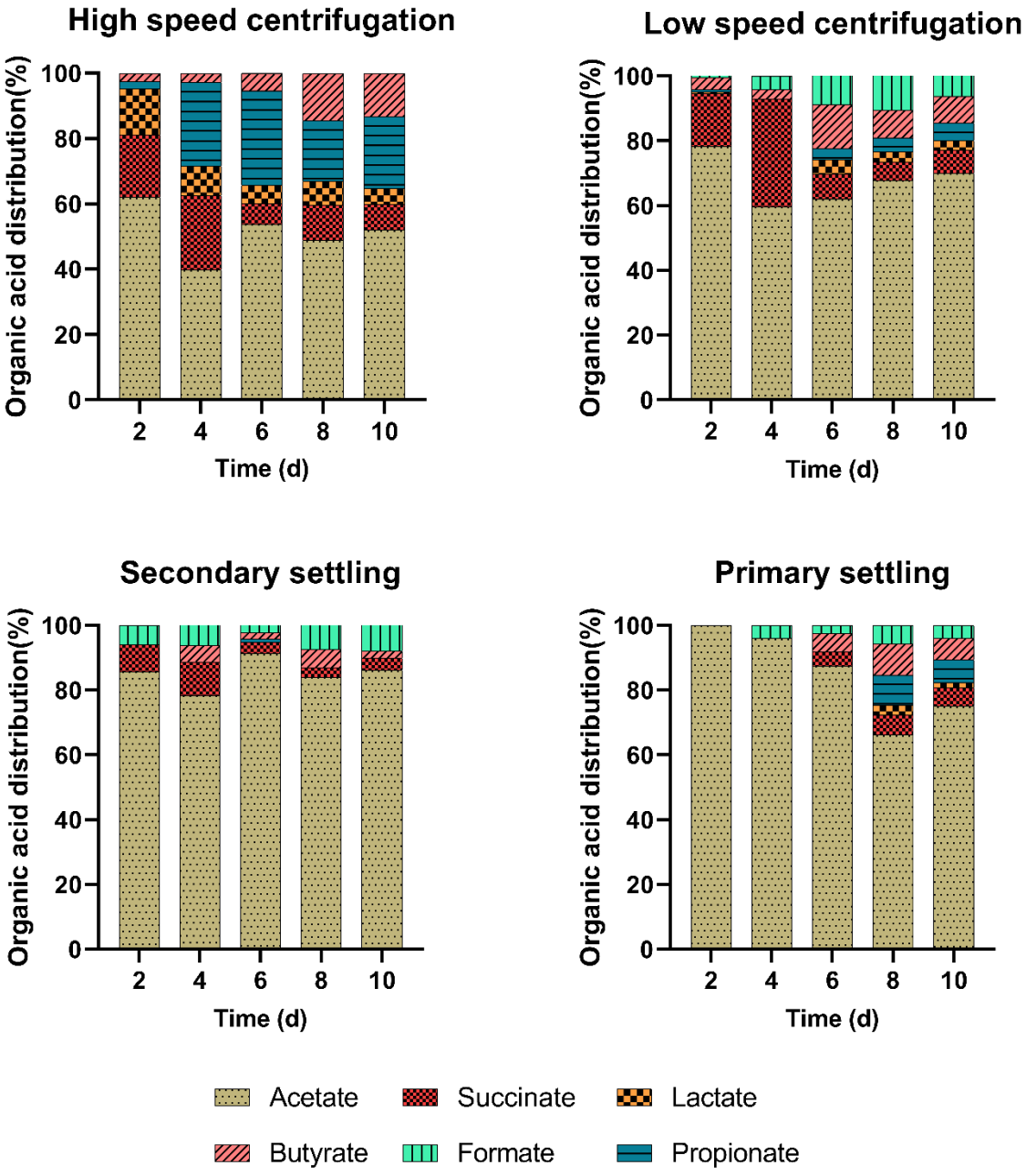

Figure 4.7. Organic acid product distribution at different concentration of highly alkaline and high pH media during 10 days of anoxic dark fermentation. Initial pH in all cases was 10.48 ± 0.02.

At the lowest solids concentration (3.04 g/L), obtained with primary settling, the organic acid production was more than 14-fold higher than at other biomass concentrations. Acetate was the

main product, with significant amounts of butyrate, propionate, and succinate co-produced. At the highest biomass concentration, there was a more balanced profile of produced organic acids. Acetate was still the most abundant, accounting for an average of 53 % of the total acids.

During dark fermentation, the complex storage molecules of the cells are first hydrolyzed to monomers. The production and accumulation of organic acid is dependent on monomer availability. High pH is beneficial for the solubilization of complex molecules, enabling their conversion and increasing organic acid yields (Liu et al., 2012). In the case of biomass harvested by primary settling the yield of soluble proteins and sugar was higher than for other harvesting methods, indicating that high pH promoted faster biomass hydrolysis (Fig 4-8).

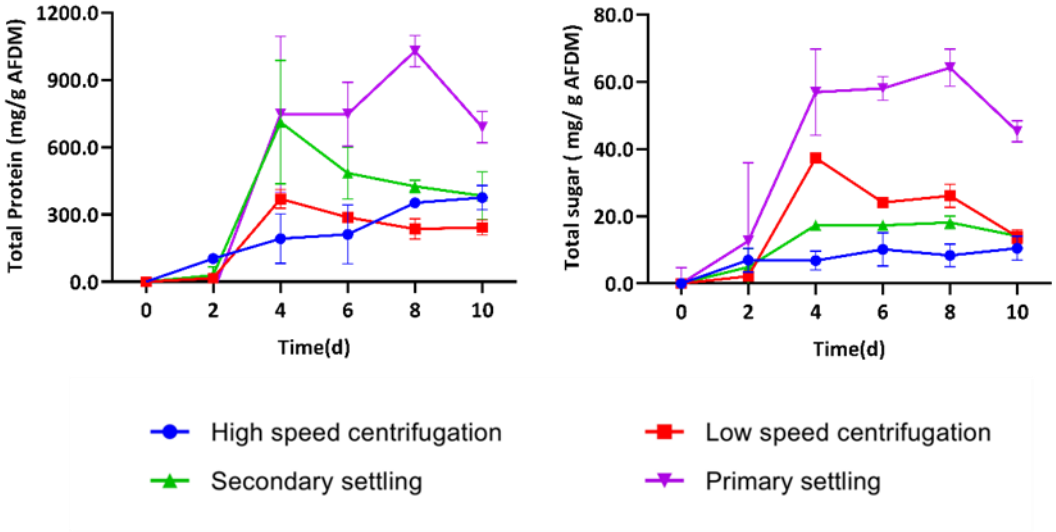

Figure 4.8. The effect of harvesting and dewatering method on soluble protein and sugar (mg per g-initial biomass) during 10 days of anoxic dark fermentation. Initial pH in all cases was 10.48 ± 0.02.

The highest acetate yield was obtained at the lowest initial biomass concentration (Figure 4-6). Acetate production has been previously shown to be higher under alkaline conditions than at

neutral or low pH (Wu et al., 2009). As acetate is an important precursor for methanogenesis that can contribute 60-70% of methane generation, an increased conversion of biomass into acetate may be beneficial for increasing methane production.

Propionate and butyrate were the second and the third most abundant organic acids at higher biomass concentrations. Propionate and butyrate serve as intermediate fermentation products and, with additional incubation time, may be converted into acetate for further methane production during anaerobic digestion.

The highest carbon recovery was observed at the lowest initial biomass concentration, with 60.4 % of the initial carbon being recovered as organic acids (Table 4-3) and about 26.5 % of the carbon present as solubilized proteins. Thus, lower initial biomass concentration favored the conversion of alkaline cyanobacterial biomass slurries during dark fermentation, resulting in higher organic acid yields obtained with lower dewatering energy needs.

Table 4-3. Carbon balance for the autofermentation of highly alkaline cyanobacterial biomass at different initial biomass concentrations. Carbon distribution results are reported after 8 days under dark anaerobic conditions.

	Recovered carbon (mg/g initial AFDM)			
	High Speed Centrifugation	Low Speed Centrifugation	Secondary Settling	Primary Settling
Initial total organic carbon in biomass	524.55	524.55	495.06	495.06
Total organic carbon in biomass at day 8	310.10	395.60	142.94	80.43
Total organic acid carbon	30.61	35.98	58.83	298.81
Acetate carbon	10.24	21.54	47.60	162.95
Succinate carbon	4.53	3.59	3.38	29.85
Formate carbon	1.22	1.65	2.08	6.86
Butyrate carbon	7.82	2.77	n.d	44.53
Propionate carbon	4.63	4.95	5.77	43.29
Lactate carbon	2.18	1.48	n.d	11.33
Total sugar carbon	4.17	13.05	9.08	32.08
Total protein carbon	183.09	122.79	260.91	221.57

4.3.3 Effect of the presence of oxygen

The cyanobacteria used in this study have significant metabolic flexibility allowing them to adapt to fluctuating redox conditions (Ataeian et al., 2021). However, little is known regarding how the cell metabolism reacts to changing oxygen levels and whether oxygen affects organic acids production and product distribution. To elucidate this effect, we studied the organic acid yield and distribution during dark fermentation of cyanobacterial biomass under conditions of anoxia (0 % O_2 in gas headspace) and hypoxia (2 % O_2 in gas headspace) as shown in Figs. 4-9 and 4-10.

The presence of oxygen significantly increased acetate and formate yields, while yields for butyrate, propionate, and lactate were higher under anoxic conditions. On the other hand, formate

was not detected under anoxic incubations. There was a more balanced distribution of organic acids under strictly anoxic conditions.

Similar organic acid carbon yield was obtained under hypoxic and anoxic conditions with 33 and 30.6 mg carbon per gram biomass respectively (Table 4-4). However, complete anoxia resulted in a longer lag-phase. The organic acid yield reached its peak at 4-6 days under hypoxic conditions, whereas this peak was delayed to day 8 under anoxic conditions. The longer lag phase observed under strictly anoxic conditions is likely the result of a longer adaptation phase needed when transitioning from oxic illuminated conditions in the photobioreactor to strict anoxia in the fermenter.

Table 4-4. Carbon balance for the autofermentation of highly alkaline cyanobacterial biomass under hypoxic and anoxic conditions at 21°C. Carbon distribution results under hypoxic and anoxic are reported after 4 and 8 days respectively.

	Recovered carbon (mg/g initial AFDM)	
Component	Hypoxic	Anoxic
Initial total organic carbon in biomass	539.72	524.55
Total organic carbon in biomass	388.70	310.10
Total organic acid carbon	33.12	30.61
Acetate carbon	25.78	10.24
Succinate carbon	4.87	4.53
Formate carbon	1.58	1.22
Butyrate carbon	n.d.	7.82
Propionate carbon	0.88	4.63
Lactate carbon	n.d.	2.18
Total sugar carbon	1.72	13.04
Total protein carbon	46.90	183.09

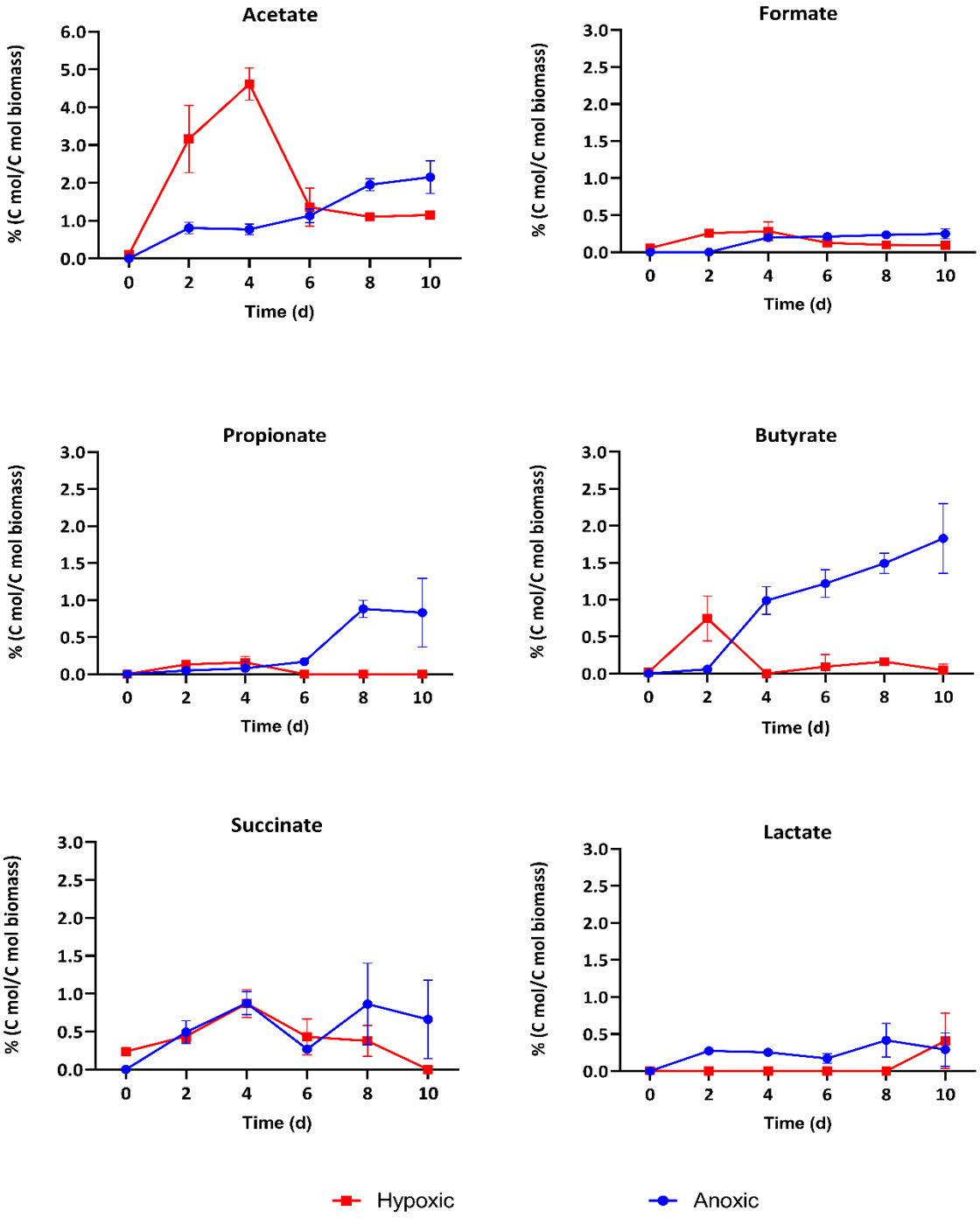

Figure 4.9. Organic acid yields (mmol-organic acids produced per g-initial biomass) during 10 days of anoxic and hypoxic dark fermentation. Initial pH in all cases was 10.35 ± 0.01.

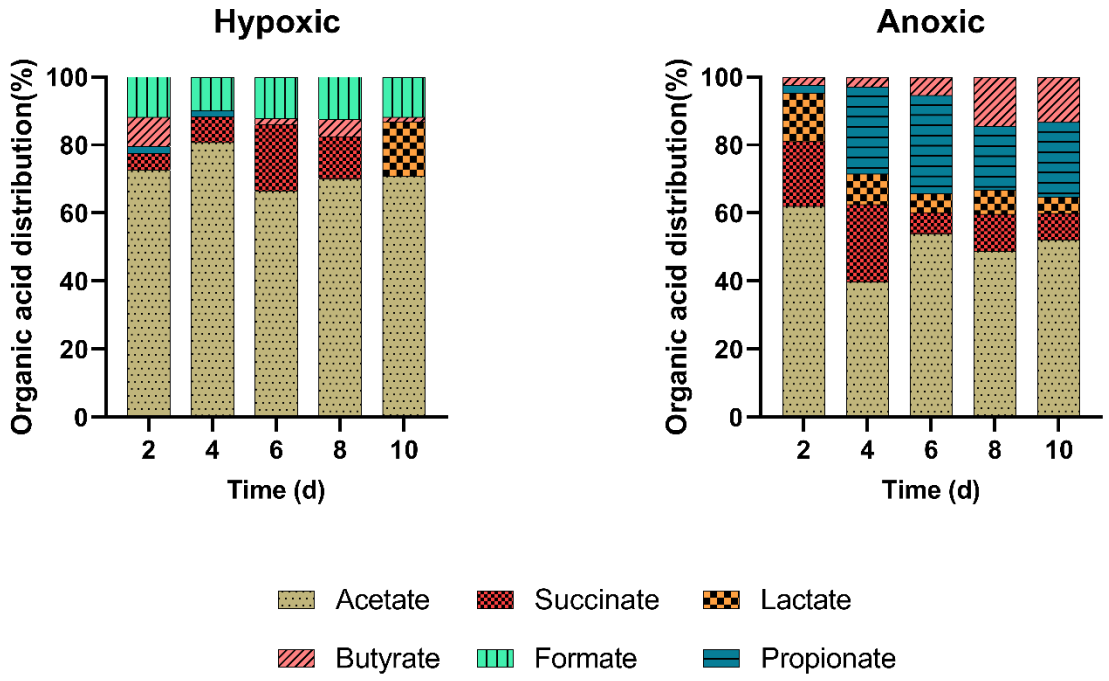

Figure 4.10. Organic acid percentage and product distribution under hypoxic and anoxic highly alkaline and high pH media during 10 days of dark fermentation. Initial pH in all cases was 10.35 ± 0.01.

4.4 CO_2 and hydrogen production

Carbon dioxide (CO_2) is a common by-product during fermentation. The high alkalinity of the fermentation medium, however, results in low or no release of CO_2 as most of it will remain dissolved as bicarbonate or carbonate. Of the initial carbon present in the biomass, only 2.2 % and 0.12 % was released as CO_2 during autofermentation at 21 °C of the biomass obtained by high-speed centrifugation and low speed centrifugation, respectively. No CO_2 release was observed at the lower concentrations obtained by natural settling. Increasing fermentation temperature translated into an increased CO_2 production at 30 °C and 37 °C of the biomass obtained by high-speed centrifugation with 16.4 % and 21.5 % of the initial carbon being released as CO_2,

respectively. Changes in fermentation oxygen content did not measurably affect the release of CO_2.

Interestingly, analysis of the produced gases by GC revealed the production of hydrogen. NADH is produced during dark fermentation as part of the cell metabolic activities. NADH needs to be recycled as NAD^+ to continue supporting ATP production via glycolysis. Hydrogenases and nitrogenases catalyze the reversible reduction of protons to H_2 coupled to NAD^+ regeneration in some cyanobacteria genera (Ananyev at al. 2012). The cyanobacterium used in this study have the genes encoding for uptake hydrogenase (*hypABCD*), bidirectional hydrogenase (*hoxEUS, hndC*), and nitrogenase (NifK, NifD, NifH,) (Ataeian et al., 2021). Thus, it is possible that the production of hydrogen during autofermentation is part of the metabolic response of *Candidatus* "Phormidium alkaliphilum".

The maximum stoichiometric hydrogen yield of biomass was calculated as 119.5 mL of H_2 per gram of biomass, based on the total sugar and protein concentration determined for the biomass and assuming that no other products, other than CO_2 and H_2, were produced. Maximum hydrogen production occurred at 21 °C and at the lowest biomass concentration (3.04 g/L). Under these conditions, a H_2 yield of 326.14 µmol/g AFDM was found, corresponding to 6.1 % of the maximum stoichiometric yield.

The increased hydrogen production at the lowest initial biomass concentration may be caused by the higher overall pH associated with autofermentation at the lowest biomass concentration. As previously indicated, harvesting via primary settling results in a slurry containing a lower ratio of biomass to total carbonates, which translates to a higher buffering capacity and a lower drop in pH during fermentation (see Table 4-2). Ananyev at al. (2012) showed that, in the cyanobacterium *Arthrospira maxima*, hydrogen production is a process operating close to thermodynamic

equilibrium under biologically relevant conditions. By removing the produced hydrogen from the culture medium, they were able to increase the net rate of hydrogen formation. As the solubility of hydrogen in aqueous medium decreases with increasing concentration of carbonate or bicarbonate ions (Engel et al., 1996). The higher carbonate amount present at the lowest biomass concentration may explain the increased hydrogen production. Additionally, as no CO_2 was released at the lowest biomass concentration, this resulted in the accumulation of pure H_2 in the headspace.

4.5 Autofermentation role within a biorefinery platform

Autofermentation effectively converts highly alkaline cyanobacterial biomass into organic acids and hydrogen. To make the overall process more economically feasible, it is important to valorize most of the fermentation products. Produced hydrogen can be separated from the headspace, while the fermentation broth can be separated into an organic acid rich fraction and a solid fraction. Furthermore, valorization of the organic acids to high value-added products (e.g., polyhydroxyalkanoates) is possible, while the remaining solid fraction can be processed into biogas using AD. Separation of the liquid phase, including solubilized proteins, also eliminates rapid ammonium accumulation in the anaerobic digestion.

Table 4-5 presents a summary of the organic acid yield and titers reached during the autofermentation of microalgal and cyanobacterial biomass. For ease of comparison with previous studies, organic acid yields shown in Table 1-5 are reported in g/ g DM.

Table 4-5. Organic acid yield and final product concentration obtained via autofermentation of microalgal and cyanobacterial biomass.

Microorganism	Organic acid yield (g/g DM)	Organic acid concentration (g/L)	Fermentation Conditions			Harvesting	Initial biomass concentration (g DM/L)	Incubation time (days)	Reference
			Temperature	pH	Added Chemicals				
Arthrospira maxima	0.55	0.825	30°C	9.80	210 mM Na^+	Filtration	1.5	2	(Carrieri et al., 2010)
Arthrospira platensis	0.011	0.22	35°C	-	NaH_2PO_4/ Na_2HPO_4 buffer solution	Filtration	50	5	(Cheng et al., 2012)
Chlorella sorokiniana	0.30	7.5	29-31°C	10.40	Carbonate/ bicarbonate buffer	Centrifugation	25	2	(Pendyala et al., 2020)
Nannochloropsis sp.	0.061	-	38°C	-	-	Centrifugation	11-29 wt%	1	(Halim et al., 2019)
Candidatus "P. alkaliphilum"[a]	0.619	2.16	21°C	10.48	-	Natural settling	3.04	8	This study
Candidatus "P. alkaliphilum"[b]	0.064	15.37	21°C	10.48	-	Centrifugation	219.36	8	This study

[a] Autofermentation at the lowest initial biomass concentration (3.04 g AFDM/L)
[b] Autofermentation at the highest initial biomass concentration (219.36 g AFDM/L)

In general, the fermentation of microalgal and cyanobacterial biomass have been shown to result in low titers, especially when compared to the fermentation of carbohydrate-rich biomasses (Tepari et al., (2019). Microalgal and cyanobacterial biomass typically have a low carbohydrate to protein content and given that carbohydrates are the primary substrates for fermentation (Moraes et al., 2019), the relatively low total organic acid titers are an expected result.

Compared to previous studies (see Table 1-5), harvesting by natural settling resulted in the highest organic acid yield at 0.616 g/g DM. This present study also corresponds to the lowest fermentation temperature, demonstrating a successful pathway for converting alkaline biomass to organic acid yield with minimal energy inputs.

The highest total organic acid concentration of 15.37 g/L, on the other hand, was obtained under solid state fermentation conditions, albeit at lower temperatures than previous studies. The energy needs and cost of recovery and purification decrease as the product concentration increases. Thus, proper bioprocess design will require to strike a balance between the initial biomass concentration (i.e., how much energy is spent in dewatering) and the final organic acid concentration (i.e., how much energy is spent in product recovery).

4.6 Conclusions

Autofermentation is a simple but highly effective pretreatment to enable the conversion of alkaline cyanobacterial biomass into methane via anaerobic digestion without the addition of energy or chemicals. In addition, it results in the production of high value added bioproducts and hydrogen. In this study, we reported autofermentation of natural mixed cyanobacterial biomass. Here, we obtained the highest organic acid yield at the lowest biomass concentration, demonstrating that extensive, energy intensive, dewatering is not needed. Although the presence of oxygen affects the organic acid yield and distribution, strict anoxia is not needed to promote the autofermentation of

alkaline cyanobacterial biomass. The successful conversion of cyanobacterial biomass into multiple products using a simple and energy efficient process was demonstrated, however, further studies are required to optimize overall processing conditions and economics.

4.7 References

Ananyev GM, Skizim NJ, Dismukes GC (2012) Enhancing biological hydrogen production from cyanobacteria by removal of excreted products. J. Biotechnol.162:97–104.

Ataeian M, Vadlamani A, Haines M, Mosier D, Dong X, Kleiner M (2021) Proteome and strain analysis of cyanobacterium *Candidatus* 'Phormidium alkaliphilum' reveals traits for success in biotechnology. iScience. 24:103405.

Cai J, Chen M, Wang G, Pan G, Yu P (2015) Fermentative hydrogen and polyhydroxybutyrate production from pretreated cyanobacterial blooms. Algal Res. 12:295–99.

Canon-Rubio KA, Sharp CE, Bergerson J, Strous M, De la Hoz Siegler H.(2016) Use of highly alkaline conditions to improve cost-effectiveness of algal biotechnology. Applied Microbiology and Biotechnology. 100:1611–22.

Carrieri D, Momot D, Brasg IA, Ananyev G, Lenz O, Bryant DA (2010) Boosting autofermentation rates and product yields with sodium stress cycling: Application to production of renewable fuels by cyanobacteria. Appl. Environ. Microbiol. 76:6455–62.

Chen Y, Cheng JJ, Creamer KS (2018) Inhibition of anaerobic digestion process: A review. Bioresour. Technol. 99:4044–64.

Cheng J, Xia A, Song W, Su H, Zhou J, Cen . (2102) Comparison between heterofermentation and autofermentation in hydrogen production from *Arthrospira* (*Spirulina*) *platensis* wet biomass. Int. J. Hydrogen Energy. 37:6536–544.

Dahiya S, Sarkar O, Swamy YV, Venkata Mohan S.(2015) Acidogenic fermentation of food waste

for volatile fatty acid production with co-generation of biohydrogen. Bioresour. Technol. 182:103–13.

Daelman MRJ, Sorokin D, Kruse O, van Loosdrecht MCM, Strous . (2016) Haloalkaline bioconversions for methane production from microalgae grown on sunlight. Trends Biotechnol. 36:450–7.

Enamala MK, Enamala S, Chavali M, Donepudi J, Yadavalli R, Kolapalli B (2018) Production of biofuels from microalgae - A review on cultivation, harvesting, lipid extraction, and numerous applications of microalgae. Renew. Sustain. Energy Rev. 94:49–68.

Engel DC, Geert F. Versteeg A, Swaaij WPM (1996) Solubility of hydrogen in aqueous solutions of sodium and potassium bicarbonate from 293 to 333 k. J. Chem. Eng. Data. 41:546–50.

Fasaei F, Bitter JH, Slegers PM, van Boxtel ABJ (2018) Techno-economic evaluation of microalgae harvesting and dewatering systems. Algal Res. 31:347–62.

Hasunuma T, Matsuda M, Kato Y, Vavricka CJ, Kondo A (2015) Temperature enhanced succinate production concurrent with increased central metabolism turnover in the cyanobacterium *Synechocystis sp*. PCC 6803. Metab. Eng. 48:10920.

Hasunuma T, Matsuda M, Kondo A (2016) Improved sugar-free succinate production by *Synechocystis sp*. PCC 6803 following identification of the limiting steps in glycogen catabolism. Metab. Eng. Commun. 3:130–41.

Halim R, Hill DRA, Hanssen E, Webley PA, Martin GJO (2019) Thermally coupled dark-anoxia incubation: A platform technology to induce auto-fermentation and thus cell-wall thinning in both nitrogen-replete and nitrogen-deplete *Nannochloropsis slurries*. Bioresour. Technol. 290:103–13.

Halim R, Hill DRA, Hanssen E, Webley PA, Blackburn S, Grossman AR (2019) Towards

sustainable microalgal biomass processing: Anaerobic induction of autolytic cell-wall self-ingestion in lipid-rich: *Nannochloropsis* slurries. Green Chem. 21:2967–82.

Jiang Y, McAdam E, Zhang Y, Heaven S, Banks C, Longhurst P (2019) Ammonia inhibition and toxicity in anaerobic digestion: A critical review. Journal of Water Process Engineering. 32:100899.

Jiunn-Jyi L, Yu-You L, Noike T (1997) Influences of pH and moisture content on the methane production in high-solids sludge digestion. Water Res. 37:1518–24.

Kassim MA and Bhattacharya S (2016) Dilute alkaline pretreatment for reducing sugar production from *Tetraselmis suecica* and *Chlorella sp*. biomass. Process Biochem. 51:1757–66.

Kuo CM, Jian JF, Sun YL, Lin TH, Yang YC, Zhang WX (2018) An efficient photobioreactors/raceway circulating system combined with alkaline-CO_2 capturing medium for microalgal cultivation. Bioresour. Technol. 266:398–406.

Liu X, Hong Y, Liu Y (2021) Cultivation of *Chlorella sp*. HQ in inland saline-alkaline water under different light qualities. Front. Environ. Sci. Eng. 16:1–10.

Liu H, Wang J, Liu X, Fu B, Chen J, Yu HQ (2012) Acidogenic fermentation of proteinaceous sewage sludge: Effect of pH. Water Res. 46:799–807.

Manyi-Loh CE, Mamphweli SN, Meyer EL, Okoh AI, Makaka G, Simon M (2013) Microbial anaerobic digestion (bio-digesters) as an approach to the decontamination of animal wastes in pollution control and the generation of renewable energy, Int. J. Environ. Res. Public Health. 10:4390.

Mattson MD (2014) Alkalinity of Freshwater. Reference module in earth systems and environmental sciences. Elsevier Inc. doi:https://doi.org/10.1016/B978-0-12-409548-9.09397-0.

Milledge JJ, Nielsen BV, Maneein S, Harvey PJ (2019) A brief review of anaerobic digestion of algae for bioenergy. Energies, 12:1–22.

Moraes BD, Dos Santos GM, Delforno TP, da Silva AJ (2019) Enriched microbial consortia for dark fermentation of sugarcane vinasse towards value-added short-chain organic acids and alcohol production. J. Biosci. Bioeng. 127(5); 594-601.

Nolla-Ardevol V, Strous M, Tegetmeyer HE (2015) Anaerobic digestion of the microalga *Spirulina* at extreme alkaline conditions: Biogas production, metagenome and metatranscriptome. Front. Microbiol. 6:1–21.

Passos F, Uggetti E, Carrère H, Ferrer I (2014) Pretreatment of microalgae to improve biogas production: A review. Bioresour. Technol. 172:403–12.

Pendyala B, Hanifzadeh M, Ameh Abel G, Viamajala S, Varanasi S (2020) Production of organic acids via autofermentation of microalgae: a promising approach for sustainable algal biorefineries. Ind. Eng. Chem. Res. 59:1772–80.

Saratale RG, Kumar G, Banu R, Xia A, Periyasamy S, Saratale GD (2018) A critical review on anaerobic digestion of microalgae and macroalgae and co-digestion of biomass for enhanced methane generation. Bioresour. Technol. 262:319–32.

Singh G, and Patidar SK (2018) Microalgae harvesting techniques: A review. J. Environ. Manage. 217:499–508.

Solé-Bundó M, Carrère H, Garfí M, Ferrer I.(2017) Enhancement of microalgae anaerobic digestion by thermo-alkaline pretreatment with lime (CaO). Algal Res. 24:199–206.

Ummalyma SB, Gnansounou E, Sukumaran RK, Sindhu R, Pandey A, Sahoo D (2017) Bioflocculation: An alternative strategy for harvesting of microalgae – An overview. Bioresour. Technol. 242:227–35.

Vadlamani A, Viamajala A, Pendyala B, Varanasi S (2017) Cultivation of microalgae at extreme alkaline pH conditions: a novel approach for biofuel production. ACS Sustain. Chem. Eng. 5:7284–94.

Vadlamani A, Pendyala B, Viamajala S, Varanasi S (2019) High productivity cultivation of microalgae without concentrated CO_2 input. ACS Sustain. Chem. Eng. 7:1933–43.

Wendt KE, Walker P, Sengupta A, Ungerer J, Pakrasi HB (2022) Engineering natural nompetence into the fast-growing cyanobacterium *Synechococcus elongatus* strain UTEX 2973. Appl. Environ. Microbiol. 88:1–16.

Wensel P, Helms G, Hiscox B, Davis WC, Kirchhoff H, Bule M (2014) Isolation, characterization, and validation of oleaginous, multi-trophic, and haloalkaline-tolerant microalgae for two-stage cultivation. Algal Res. 4:2–11.

Weschler MK, Barr WJ, Harper WF, Landis AE (2014) Process energy comparison for the production and harvesting of algal biomass as a biofuel feedstock. Bioresour. Technol. 153:108–15.

Wu H, Yang D, Zhou Q, Song Z (2009) The effect of pH on anaerobic fermentation of primary sludge at room temperature. J. Hazard. Mater. 172:196–201.

CHAPTER 5

Enabling the anaerobic digestion of Alkaline Cyanobacterial Biomass

This chapter provides information on batch anaerobic digestion experiments to determine biochemical methane potential of fresh and autofermented alkaline cyanobacterial biomass with different inoculum sources at low temperature to reduce the energy input.

5.1. Introduction

Autofermentation of alkaline cyanobacterial biomass resulted in multiple valuable products, as discussed in Chapter 4. The recovery of these valuable products, as well as the utilization of biomass waste after product recovery into an energy product, improves the economic viability of a cyanobacterial biomass biorefinery. Anaerobic digestion (AD), a promising technology that transforms organic matter into renewable biogas energy, has been stated as the most suitable technology to maximize product recovery from waste biomass (Romero-Güiza et al., 2016). Integration of autofermentation and AD maximizes product recovery by converting waste cyanobacterial biomass into an energy product, biogas.

AD is a sequence of processes through which microorganisms break down organic matter. These processes are hydrolysis, acidogenic fermentation, hydrogen-producing acetogenesis, and methanogenesis. In the first step, complex organic substances are decomposed into soluble monomers (sugars, amino acids, and fatty acids). In the acidification step, acidogenic bacteria convert soluble monomers into terminal products, such as volatile fatty acids (VFA) and CO_2. In the third step, hydrogen-producing acetogens convert VFAs into acetic acid and hydrogen. In the last step, anaerobic methanogenic bacteria convert acidification products (such as acetic acid, formic acid, CO_2/H_2, etc.) into methane (Li et al., 2019). Among the microbes involved in each of these steps, methanogenic bacteria are the most sensitive ammonium, which is a product of protein degradation during the hydrolysis step (Rajagopal et al., 2013; Yenigün and Demirel, 2013). The high alkalinity and pH of the cyanobacterial biomass, combined with its high protein content, increase the risk of ammonia inhibition, and reduce the efficiency of waste biomass utilization in methane conversion (Jiang et al., 2019). Autofermentation of cyanobacterial biomass reduces the pH due to organic acid production, therefore eliminating the risk of ammonium inhibition.

Moreover, it can replace the first three steps of anaerobic digestion, and the separation of these three steps can allow better control over fermentative bacteria and methanogenic bacteria to improve methane productivity. However, the integration of autofermentation and AD of alkaline cyanobacterial biomass still requires evaluation of different process parameters, such as temperature, pH, and the identification of a suitable methanogenic inoculum for maximum methane production.

Biochemical methane potential (BMP) tests are batch AD tests that are widely used to evaluate the anaerobic biodegradability of organic substrates and to identify key variables that affect AD (Kafle and Chen, 2016). BMP tests are usually performed by mixing organic substrate with inoculum and incubating for a period of 30 to 60 days under stable temperatures usually between 35 to 55 °C (Filer et al., 2019). The most researched parameters are the origin of inoculum, digestion temperature, the effect of pretreatment techniques, and co-digestion of different substrates. These parameters are important to assess the feasibility of a full-scale AD plant, as well as to provide critical data to support process design and optimization. Among these parameters, the origin of the inoculum is important as the digestion of high protein content and alkaline cyanobacterial biomass may result in ammonia toxicity (Mahdy et al., 2017). Methanogenic inoculums obtained from sewage sludge and wastewater treatment systems have low ammonia tolerance as they are typically exposed to a low concentration of ammonia (Capson-Tojo et al., 2020). Thus, these methanogenic microbial populations may not be able to cope with the high protein loads and alkaline conditions. Another important parameter is temperature, as it affects the degradability of the substrate and the energy requirement of the process (Nie et al., 2021). AD digestion systems can be classified based on the operating temperatures as: psychrophilic (<25 °C), mesophilic (25-37 °C), and thermophilic (55-65 °C) (McKeown et al., 2012). The majority of today's AD processes operate in mesophilic

or thermophilic temperature ranges. Inoculums obtained from these systems are adapted to mesophilic or thermophilic temperature ranges and thus require additional energy for heating. Although higher operational temperatures provide a higher microbial growth rate and methane production, the high energy requirements of mesophilic and thermophilic temperatures may reduce net energy production (Zupančič and Roš, 2003). To maximize net energy production from AD of autofermented cyanobacterial biomass, the application of a lower operational temperature may be beneficial to reduce the energy input. Therefore, performance evaluation of different inocula at lower operational temperatures (21 °C) becomes important for the development of a low-cost, high net energy production bioprocess.

Other than process parameters, pretreatment is a significant step required to improve the degradability of cyanobacterial biomass and enhance methane production. Pretreatment methods applied to cyanobacterial biomass can be classified as physical, thermal, chemical, biological, or a combination of these methods (Ariunbaatar et al., 2014). Physical methods (ultrasound, microwave, or shear forces) and thermal methods require high energy input, which negatively affects process economics (Amin et al., 2017). Chemical pretreatments may contaminate final products or be corrosive to materials and instruments (López Torres and Espinosa Lloréns, 2008). Biological pretreatment is based on the use of microorganisms or enzymes (Mlaik et al., 2019; Yuan et al., 2014). Low capital and operational costs are important parameters for the selection of the pretreatment method. In addition, pretreatment methods with a positive energy balance are advantageous. Autofermentation is a low-cost and efficient pretreatment method to enable the AD of alkaline biomass as it reduces pH by producing organic acid during fermentation. Furthermore, autofermentation fits perfectly into the biorefinery concept as a variety of valuable products (organic acid, pigments, and hydrogen) are produced.

In this chapter, the anaerobic digestion of fresh and autofermented cyanobacterial biomass was performed with three different inoculums at two different temperatures. The digestion capabilities of digested manure, digested sewage sludge, and soda lake sediment were evaluated for low-temperature anaerobic digestion. The effects of temperature and pretreatment on COD removal, pH, and NH_4^+ were also investigated.

5.2. Characteristics of biomass and inocula

To evaluate different inoculums for their capability of converting fresh (high pH) and autofermented alkaline cyanobacterial (neutral pH) biomass into methane, a wide range of physical, chemical, and composition analyses were done, as shown in Tables 5-1 and 5-2. Across all inocula and biomass evaluated, the ash content was between 5 and 10 %. The pH of fresh biomass and soda lake sediment was higher compared to autofermented biomass and other inoculums. Fresh cyanobacterial biomass has a protein content of 60.9 %, a carbohydrate content of 12.5 %, and a lipid content of 12.5%. The high content of protein resulted in a low C/N ratio of 4.34 for fresh biomass and 5.37 for autofermented biomass. Although autofermented biomass had a higher C/N ratio compared to fresh biomass due to the separation of fermentation broth rich in proteins, a C/N ratio lower than 20–30 is not favorable for anaerobic digestion due to the conversion of nitrogen in proteins into inhibitory compounds such as NH_3 and NH_4^+ (Park et al., 2018). Although NH_3 and NH_4^+ are important sources of nitrogen for bacteria and low concentrations of ammonia (below 10–11 mM) are beneficial to the process, high concentrations of these compounds are shown to reduce the methanogenic activity (Rajagopal et al., 2013).

NH_4^+ was not detected in freshly harvested biomass, while autofermentation resulted in the degradation of proteins and the production of 15–25 mM NH_4 (Table 5-2). Digested manure and soda lake sediment had similar NH_4^+ concentrations (Table 5-1). NH_4^+ was further produced and

reached a concentration of 60 mM, 135 mM, and 270 mM for AD with digested manure, digested sewage sludge, and soda lake sediment, respectively.

Table 5-1. Characterization of inocula in terms of physicochemical properties.

	Temperature (°C)	**pH**	**TS (g/L)**	**VS (g/L)**	**Ash content (%)**	**COD (g/L)**	**NH_4^+ (mM)**
Digested sewage sludge	35	7.5	20	18	10	31	2
Digested manure	38	8	34	32	5.8	46	23
Soda lake sediment	15	10.2	18	8	5.5	18	27

Table 5-2. Characterization of fresh biomass and autofermented biomass.

	Temperature (°C)	**pH**	**TS (g/L)**	**VS (g/L)**	**Ash content (%)**	**C/N ratio**	**COD (g/L)**	**NH_4^+ (mM)**
Autofermented biomass	21	7	143	130	8.9	4.34	16	15-25
Fresh biomass	21	10.4	241	219	9.3	5.37	13	-

5.3. Effect of inoculum on methane production at different temperatures

In the BMP tests, three different inoculums, digested manure, digested sewage sludge, and soda lake sediment, were evaluated for methane yield, COD, and NH_4^+ concentrations at 21 °C and 35 °C. The methane yield from the AD of fresh and fermented cyanobacterial biomass is presented in Figure 5-1. Digested manure and digested sewage sludge were not successful at converting fresh biomass into methane at both temperatures due to the high pH (10.4) and alkalinity of the fresh biomass. High pH and alkalinity inhibited methanogenesis, resulting in almost no methane production. Although methanogenesis was inhibited, acidification microorganisms were still able to continue to degrade the biomass and produce hydrogen because of the degradation process. Hydrogen gas was present in the headspace of AD bottles, in which no methane production was seen. The highest methane yield from fresh biomass was obtained by the soda lake sediment inoculum at 35 °C. Both cyanobacterial biomass and soda lake sediment were originally collected from the same soda lakes. For this reason, the microbial community in the soda lake sediment inoculum was already acclimated to the high pH and high alkalinity conditions. Although soda lake sediment was able to produce methane, the methane yield was not high enough for successful AD.

The high pH of fresh biomass was decreased due to organic acid accumulation during the autofermentation pretreatment step, as mentioned in Chapter 4. A decreased pH to neutral conditions enabled the successful conversion of cyanobacterial biomass into methane by reducing the risk of NH_4^+ inhibition. AD of autofermented cyanobacterial biomass at 35 °C resulted in a higher methane yield than at 21 °C. The highest methane yield was obtained from AD with digested sewage sludge, with a yield of 314 mL CH_4/ g VS.

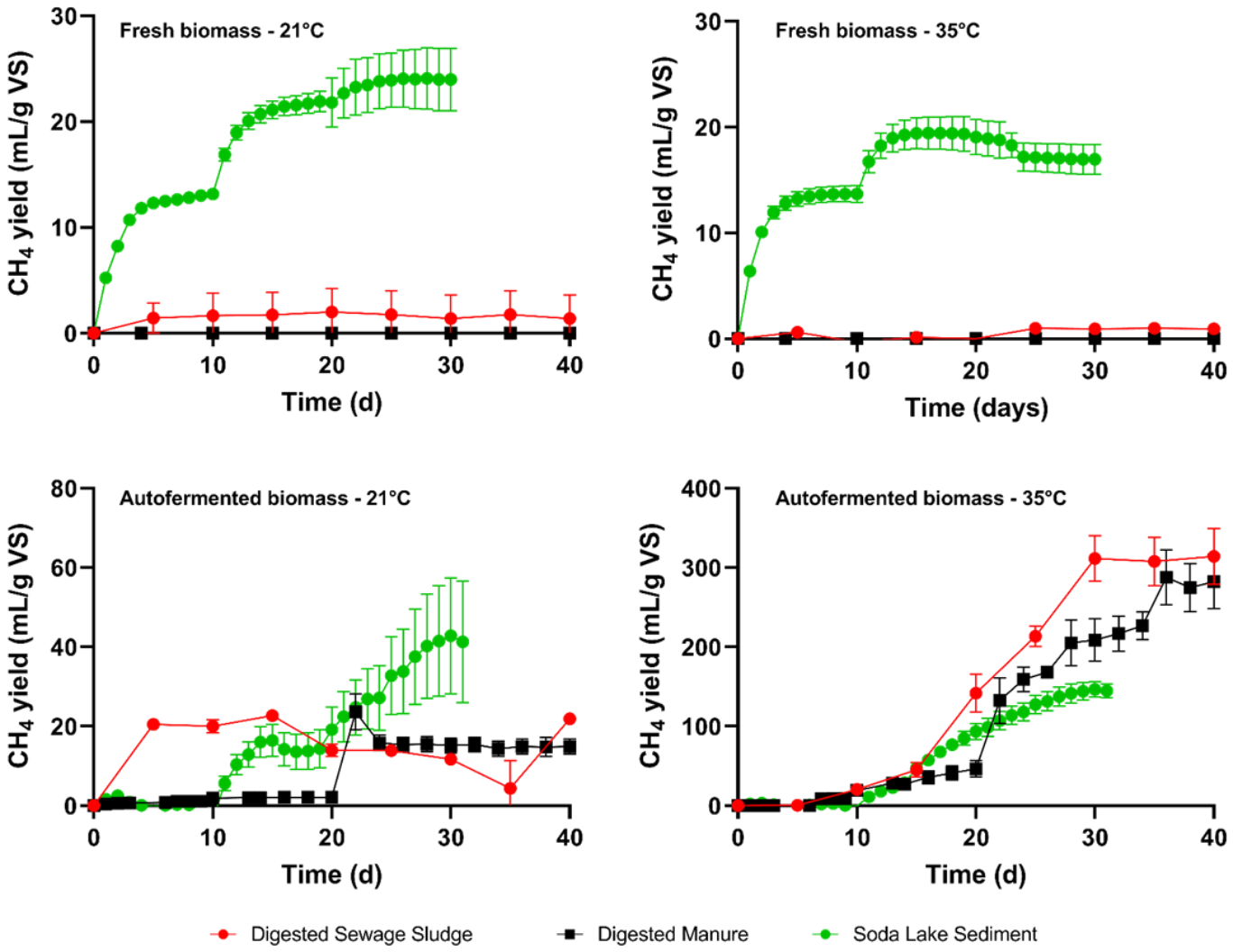

Figure 5.1. Methane yield from anaerobic digestion of fresh and fermented cyanobacterial biomass with digested sewage sludge, digested manure, and soda lake sediment at 21 °C and 35 °C

This was followed by digested manure with a yield of 291 mL CH_4/ g VS. The methane content in the headspace was 65 % and 60 % for digested sewage sludge and digested manure, respectively. Soda lake sediment produced more methane than fresh biomass, with 144 mL CH_4/ g VS. Although digested sewage sludge and digested manure were successful at converting autofermented cyanobacterial biomass at 35 °C, the methane yield obtained using these inocula was significantly lower at 21 °C, with 14 mL CH_4/ g VS and 14.9 mL CH_4/ g VS, respectively. Inoculation with soda lake sediment resulted in the highest methane yield at 21 °C with 25.9 mL CH_4/ g VS.

5.4. COD removal performance and NH_4^+ accumulation

Fig. 5-2 shows the COD removal performance during AD of either fresh or autofermented cyanobacterial biomass at 21 °C and 35 °C, while Fig. 5-3 shows the accumulation of NH_4^+. Digested manure was able to degrade the organic material in the fresh biomass and reduce COD, although there was not significant methane production. In the AD of fresh biomass with digested sewage sludge and soda lake sediment there was no significant reduction in COD. During the AD of autofermented biomass, on the other hand, COD reduction was observed in all the experiments done with the different inocula, with an average of 60 % COD conversion into methane.

There was a significant increase in NH_4^+ concentration in each experiment. However, the highest NH_4^+ accumulation was observed in AD with soda lake sediment. The NH_4^+ concentration increased from 25 mM to 327 mM in the AD of fresh biomass and from 58 mM to 270 mM in the AD of autofermented biomass. The final NH_4^+ concentration in AD with digested sewage sludge and digested manure was lower than AD with soda lake sediment, with 127 mM and 88 mM for digested sewage sludge and digested manure, respectively. NH_4^+ concentrations higher than 1700–1800 mg/L (around 100 mM) have been shown to inhibit methanogenesis. The

change in pH during AD is given in Figure 5-4. The high pH of fresh biomass in AD increases the inhibitory effect of NH_4^+ by deprotonation. The deprotonated NH_3 is more permeable through the cell membrane than NH_4^+ thus causing changes in intracellular pH and leading to cytotoxicity. Although the NH_4^+ concentration was high in the AD of autofermented biomass, the pH was low enough (almost neutral) to prevent inhibition of methanogenesis.

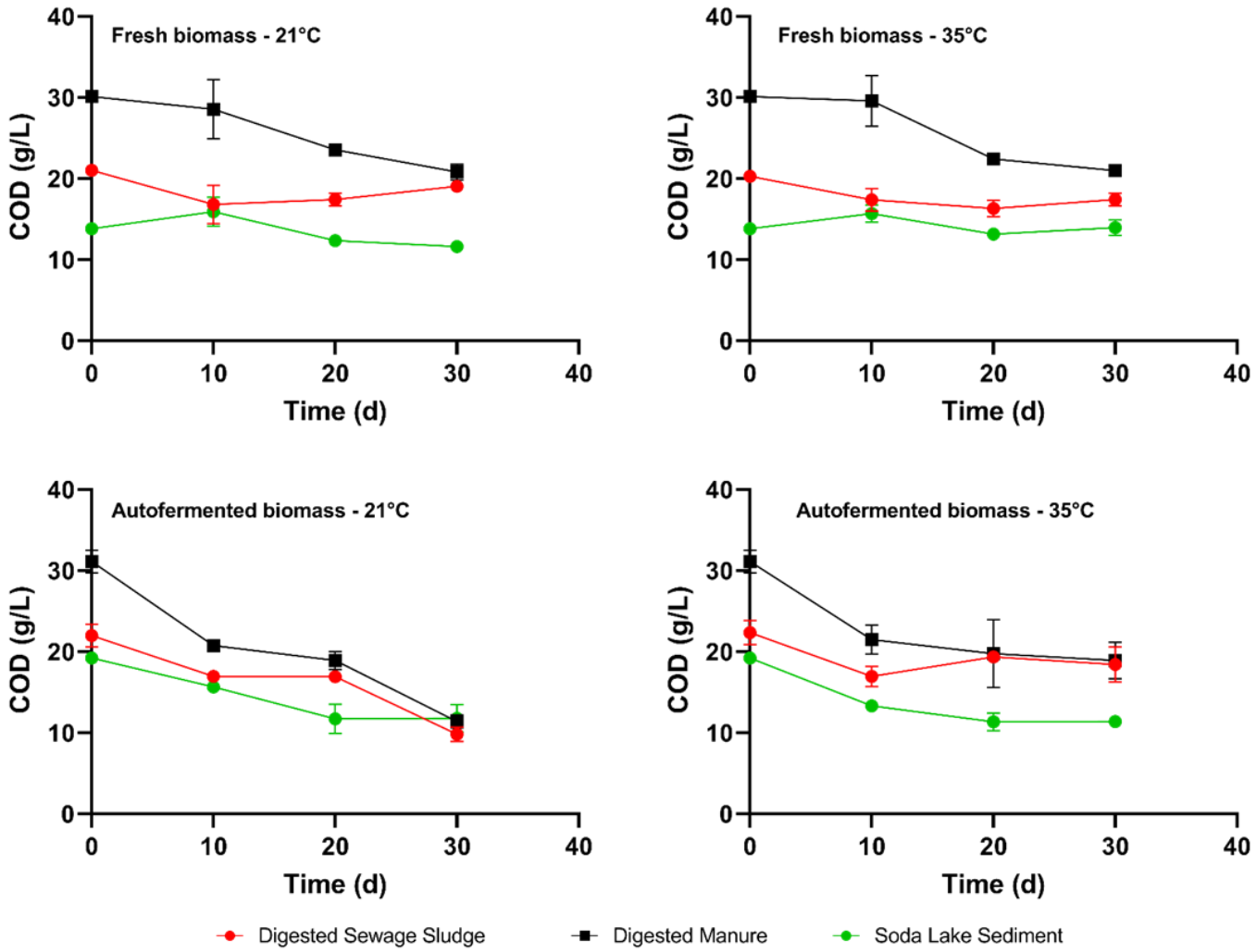

Figure 5.2. Change in COD concentration during anaerobic digestion of fresh and fermented cyanobacterial biomass with digested sewage sludge, digested manure, and soda lake sediment at 21 °C and 35 °C.

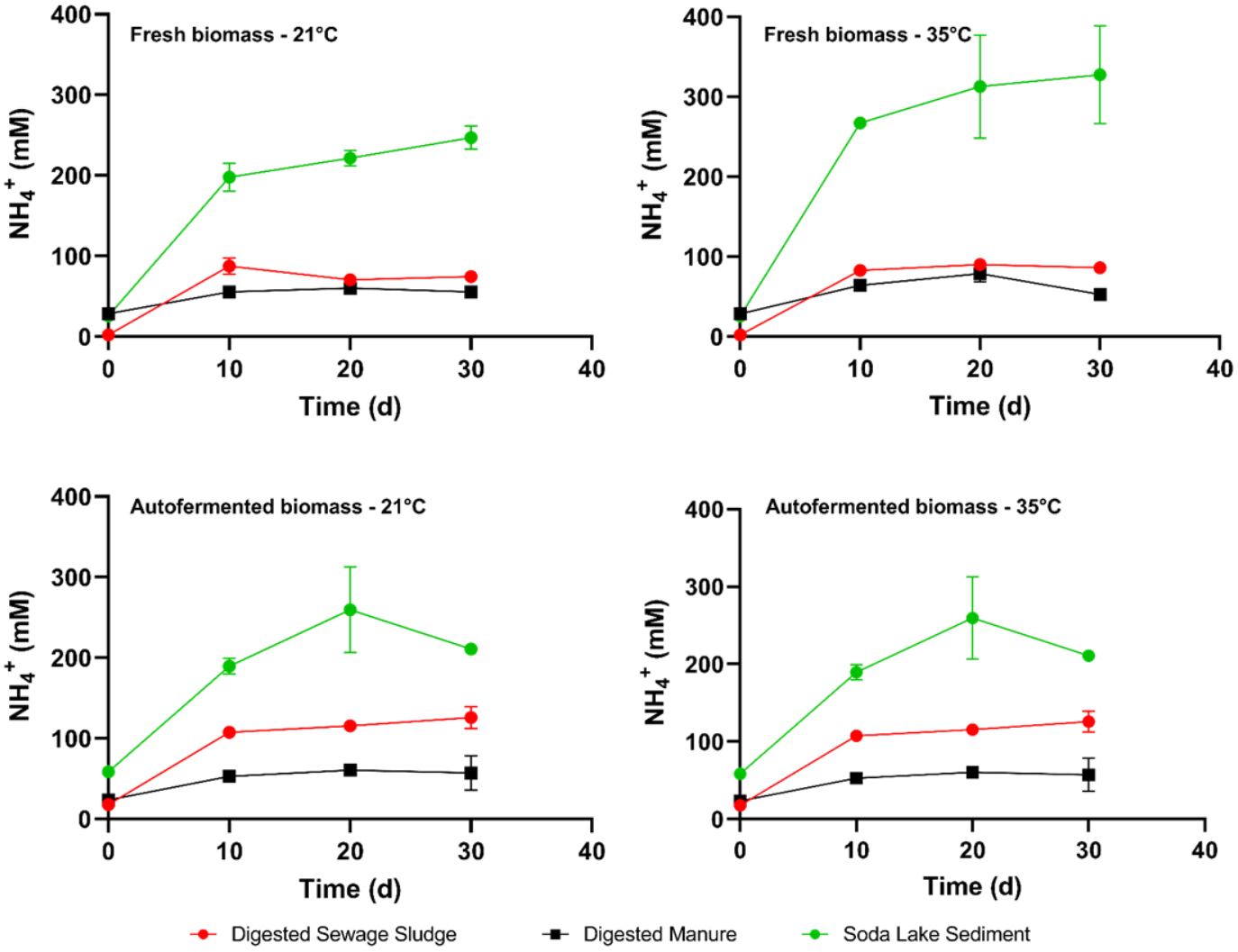

Figure 5.3. Change in NH_4^+ concentration during anaerobic digestion of fresh and fermented cyanobacterial biomass with digested sewage sludge, digested manure, and soda lake sediment at 21 °C and 35 °C.

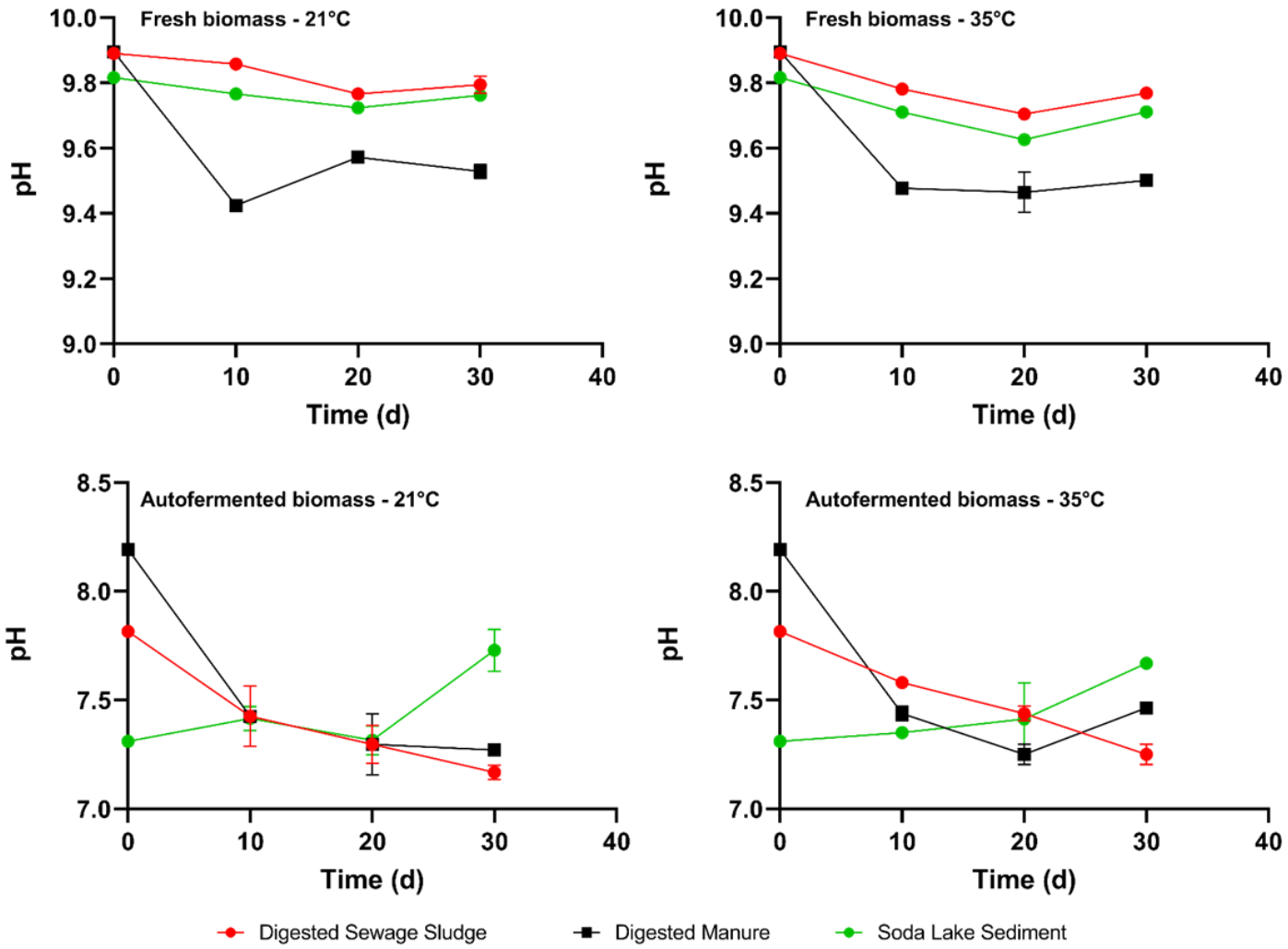

Figure 5.4. Change in pH during anaerobic digestion of fresh and fermented cyanobacterial biomass with digested sewage sludge, digested manure, and soda lake sediment at 21 °C and 35 °C.

5.5. Organic acid profile

The concentration of volatile fatty acids (VFAs), including butyrate, acetate, propionate, and lactate, during AD is an important parameter to determine the success of the AD. Among these organic acids, acetate is the most important precursor for methanogenesis. Rapid consumption of VFAs indicates a successful AD process, while accumulation of VFAs occurs due to low or no consumption because of inhibition of methanogenesis (Park et al., 2018). Under high pH and high alkaline conditions, VFA accumulation occurred due to inhibition of methanogenesis (Figure 5-5).

The change in VFA concentration during AD of fresh and autofermented biomass with soda lake sediment inoculum at 21 °C and 35 °C is given in Figure 5-5. An increase in acetate concentration occurred in the AD of fresh biomass at both temperatures due to the degradation of fresh biomass, however. After day 20, the acetate concentration decreased in the AD of fresh biomass at 35 °C. In the case of autofermented biomass, acetate was present in the media due to pretreatment. Low pH resulted in the complete consumption of acetate and high methane production compared to fresh biomass.

The capability of methane production at low temperatures was an important criterion for the next phase of these experiments to obtain net energy-positive methane production. Because soda lake sediment was the only inoculum capable of performing well at low temperatures, VFA analyses were performed only for the soda lake sediment experiment to determine the required process conditions for a semi-continuous AD process.

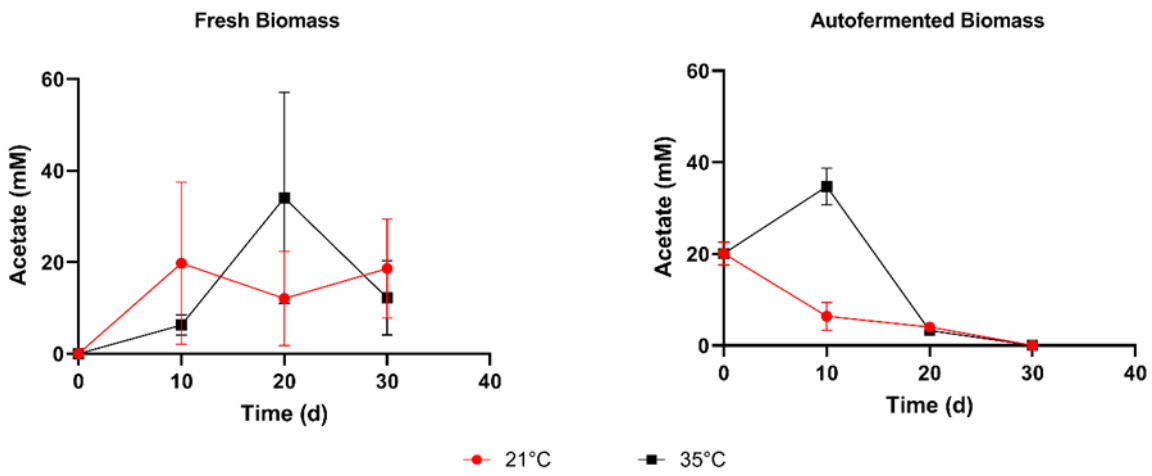

Figure 5.5. Change in organic acid concentration during anaerobic digestion of fresh and fermented cyanobacterial biomass with soda lake sediment at 21 °C and 35 °C.

5.6 Conclusion

In this chapter, a series of batch BMP tests were completed to determine the most successful inoculum source that can convert fresh and autofermented cyanobacterial biomass into methane at low temperature (21 °C) to reduce energy requirements for the AD process. The soda lake sediment inoculum was found to be the most successful for converting both fresh (high pH) and autofermented cyanobacterial biomass into methane at 21 °C. Furthermore, the relationship between pH and methane yield showed that how pH level can affect the ammonium inhibition. Although exactly same substrate concentration was added in each experiment, high pH caused inhibition of methanogenesis and resulted in no methane production. Changes in ammonia accumulation and VFA concentration provided important information on performance of AD. This knowledge will be important in design and operation of semi-continuous AD process.

5.7 References

Amin FR, Khalid H, Zhang H, Rahman S, Zhang R, Liu G, Chen C (2017) Pretreatment methods of lignocellulosic biomass for anaerobic digestion. AMB Express 7(1): 1–12.

Ariunbaatar J, Panico A, Esposito G, Pirozzi F, Lens PNL (2014) Pretreatment methods to enhance anaerobic digestion of organic solid waste. Appl. Energy. 123: 143–156.

Capson-Tojo G, Moscoviz R, Astals S, Robles, Steyer JP (2020) Unraveling the literature chaos around free ammonia inhibition in anaerobic digestion. Renew. Sustain. Energy Rev. 117: 109487.

Filer J, Ding HH, Chang S (2019) Biochemical Methane Potential (BMP) Assay Method for Anaerobic Digestion Research. Water. 11(5): 921.

Jiang Y, McAdam E, Zhang Y, Heaven S, Banks C, Longhurst P (2019) Ammonia inhibition and toxicity in anaerobic digestion: A critical review. J. Water Process Eng. 32: 100899.

Kafle GK, Chen L (2016). Comparison on batch anaerobic digestion of five different livestock manures and prediction of biochemical methane potential (BMP) using different statistical models. Waste Manag. 48: 492–502.

Li Y, Chen Y, Wu J (2019) Enhancement of methane production in anaerobic digestion process: A review. Appl. Energy. 240: 120–137.

López Torres M, Espinosa Lloréns M del C (2008) Effect of alkaline pretreatment on anaerobic digestion of solid wastes. Waste Manag. 28(11): 2229–2234.

Mahdy A, Fotidis IA, Mancini E, Ballesteros M, González-Fernández C, Angelidaki I (2017) Ammonia tolerant inocula provide a good base for anaerobic digestion of microalgae in third generation biogas process. Bioresour. Technol. 225: 272–278.

McKeown RM, Hughes D, Collins G, Mahony T, O'Flaherty V (2012) Low-temperature anaerobic digestion for wastewater treatment. Curr. Opin. Biotechnol. 23(3): 444–451.

Mlaik N, Khoufi S, Hamza M, Masmoudi MA, Sayadi S (2019) Enzymatic pre-hydrolysis of organic fraction of municipal solid waste to enhance anaerobic digestion. Biomass and

Bioenergy. 127: 105286.

Nie E, He P, Zhang H, Hao L, Shao L, Lü F (2021) How does temperature regulate anaerobic digestion? Renew. Sustain. Energy Rev. 150: 111453.

Park JG, Lee B, Jo SY, Lee JS, Jun HB (2018) Control of accumulated volatile fatty acids by recycling nitrified effluent. J. Environ. Heal. Sci. Eng. 16(1): 19.

Rajagopal R, Massé DI, Singh G (2013) A critical review on inhibition of anaerobic digestion process by excess ammonia. Bioresour. Technol. 143: 632–641.

Romero-Güiza MS, Vila J, Mata-Alvarez J, Chimenos JM, Astals S (2016) The role of additives on anaerobic digestion: A review. Renew. Sustain. Energy Rev. 58: 1486–1499.

Yenigün O, Demirel B (2013) Ammonia inhibition in anaerobic digestion: A review. Process Biochem. 48(5–6): 901–911.

Yuan X, Wen B, Ma X, Zhu W, Wang X, Chen S, Cui Z (2014) Enhancing the anaerobic digestion of lignocellulose of municipal solid waste using a microbial pretreatment method. Bioresour. Technol. 154: 1–9.

Zupančič GD, Roš M (2003) Heat and energy requirements in thermophilic anaerobic sludge digestion. Renew. Energy. 28(14): 2255–2267.

CHAPTER 6

Energy Positive Methane Production from Fermented Cyanobacteria

This chapter is currently under preparation for submission in Bioresource Technology Journal.

Authors' contributions: Here, I designed and carried out all the experimentation, methodology, data analysis, visualization and writing the original draft. Dr. Tervahauta contributed to the methodology and experimentation of anaerobic digestion. Dr. Tervahauta, Prof De la Hoz Siegler, and Prof Strous supervised the project, contributed to the methodology, conceptualization, reviewed and edited the manuscript.

Abstract

The use of a high-pH and high-alkalinity growth medium improves the sustainability of cyanobacteria cultivation systems. However, these conditions make methane production from the cyanobacteria more challenging. Fermentation can be used as a low-cost, zero-energy pre-treatment method to break down cyanobacteria and lower the pH prior to anaerobic digestion. Here, we show that fermented cyanobacteria can be digested to biogas at ambient temperature, using sediments from alkaline soda lakes as inoculum. Increased concentrations of ammonium were shown to decrease methane production. However, despite fluctuating ammonium concentrations, fermented cyanobacteria were successfully digested for 550 days in duplicated semi-continuous digesters (3 L) operated at a temperature of 21°C with an average methane yield of 471 mL/gVS and 62% of the biomass converted to biogas. This digestion system had a higher net energy production than previously described microalgae digestion systems.

6.1. Introduction

Cyanobacteria are natural bio-factories for diverse biotechnological applications owing to their capacity to gather solar energy and fix carbon dioxide into valuable bioactive compounds such as proteins and pigments (Garlapati et al., 2019; Knoot et al., 2018; Noreña-Caro and Benton, 2018). However, the deployment of large-scale cyanobacteria cultivation is hindered by major limitations such as water evaporation, CO_2 losses, and contamination with unwanted species, which may lead to low biomass productivity (Udayan et al., 2022). These limitations need to be addressed to obtain optimum outputs in large-scale cyanobacterial cultures with minimal operating cost. Strategies suggested to address these limitations include using wastewater to supply nutrient needs (Mohsenpour et al., 2021), improving the efficiency of the delivery of CO_2 to the cells (Zheng et al., 2018), and selecting and isolating robust species (Geada et al., 2017).

The use of high pH (>10) and high alkalinity has been proposed to address the slow growth rate of cultures due CO_2 losses and high cost of CO_2 pumping to the cultivation system (Kuo et al., 2018; Vadlamani et al., 2017). High pH and high alkalinity increase CO_2 mass transfer rates, while providing buffering capacity for CO_2 absorption into the culture medium (Canon-Rubio et al., 2016). Furthermore, high pH reduces the risk of contamination and frequent culture crashes, as many microorganisms are not capable of growing at high pH. In this study, we use the cyanobacterium *Candidatus* "Phormidium alkaliphilum", which can grow at pH 11, enabling the direct capture of CO_2 from the air and into the medium and eliminating the cost of a concentrated CO_2 supply.

Downstream processing of cyanobacterial biomass also has a significant effect on the economic viability and environmental footprint of the bioproducts (Khanra et al., 2018). There are several pathways for processing harvested biomass into bioproducts, such as solvent extraction for

pigments and proteins, transesterification of neutral lipids, fermentation to bioethanol, anaerobic digestion to biogas, thermochemical conversion to bio-crude (Khanra et al., 2018; Nitsos et al., 2020). Most of the downstream processes have disadvantages such as the need for water removal, the use of large amounts of solvent, high energy requirement to heat the reactors for thermochemical processes, and removal of chemicals. Anaerobic digestion (AD) is one of the most cost-effective technologies due to low operational temperatures compared to thermochemical processes, resulting in lower energy requirements (Yukesh Kannah et al., 2021). Integrating cyanobacterial biomass production with AD allows the simultaneous reduction of carbon emissions and the generation of bioenergy and bioproducts for the circular economy. However, the high protein content of the cyanobacterial biomass results in the accumulation of the inhibitory compounds ammonia (NH_3) and ammonium (NH_4^+) during the degradation of the biomass (Solé-Bundó et al., 2019). Furthermore, high pH and high alkalinity biomass cultivation increases the inhibitory effect of NH_4^+ by deprotonation into NH_3, which can inhibit methanogenic activity and reduce biogas production (Bonk et al., 2018). For successful AD, a pH range between 6.5 and 8.5 is required to avoid inhibition (Cioabla et al., 2012). In a previous study, Nolla-Ardevol (2015) used microbial communities obtained from haloalkaline sediments to enable AD under high pH and high alkalinity conditions. This study reported that the digestion of *Spirulina* biomass under highly alkaline conditions (pH 10, 2.0 M Na^+) into methane-rich (96 %) biogas was possible. However, only 7 % of the initial biomass was converted to methane due to the inhibitory effect of NH_3-N, with volatile fatty acids accumulating instead.

To address these challenges, we integrated autofermentation as a low-cost and energy-efficient pre-treatment with the AD process to reduce the pH of the harvested biomass. Autofermentation is a process in which cyanobacteria can produce volatile fatty acids by catabolizing their storage

molecules, such as carbohydrates (Hasunuma et al., 2016; Pendyala et al., 2020). In Chapter 4, it was showed that the formation of volatile fatty acids (VFAs) during autofermentation can decrease the pH of the biomass slurry and reduce the risk of ammonia inhibition. Direct autofermentation after primary settling also reduces the energy requirement associated with extensive dewatering, while avoiding the use of any additional chemicals. In cultures of *Candidatus* "P. alkaliphilum", autofermentation also triggers the release of phycocyanin, a high-value protein-based colorant used in the food industry.

Application of AD at low temperatures is an interesting option as may increase the energy efficiency of the process by avoiding the need to heat the digester. However, studies on AD at low temperatures show that the reduced temperature decreases the rate of methane production and increases the retention time needed (Liu et al., 2016). Digested manure and sewage sludge are commonly used inoculums for anaerobic digestion but may be unable to successfully produce methane at lower temperatures (<35 °C) (McKeown et al., 2012). Soda Lake sediment may be a better inoculum for digestion of cyanobacteria at ambient temperature (21 °C).

In this study, we report conversion of cyanobacterial biomass grown at high pH and alkalinity to methane by integrating autofermentation and AD at room temperature with two duplicate semi-continuous digesters. To select the best inoculum for the semi-continuous AD, we evaluate different inocula and their performance at two different temperatures (21 °C and 35 °C) for successful conversion of fermented biomass into methane. Furthermore, we report the energy balance of semi-continuous digestion of fermented cyanobacterial biomass at room temperature.

6.2 Batch digestion of fermented cyanobacteria

Table 6-1 presents the methane yield in the batch digestion of fermented cyanobacteria with different inocula at 21 °C and 35 °C, as well as the initial characteristics of the inocula. Methane

production at 21 °C using digested manure and digested sewage sludge was lower compared to the methane production at 35 °C. This could be explained by the fact that the digested manure and the digested sewage sludge were obtained from digesters operating at 35 °C and 38 °C, respectively. The use of low operational temperature in anaerobic digestion with these inocula may result in reduced substrate utilisation, microbial growth and metabolic activity, and increased methane solubility in the reactor. Although the methane production using soda lake sediment was lower at 21 °C compared to 35 °C, it was still higher than with the other inocula. The fermentative bacteria and methanogenic archaea from soda lake sediments can be expected to be adapted to low temperatures as they can survive through the cold winter at extremely low temperature in the Cariboo Plateau in British Columbia (Triwari et al., 2021). Furthermore, soda lake sediment samples were taken in in summer 2019, when the average summer temperature in Cariboo Plateau was 15°C, which explains the quick adaptation of soda lake sediment to the anaerobic digestion at 21°C.

Table 6-1 also shows the highest NH_4^+ concentration measured in batch tests with different inocula at 21°C. Even though, the bottles inoculated with soda lake sediment had the highest NH_4^+ concentration, the methane yield was higher than with the other inocula. A possible explanation for this is that the inhibition risk of rapid NH_4^+ accumulation is reduced at low temperatures because temperature influences the dissociation constant of ammonia nitrogen (Rajagopal et al., 2013).

Table 6-1. Batch digestion of fermented cyanobacteria with different inoculums at 21°C and 35°C

Inoculum	Methane yield (mL/gVS) at 30 d of incubation		Inoculum source	Source temperature	Initial pH of the inoculum	VS	COD	NH_4^+ Concentration at 21°C
	35°C	**21**°C				**g/L**	**g O_2/L**	**mM**
Digested manure	222	3.4	Lethbridge Biogas	38°C	8.0	32	46	60 mM
Digested sewage sludge	312	12	Bonnybrook Wastewater Treatment Plant	35°C	7.5	18	31	135 mM
Soda lake sediment	144	42	Soda lake, Cariboo plateau	15°C	10.2	8	18	270 mM

Massé et al. (2003) showed that ammonium inhibition can be prevented by performing AD at a low temperature. They reported a threefold increase in free ammonia nitrogen (FAN) from 62 mg/L to 185 mg/L when temperature was increased from 10 °C to 20 °C. A further increase in temperature increased FAN concentrations from 304 to 448 mg/L at 35 °C, although there was no difference in pH and total ammonia nitrogen. Therefore, low operating temperature in the anaerobic digestion of fermented cyanobacteria is a feasible option to reduce ammonia inhibition.

6.3 Ammonium inhibition in the digestion of acetate using soda lake sediment as an inoculum

The ammonium (NH_4^+) concentration in batch AD tests inoculated with soda lake sediment reached to a higher level compared to other inocula. In previous studies, inhibition of methanogenesis and a drop in methane production was reported above 1700–1800 mg/L of total free ammonia (NH_3) nitrogen and NH_4^+ nitrogen concentrations with using sludge (Yenigün and Demirel, 2013). Although there was methane production in the batch, AD tests inoculated with soda lake sediment, it was important to determine the threshold NH_4^+ concentration for inhibition as it was not reported before for soda lake sediment. In addition, this high NH_4^+ concentration may be already inhibitory, and it was the reason of lower methane yield compared to other inocula. This was determined in anoxic incubations of the soda lake sediment with acetate at pH 7 using a range of NH_4^+ concentrations, from 0 to 60 mM (Figure 6-1). The highest methane yield of 74 mL/ g acetate was obtained at 0 mM of NH_4^+. A significant decrease of 74 % in the methane yield occurred at 60 mM of NH_4^+. The lag phase was also longer at higher NH_4^+ concentrations. Methane production started after 5 days of incubation at 60 mM of NH_4^+ compared to lower NH_4^+ concentrations (1 day), which could indicate an acclimation period of methanogens to a high NH_4^+ concentration.

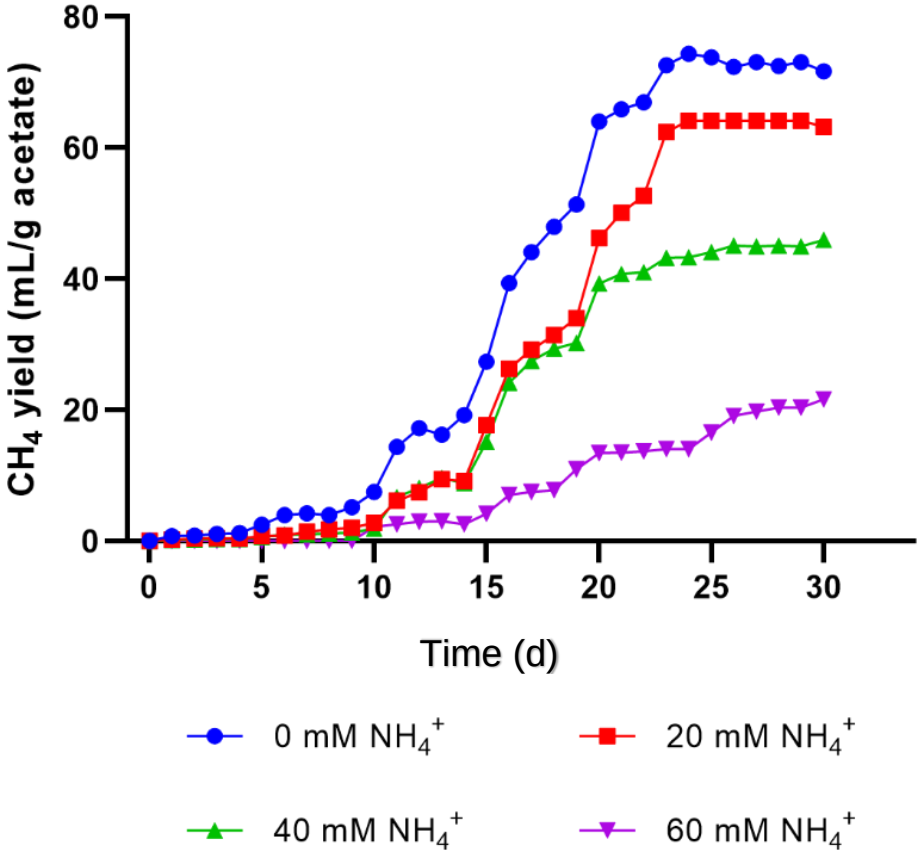

Figure 6.1. Ammonium inhibition in the digestion of acetate using soda lake sediment as an inoculum.

6.4 Anaerobic digestion of fermented cyanobacteria in semi-continuous digesters

After evaluating the different inocula sources to produce methane from fermented cyanobacterial biomass, we studied semi-continuous AD of fermented cyanobacterial biomass at 21 °C. As a low-temperature inoculum, soda lake sediment was used in the duplicate semi-continuous digesters operating at 21 °C. Figure 3 presents the cumulative methane production and NH_4^+ concentration in the anaerobic digesters during the first 550 days of operation.

Digesters operated with an average OLR of 0.1 g VS/Ld during the 550 days of operation. After 223 days, recycling of digester biomass was implemented to improve SRT and prevent biomass washout. 50 % of the solids in the effluent was recycled back into the digesters, which resulted in increased SRT from 44 days to 89 days. Recycling of digester biomass stimulated methane production while the NH_4^+ concentration remained similar to before recycling. The methane yield at 550 days was 465 mL/g VS and 476 mL/g VS with a methane conversion of 59 % and 64 % for Digester 1 and Digester 2, respectively. Although, the average NH_4^+ concentration was below the 60 mM, which caused 74% decrease in methane production, determined by the NH_4^+ inhibition batch test with a concentration of 32 mM in Digester 1 and 36 mM in Digester 2 (Figure 6-2).

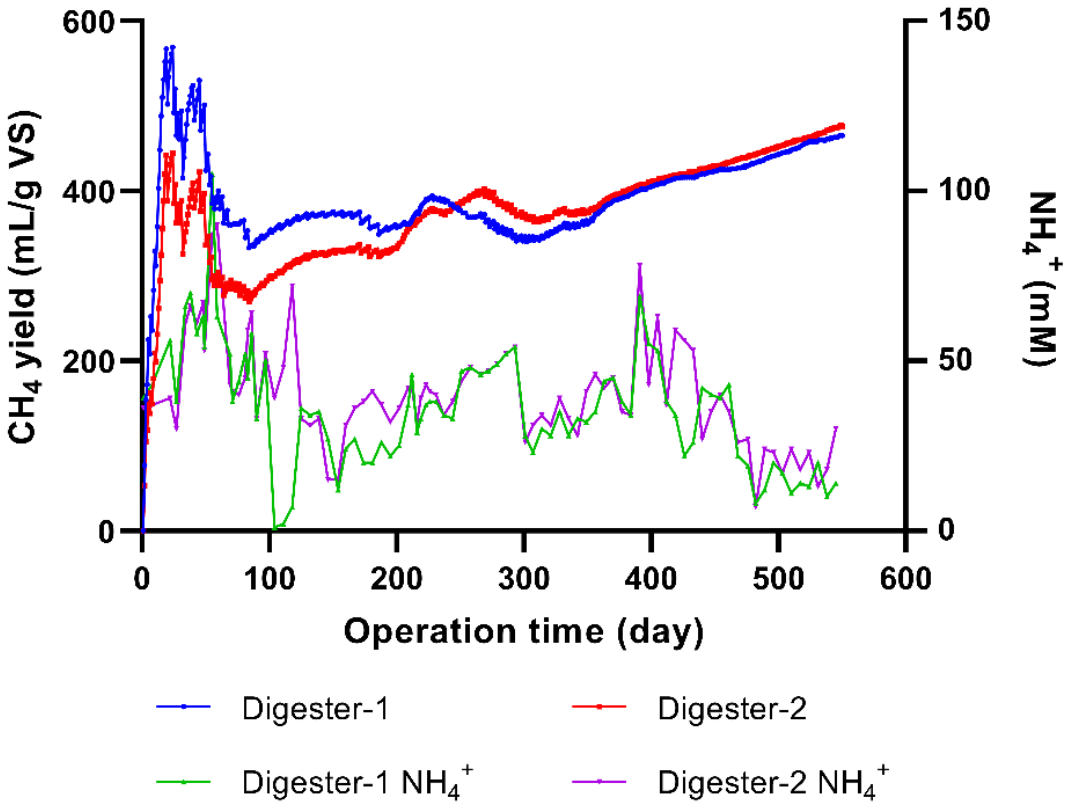

Figure 6.2. Anaerobic digestion of fermented cyanobacteria in duplicate digesters at 21°C using soda lake sediment as inoculum with average loading rate of 0.1 g VS/L d during 550 days of operation.

After 550 days of operation, the OLR was gradually increased to 0.4 g VS/Ld. The methane yield reached a peak at 663 days at about 626 mL/g VS for digesters (Figure 6-3). The NH_4^+ concentration also increased with increased increasing OLR to the highest NH_4^+ value of 495 mM in Digester 1 and 411 mM in Digester 2. These high concentrations of NH_4^+ were above the highest NH_4^+ concentration in batch test, which resulted in 74 % reduction in methane production. Before the NH_4^+ concentration peaked, the methane yield continued to increase. However, when the NH_4^+ concentration reached the peak value, methane yield started to decrease to the last measured value of 400 mL/g VS for Digester 1 and 109 mL/g VS for Digester 2 at 790 days. The average NH_4^+ concentration was 215 mM in Digester 1 and 212 mM in Digester 2, which is about 3.5 times higher than the highest NH_4^+ concentration (60 mM) used in the NH_4^+ inhibition batch tests (Figure 6-1) after increasing the OLR.

The OLR is an important constraint during the AD of cyanobacteria due to a high risk of potential NH_4^+ inhibition. The protein content of the cyanobacterial biomass used in this study was determined to be 61% as shown in Chapter 4. High NH_4^+ accumulation due to degradation of this high protein content limited methane production during AD at high OLR. Samson and LeDuyt (1986) studied AD of protein rich cyanobacterium *Spirulina maxima* biomass (up to 60 % protein) at an OLR of 2.5–10 g /Ld. They reported total ammonia nitrogen accumulation of up to 7000 mg/L (500 mM) causing inhibition of methanogenesis. Using a lower OLR might be beneficial to prevent rapid NH_4^+ accumulation, reducing the risk of inhibition of methanogenesis. A low OLR combined with a low operational temperature (Table 6-2) resulted in a higher methane yield during digestion of protein-rich biomass compared to previous studies.

V

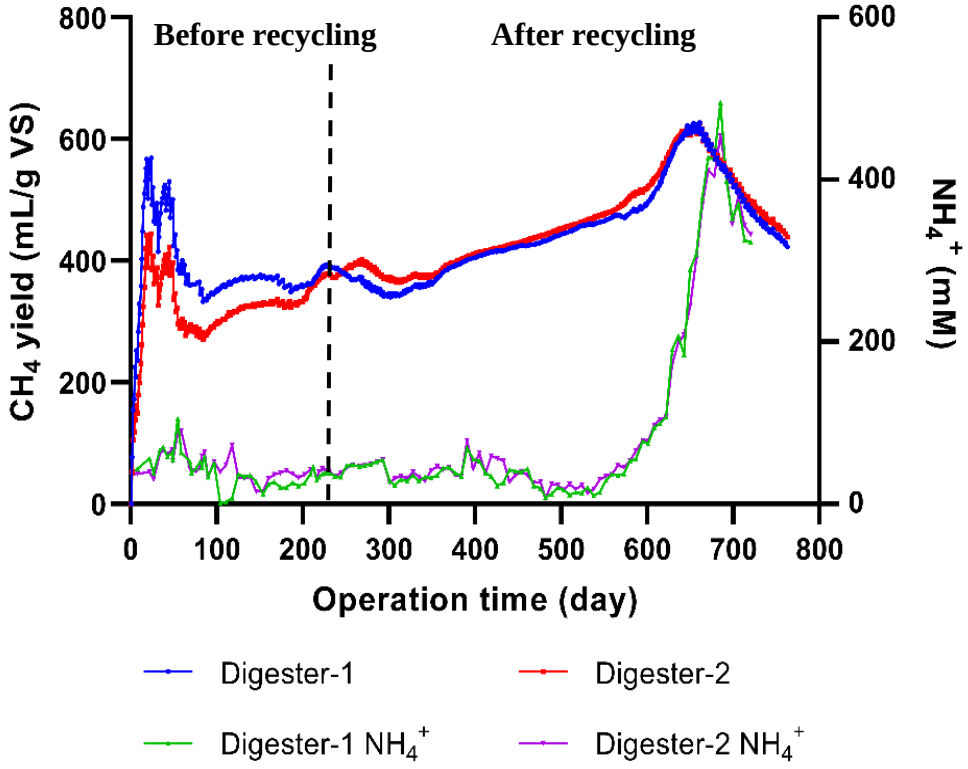

Figure 6.3. Anaerobic digestion of fermented cyanobacteria in duplicate digesters at 21°C using soda lake sediment as inoculum with average loading rate of 0.4 g VS/L d after 550 days of operation.

VFA concentration in both digesters and feed is reported in Figure 6-4. During the 550 days of operation of digesters, average total VFAs concentration in feed, Digester 1 and Digester 2 was 30 mM, 2.3 mM, and 4 mM, respectively. Average VFA conversion into methane was 85 % in Digester 1 and 72 % in Digester 2 during the 550 days of operation. After increasing OLR, NH_4^+ inhibition caused VFA to accumulate up to 113 mM in Digester 1 and 178 mM in Digester 2 due to reduced methanogenic activity and methane conversion.

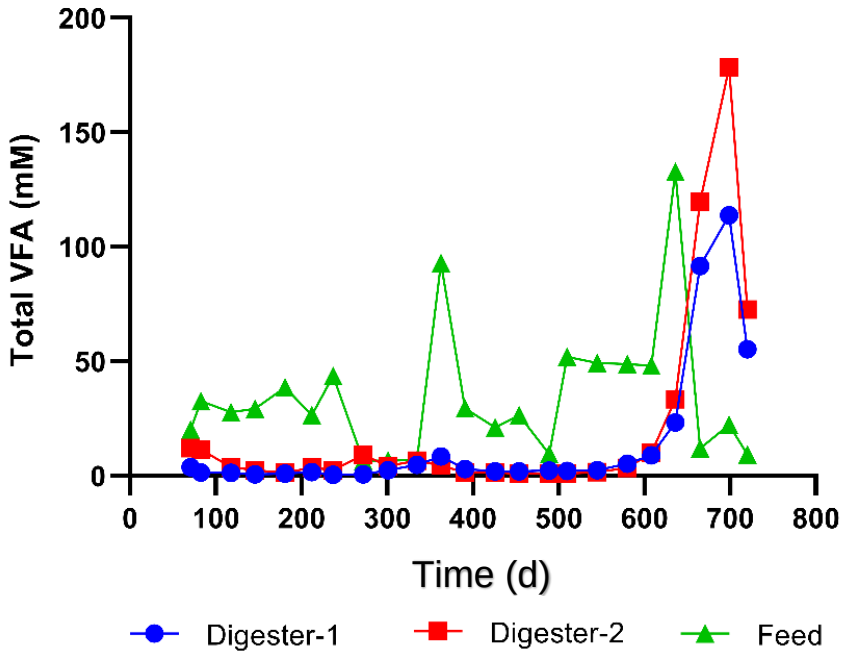

Figure 6.4. Total VFA concentration in feed and in duplicate digesters at 21°C using soda lake sediment as inoculum.

In this study, we used fermentation of cyanobacterial biomass as a pretreatment for anaerobic digestion. This fermentation process was previously shown to produce volatile fatty acids and degrade cyanobacterial cells, resulting in the solubilization of cyanobacterial proteins (Demirkaya et al. 2022). About 10 % (w/w) of the protein consisted of phycocyanin, a high value-added protein-based pigment with applications in food, pharmaceutical and cosmetics industries (Vadlamani et al, 2021). Recovery of phycocyanin as a high value added bioproduct might be beneficial to anaerobic digestion, as it would reduce the protein content in the feed.

6.5 Energy positive methane production from fermented cyanobacteria

Table 6-2 compares the net energy production of experimental microalgae digestion systems. The main components contributing to the energy balance were the energy required for heating ($E_{heating}$)

and the energy produced in the form of methane ($E_{methane}$). High operational temperature and volume of the digester contributed to a higher energy use for heating, while high OLR decreased the value of $E_{heating}$. The amount of energy produced from methane was linearly correlated to the methane yield of each digester. The energy required for pumping and mixing was two to four orders of magnitude smaller than the energy required for heating. The results reported in the present study compare very favourably with previous studies. Indeed, the high methane yield, obtained without heating, led to a positive energy yield. The studies of (González-Fernández et al., 2012) and (Passos and Ferrer, 2015) resulted in negative energy production due to low methane yield and a high operating temperature of the digester. When the heating energy required for the pre-treatment system was included, two other studies of (Schwede et al., 2013) and (Passos and Ferrer, 2014) resulted in a net negative energy production due to the high operating temperature of the pre-treatment systems. This highlights that although pre-treatment systems can be used to increase energy production from microalgae, they often require more energy than they create, and should be critically evaluated through a complete energy balance. Together with the present study, the study of (Golueke and Oswald, 1959) was the only one that resulted in a positive energy balance. That system did not include a pre-treatment step.

The sensitivity of the energy balance to ambient temperature was explored. The threshold ambient temperature at which the present study is no longer energy positive is 12°C. This temperature corresponds to the average temperature of the growing season (May to September) in high latitude countries like Nothern Canada and Scandinavia, demonstrating wide applicability of this treatment system in other areas in the world with warmer climates.

Table 6-2.Energy balance of microalgae digestion systems

Microalgae/Cyanobacteria	**Pre-treatment**	**T**	**HRT**	**OLR**	**CH_4 yield**	**E_{total}**	**$E_{total\ with\ pre\text{-}treatment}$**
		(°C)	*(d)*	*(kgVS/m^3d)*	*(L/kgVS)*		*MJ/kgVS*
Scenedesmus sp[1]	Thermal (90°C, 3h)	35	23	1.7	100	-1.9	-12
Nannochloropsis salina[2]	Thermal (120°C, 8h)	38	120	2.0	270	3.5	-16
Mixed culture[3]	Thermal (95°C, 10h)	37	20	0.73	310	1.5	-22
Mixed culture[4]	Hydrothermal (130°C, 15min)	37	20	0.71	170	-3.6	-17
Mixed culture[5]	No pre-treatment	45	20	nd	402	2.2	2.2
Cyanobacterial consortium	Fermentation (21°C)	21	44	0.1	471	17.8	17.8

HRT = Hydraulic Retention Time

OLR = Organic Loading Rate

nd = not determined, assumed 1.0 as the average loading rate

1 Gonzalez-Fernandez et al., 2012

2 Schwede et al., 2013

3 Passos and Ferrer, 2014

4 Passos and Ferrer, 2015

5 Golueke and Oswald, 1959

* This study

6.6 Conclusion

In this work, we showed successful conversion of fermented cyanobacterial biomass, grown at high pH and alkalinity, into methane at room temperature. Pre-treatment with autofermentation reduces pH and releases high value products (proteins and pigments) while decreasing the pH and ammonia inhibition risk, thus enabling successful AD. Risk of rapid NH_4^+ accumulation and inhibition of methane production due to high protein content was prevented by applying a low OLR and operation at low temperature. Furthermore, this non-heated digestion system had a higher net energy production compared to previous microalgae digestion systems.

6.7 References

Bonk F, Popp D, Weinrich S, Sträuber H, Kleinsteuber S, Harms H, Centler F (2018) Ammonia inhibition of anaerobic volatile fatty acid degrading microbial communities. Front. Microbiol. 9: 2921.

Canon-Rubio KA, Sharp CE, Bergerson J, Strous M, De la Hoz Siegler H (2016) Use of highly alkaline conditions to improve cost-effectiveness of algal biotechnology. Appl. Microbiol. Biotechnol. 100 (4): 1611–1622.

Cioabla AE, Ionel I, Dumitrel GA, Popescu F (2012) Comparative study on factors affecting anaerobic digestion of agricultural vegetal residues. Biotechnol. Biofuels 5: 39.

Demirkaya C, Vadlamani A, Tervahauta T, Strous M, De la Hoz Siegler H (2022) Co-production of hydrogen and organic acids from alkaline cyanobacterial biomass via dark autofermentation. SSRN Electron. http://dx.doi.org/10.2139/ssrn.4082772.

Garlapati D, Chandrasekaran M, Devanesan AA, Mathimani T, Pugazhendhi A (2019) Role of cyanobacteria in agricultural and industrial sectors: an outlook on economically important

byproducts. Appl. Microbiol. Biotechnol. 103: 4709–4721.

Geada P, Vasconcelos V, Vicente A, Fernandes B (2017) Microalgal biomass cultivation. Algal Green Chem. Recent Prog. Biotechnol. 257–284.

Golueke CG, Oswald WJ (1959) Biological conversion of light energy to the chemical energy of methane. Appl. Microbiol. 7: 219.

González-Fernández C, Sialve B, Bernet N, Steyer JP (2012) Thermal pretreatment to improve methane production of *Scenedesmus* biomass. Biomass and Bioenergy 40: 105–111.

Hasunuma T, Matsuda M, Kondo A (2016) Improved sugar-free succinate production by *Synechocystis* sp. PCC 6803 following identification of the limiting steps in glycogen catabolism. Metab. Eng. Commun. 3: 130–141.

Khanra S, Mondal M, Halder G, Tiwari ON, Gayen K, Bhowmick TK (2018) Downstream processing of microalgae for pigments, protein and carbohydrate in industrial application: A review. Food Bioprod. Process. 110: 60–84.

Knoot CJ, Ungerer J, Wangikar PP, Pakrasi HB (2018) Cyanobacteria: Promising biocatalysts for sustainable chemical production. J. Biol. Chem. 293: 5044.

Kuo CM, Jian JF, Sun YL, Lin TH, Yang YC, Zhang WX, Chang HF, Lai JT, Chang JS, Lin CS, (2018) An efficient photobioreactors/raceway circulating system combined with alkaline-CO_2 capturing medium for microalgal cultivation. Bioresour. Technol. 266: 398–406.

Liu D, Zhang L, Chen S, Buisman C, Ter Heijne A (2016) Bioelectrochemical enhancement of methane production in low temperature anaerobic digestion at 10 °C. Water Res. 99: 281–287.

McKeown RM, Hughes D, Collins G, Mahony T, O'Flaherty V (2012) Low-temperature anaerobic

digestion for wastewater treatment. Curr. Opin. Biotechnol. 23: 444–451.

Mohsenpour SF, Hennige S, Willoughby N, Adeloye A, Gutierrez T (2021) Integrating micro-algae into wastewater treatment: A review. Sci. Total Environ. 752: 142168.

Nitsos C, Filali R, Taidi B, Lemaire J (2020) Current and novel approaches to downstream processing of microalgae: A review. Biotechnol. Adv. 45: 107650.

Nolla-Ardèvol V, Strous M, Tegetmeyer HE (2015) Anaerobic digestion of the microalga Spirulina at extreme alkaline conditions: biogas production, metagenome, and metatranscriptome. Front. Microbiol. 6: 597.

Noreña-Caro D, Benton MG (2018) Cyanobacteria as photoautotrophic biofactories of high-value chemicals. J. CO_2 Util. 28: 335–366.

Passos F, Ferrer I (2014) Microalgae Conversion to Biogas: Thermal Pretreatment Contribution on Net Energy Production. Environ. Sci. Technol. 48: 7171–7178.

Passos F, Ferrer I (2015) Influence of hydrothermal pretreatment on microalgal biomass anaerobic digestion and bioenergy production. Water Res. 68: 364–373.

Pendyala B, Hanifzadeh M, Ameh Abel G, Viamajala S, Varanasi S (2020) Production of organic acids via autofermentation of microalgae: a promising approach for sustainable algal biorefineries. Ind. Eng. Chem. Res. 59 (5): 1772–1780.

Samson R, LeDuyt A (1986) Detailed study of anaerobic digestion of *Spirulina maxima* algal biomass. Biotechnol. Bioeng. 28: 1014–1023.

Schwede S, Rehman ZU, Gerber M, Theiss C, Span R (2013) Effects of thermal pretreatment on anaerobic digestion of *Nannochloropsis salina* biomass. Bioresour. Technol. 143: 505–511.

Solé-Bundó M, Passos F, Romero-Güiza MS, Ferrer I, Astals S (2019) Co-digestion strategies to enhance microalgae anaerobic digestion: A review. Renew. Sustain. Energy Rev. 112: 471–482.

Udayan A, Sirohi R, Sreekumar N, Sang BI, Sim SJ (2022) Mass cultivation and harvesting of microalgal biomass: Current trends and future perspectives. Bioresour. Technol. 344: 126406.

Vadlamani A, Viamajala S, Pendyala B, Varanasi S (2017) Cultivation of microalgae at extreme alkaline ph conditions: a novel approach for biofuel production. ACS Sustain. Chem. Eng. 5: 7284–7294.

Vadlamani A, Demirkaya C, Zorz J, De la Hoz Siegler H, Strous M (2021) Alkaliphilic consortium shifting for production of phycocyanins and biochemicals.

Yenigün O, Demirel B (2013) Ammonia inhibition in anaerobic digestion: A review. Process Biochem. 48: 901–911

Yukesh Kannah R, Kavitha S, Parthiba Karthikeyan O, Rene ER, Kumar G, Rajesh Banu J (2021) A review on anaerobic digestion of energy and cost effective microalgae pretreatment for biogas production. Bioresour. Technol. 332: 125055.

Zheng Q, Xu X, Martin GJO, Kentish SE (2018) Critical review of strategies for CO_2 delivery to large-scale microalgae cultures. Chinese J. Chem. Eng. 26: 2219–2228.

CHAPTER 7

Pre-feasibility Study of a Cyanobacteria-based Biorefinery

This chapter provides a preliminary assessment of the technoeconomic feasibility of a cyanobacterial based biorefinery to produce phycocyanin, hydrogen, oxygen, and methane via autofermentation and anaerobic digestion.

7.1 Introduction

Cyanobacteria are potential feedstocks for the production of biofuels and value-added products. Consideration for their use towards a possible biorefinery have increased in recent years due to the following advantages: high fixation rate of carbon dioxide, elevated biomass growth rate; high protein content, and potential to produce several value-added products such as polysaccharides, peptides, biopolymers, antioxidants, and pigments. However, the main bottlenecks of cyanobacterial-based biofuels and value-added products are the elevated production costs and the high energy requirements of harvesting and downstream processing. Hence, new cultivation, harvesting and downstream processing approaches are required to enable the success of cyanobacteria-based bioprocesses. The use of high pH and alkalinity has been identified as an alternative production pathway to increase the feasibility of cyanobacterial systems.

A biorefinery approach, with multiple concomitant high value-added products as well as one or more energy products, also allows for enhanced economic feasibility. As shown in previous chapters, the autofermentation of the alkaline cyanobacterial biomass results in the formation of multiple valuable products (phycocyanin, organic acids, and hydrogen), and the anaerobic digestion of the residual biomass produces an energy product (i.e., methane); thus, the proposed processes are suitable to be combined in a biorefinery approach.

Autofermentation under solid state conditions resulted in the release of a valuable protein-based pigment from the cyanobacterial biomass (Zorz et al., 2022). Phycocyanin is a natural blue pigment that is used as a colorant for food and cosmetic industries and is one of the most valuable protein-based products that can be obtained from cyanobacteria. Direct production of phycocyanin from cyanobacteria is expensive as it requires the degradation of cells, extraction, and separation of phycocyanin. However, during the autofermentation process, lysis of the cyanobacterial cells

released phycocyanin without any additional pretreatment or extraction steps. Furthermore, autofermentation at solid state conditions results in more concentrated phycocyanin content than other extraction processes (e.g., freezing and thawing, homogenizer, ultrasound, microvave), which makes the separation process easier and more energy efficient.

The market for phycocyanin has been expanding due to the growing demand for natural ingredients and functional foods (Thevarajah et al., 2022). To support market expansion and to ensure the sustainability of this emerging industry, further optimization of current methods for the production, extraction, and purification of phycocyanin is needed. The integration of direct air capture of carbon dioxide with alkaline cyanobacterial biomass production, autofermentation, and AD is a promising pathway to simultaneously produce phycocyanin, hydrogen, organic acids, and methane. Phycocyanin, which commands the highest market price, provides a key economic driver, while methane and hydrogen, with a much higher market volume albeit lower price, help to provide scalability. The direct capture of CO_2 provides additional environmental benefits and results in a fully circular process.

In this chapter, a preliminary assessment of an integrated cyanobacterial biorefinery is conducted. Mass and energy balances were performed for a pilot-scale facility able to process the output of a 1 ha (i.e., 10000 m^2) alkaline cyanobacterial biomass cultivation system. Sizing and preliminary capital cost estimation for each required processing equipment was used in combination with the expected biorefinery revenues to estimate the potential economic profitability of this pilot facility.

7.2 Process description

The integrated process for the cultivation of cyanobacteria at high alkaline and high pH conditions and conversion of this biomass into high value-added products and methane, consists of photobioreactors (PBRs), harvesting (centrifugation/settling), autofermentation, anaerobic digestion, air/flue gas contactor, and CO_2 scrubber, as shown in Figure 7-1. In the air/flue gas contactor, recovered media after harvesting is purged with air/flue gas to absorb CO_2. The high pH and alkalinity of the liquid culture medium enable an enhanced CO_2 absorption rate from the flue gas entering the system. The CO_2 enriched stream goes to the CO_2 scrubber to separate CO_2 and CH_4 coming from the AD process to allow further CO_2 capture and carbon neutral process. The pH of the culture medium decreases as CO_2 is absorbed into it (Caceres-Falla, 2020).

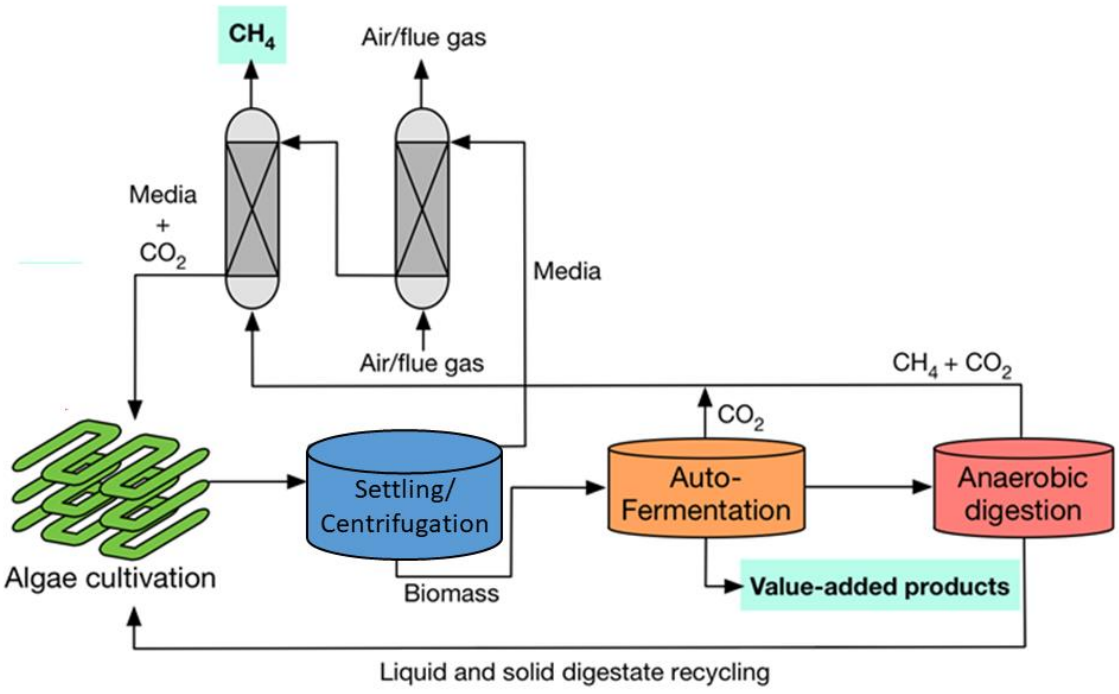

Figure 7.1. Process Flow Diagram for the integrated high alkaline and high pH cyanobacteria cultivation process and high value-added product recovery process.

The alkaline medium that leaves the CO_2 scrubbers is then fed to the tubular PBRs. The tubular polyethylene PBRs are ideal to maximize light capture as well as easy to manufacture, scale up, and more sustainable for outdoor use due to their large illumination surface area. The use of high alkalinity and high pH allows more buffering capacity and CO_2 supply which then improves volumetric biomass productivity. Increased cell density further makes the harvesting process easy, eliminates the need for cost intensive harvesting methods (centrifugation), and improves cost-effectiveness.

In this process, two types of separation processes, natural settling, and centrifugation are used to harvest and recover the biomass. The cyanobacteria *Candidatus* "P. alkaliphilum" can settle naturally. Harvesting biomass by natural settling is a cost-effective, effortless, and simple technique, as the process does not require any energy input or the addition of chemicals. However, this process is time consuming and does not remove all the alkaline, high pH media, which is inhibitory to the anaerobic digestion step, as shown in Chapter 5. Furthermore, most of the valuable proteins including phycocyanin are degraded during fermentation after natural settling due to high pH. Therefore, centrifugation is used here to further concentrate the biomass and remove most of the alkaline, high pH media. A combination of centrifugation and natural settling reduces the cost and energy requirements compared to direct centrifugation as most of the media is removed via natural settling and centrifugation only processes a reduced volume of pre-concentrated biomass slurry. By settling, the concentration of biomass can be increased up to 1% total solid. By centrifugation the concentration of biomass can be increased up to 20% total solid.

After harvesting, the biomass slurry is pumped into the autofermentation tank; autofermentation serves the purpose of reducing the pH of the cyanobacterial slurry, which limits the potential for inhibition of methanogens during the anaerobic digestion step. During autofermentation storage

carbohydrates are converted into organic acid, which reduces high pH of the cyanobacterial slurry. Therefore, it enables anaerobic digestion of the cyanobacterial slurry. Autofermentation results in the production of valuable products such as phycocyanin and hydrogen that can be recovered to improve the economic viability of the process.

Recovery of hydrogen can be directly done by pumping out and the compression of the head space from the fermentation process as autofermentation results in pure hydrogen production as produced CO_2 is absorb due to high pH. During fermentation, liquefaction occurs and up to 50% of the biomass solubilizes due to the degradation of cells, release of cell content, and conversion of soluble organic content into organic acids. Extraction and separation of phycocyanin from the fermentation broth is critical for this process, as the recovery of phycocyanin can significantly improve the economic viability of the process. Dilution of slurry can be done in 1:1 ratio just to enable separation of biomass and liquid phase with a filtration system. The rotary drum is partially submerged in the harvested algal feed. Water in the algae feed is drawn into the drum through the filter medium to the low-pressure zone with a vacuum pump. Biomass accumulates on the outer surface of the filter and forms a cake layer. The water separated from biomass can be removed with a water pump. After separation of gas phase and liquid phase, waste biomass is used as feedstock for biogas production via anaerobic digestion for further utilization of the biomass to produce energy. The organic loading rate was assumed as 0.11 kgVS/m^3d with a biomass feed of 43 kgVS/d. Based on Chapter 6, hydraulic retention time was assumed as 44 days. Biogas usually consists of 65% methane and up to 35% CO_2. CO_2 from the AD process is used to replenish bicarbonate concentration in the recovered media for microalgae growth via CO_2 absorption column. The bicarbonate ions decrease in the recovered media because the oxygen, carbon and hydrogen are being used by the algae in its growth cycle. As a result, the equilibrium is displaced

increasing the concentration of carbonate ions, elevating the pH at the end of cultivation. The change in the equilibrium allows carbon in the media to be replenished by introducing CO_2, which is an acid gas, to lower down the pH to normal cultivation values and replenish the CO_2. Furthermore, the CO_2 amount obtained from AD process is not enough to replenish the carbon content of the media thus, thus additional CO_2 from flue gas is needed. After AD, solid digestate is recycled back to AD to prevent microbial loss, while the liquid digestate is used as a nutrient source for cyanobacterial growth. Furthermore, recycling both digestate streams aims to reduce the waste and cost of cyanobacterial biomass cultivation by reducing nutrient needs.

7.3 Overall mass balance

The mass balance around each unit was done based on the experimental values obtained in previous chapters. Major assumptions and methodological simplifications are described below.

7.3.1 Assumptions

The mass balance around the plant was calculated on a total mass basis of each component for each unit in the process per day. Initial assumptions for calculations are given below.

- The cyanobacterial biomass is 50% carbon in total dry biomass.
- The initial inoculum is 0.2 kg dry cyanobacterial biomass/L.
- Cultivation period of 4 days.

The yearly production of cyanobacterial biomass as estimated based on average solar radiation is received in Calgary each month. The average monthly solar radiation and temperature data were obtained from Engineering Climate Datasets - Environment and Climate Change Canada (2022). The average of 5 previous years of solar radiation was used to calculate the biomass growth for each month. The relationship between solar radiation each month and biomass productivity data are given in Figure 7-2. Average yearly biomass production was determined as 3631 kg/day.

The water and nutrient requirements to reach the target biomass production are given in Table 7-1. The main nutrients consumed during cultivation are bicarbonate, nitrate, ammonium, and iron. Potassium, manganese, cobalt, nickel, copper, and zinc are also consumed, although in smaller quantities. These nutrients need to be replenished after each cultivation cycle. After settling, up to 90% of the media can be separated and recycled back to the cultivation process further to reduce the water and nutrient requirement of the cultivation system. Ten percent of the concentrated biomass is also recycled back to the cultivation system to start the new growth cycle.

Figure 7-3 and Figure 7-4 provide information on the mass of each streams enter and leave each unit.

7.3.2 Input data from experimental results

After settling, the biomass slurry is further concentrated to 20% solid content (i.e., 219 g DW/ L) via centrifugation. Phycocyanin with a high purity is released due to the degradation of cyanobacterial cells during autofermentation at this biomass concentration. Up to 0.68 gr phycocyanin per kg biomass can be recovered from fermentation. Under these conditions up to 0.15 kg of organic acid and 0.006, m^3 of H_2 can be produced per kg of biomass. Although the organic acid and H_2 production are significantly lower than the natural settling, six times higher methane conversion (0.60 kg COD CH_4/ kg COD) occurs due to neutral pH. 0.36 m^3 of CH_4 can be obtained per kg of biomass.

Table 7-1. Water and nutrient requirement for 1 ha cyanobacterial biomass cultivation system.

Material	System Requirement	After the growth	Unit
Cyanobacterial Biomass	288.70	3175.71	kg/day
Water	3.261983.1985	3.262258.7465	Gg/day
Carbonate	41.29	47.04	ton/day
Bicarbonate	15.49	3.80	ton/day
Nitrate	618.91		kg/day
Ammonium	54.13		kg/day
Potassium	1.14	1.10	ton/day
Phosphate	450.95	381.96	kg/day
Calcium	22.22	18.76	kg/day
Magnesium	79.28	69.96	kg/day
Sulfate	313.34	267.32	kg/day
Iron	7.28	1.40	kg/day
Manganese	226.4	4.2	mg/day
Cobalt	12.1	5.1	mg/day
Nickel	8.1		mg/day
Copper	18.2		mg/day
Zinc	31.3		mg/day
Boron	342.2	316.1	mg/day
Sodium	37.71	37.71	ton/day
Chloride	804.83	804.83	ton/day

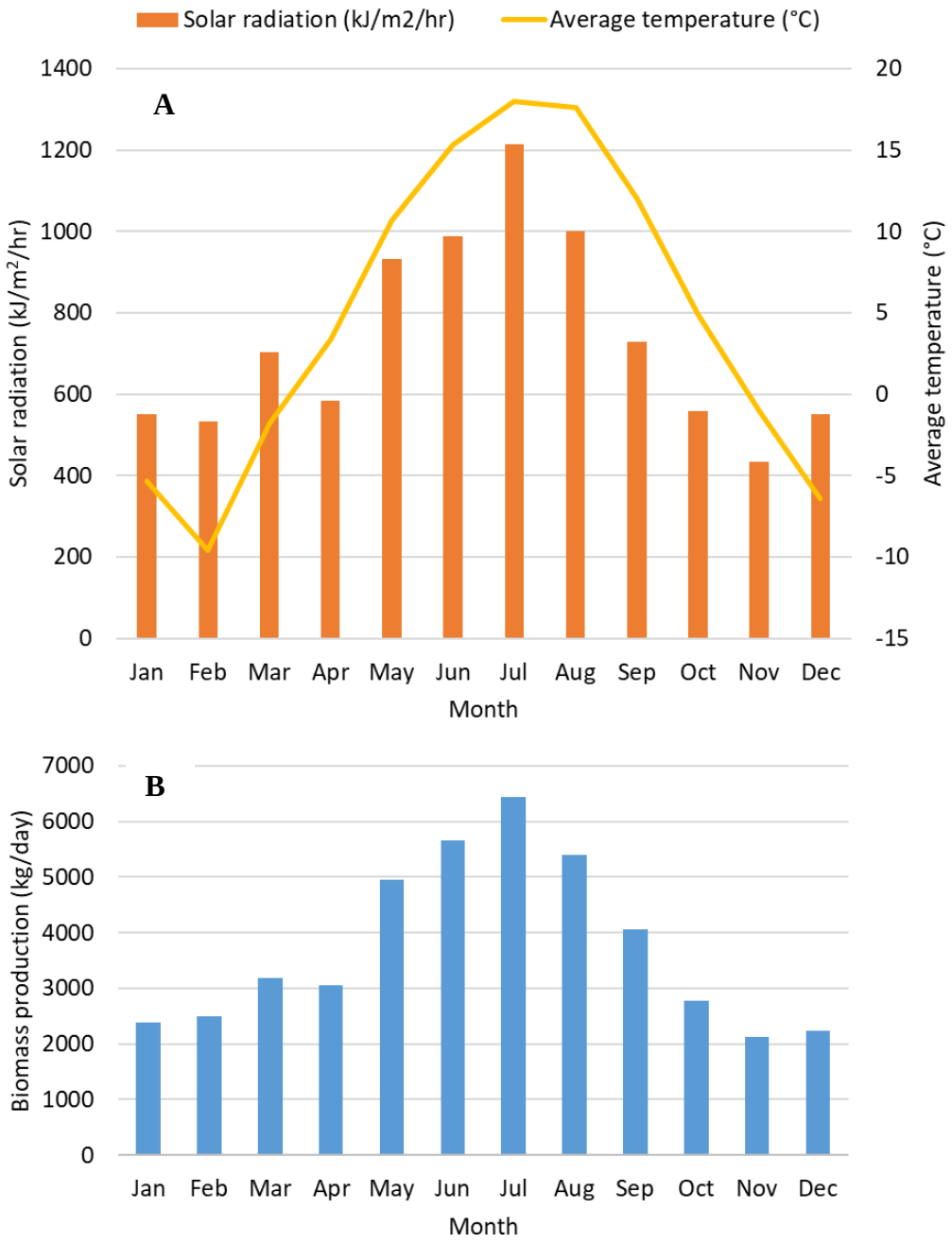

Figure 7.2. (A) Monthly solar radiation and average temperature in Calgary and (B) biomass productivity of the 1-ha tubular PBR system.

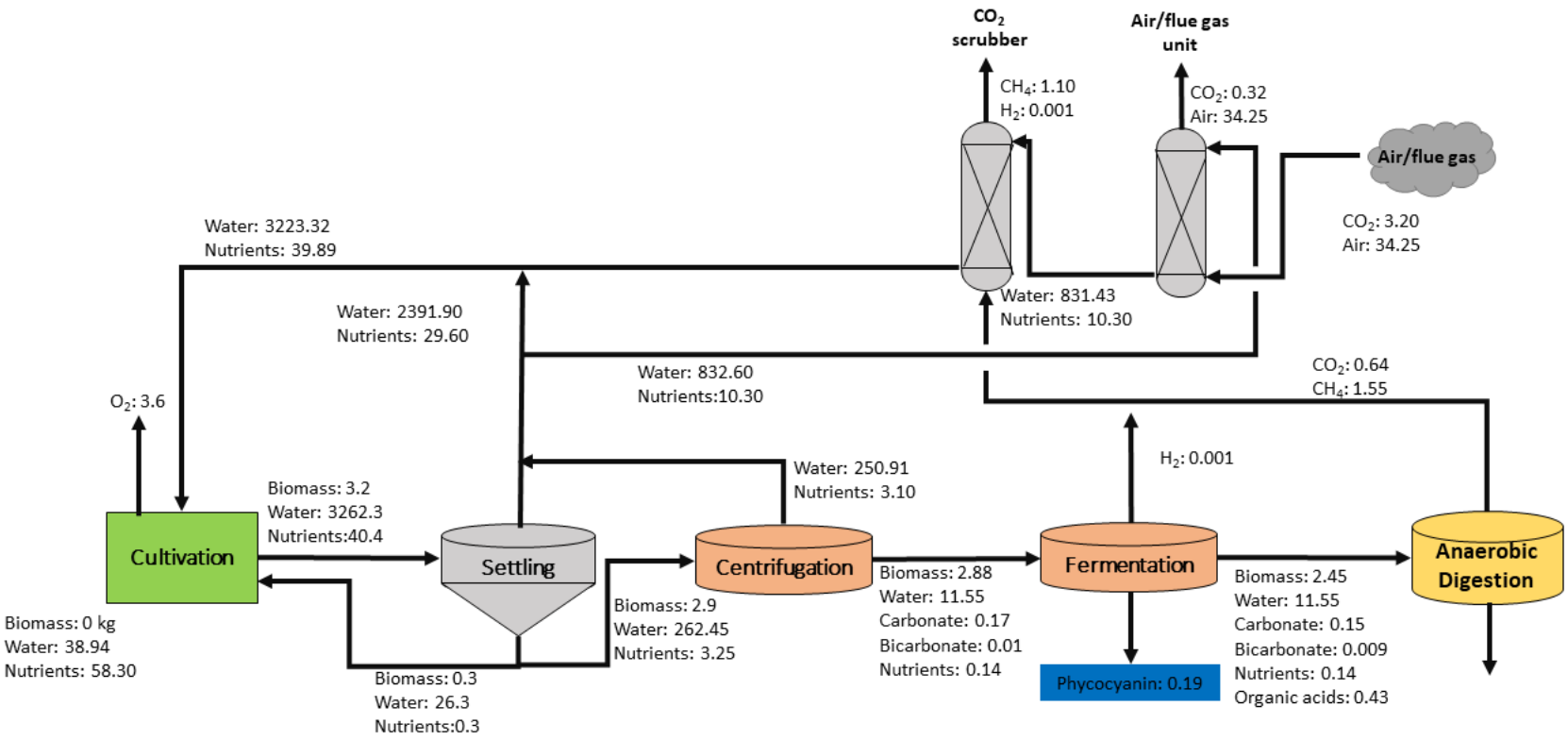

Figure 7.3. Mass balance for the integrated high alkaline and high pH cyanobacteria cultivation process and high value-added product recovery process. Mass flows are given in tons/day.

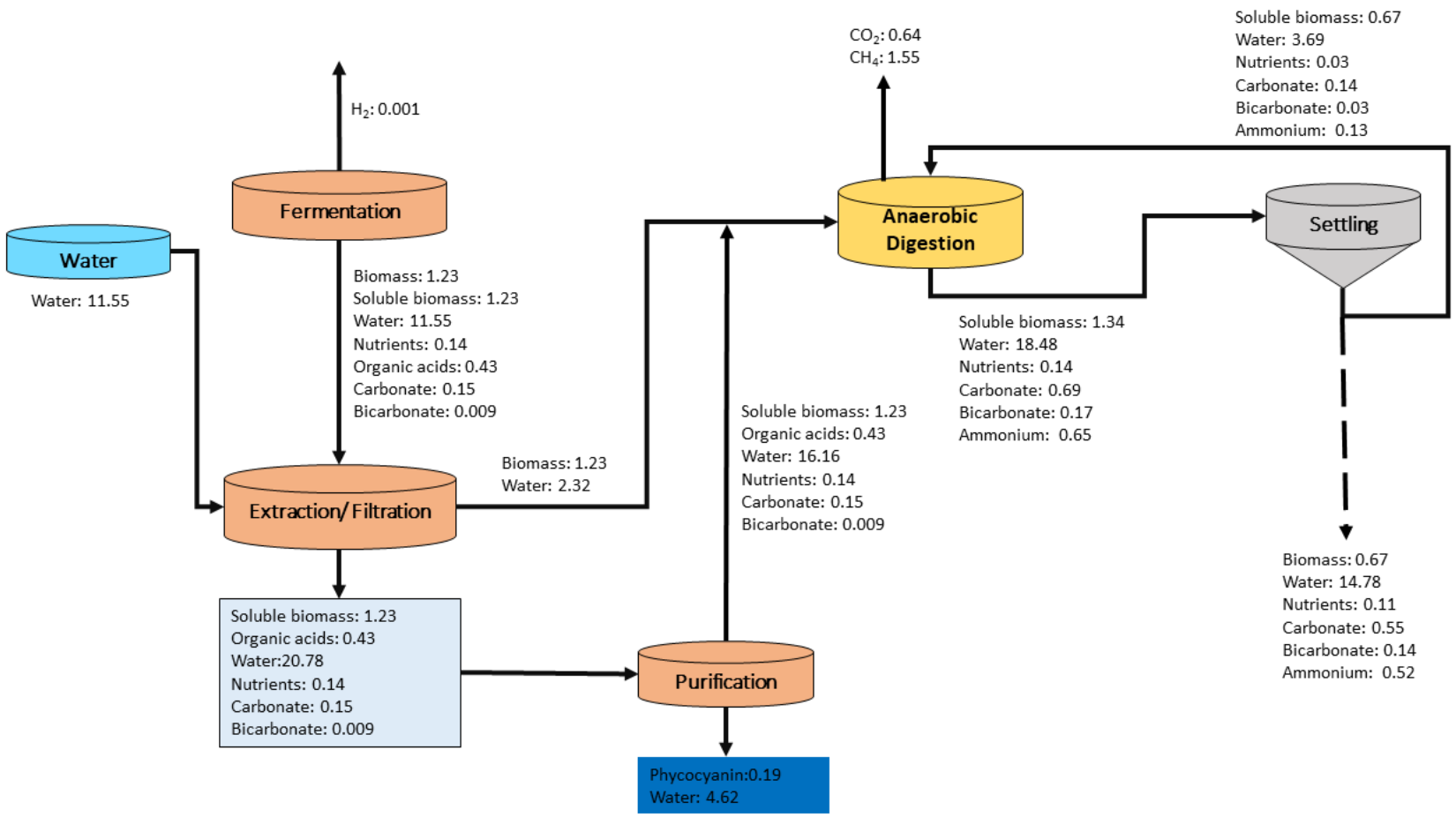

Figure 7.4. Mass balance for the integrated high alkaline and high pH cyanobacteria cultivation process and high value-added product recovery process. Mass flows are given in tons/day.

7.4. Equipment sizing and energy calculations

7.4.1. PBR

Biomass productivity (g $m^{-2}day^{-1}$) in tubular photobioreactors (PBRs) is affected by seasonal variability, tube spacing, PBR directional orientation, and culture conditions such as pH, temperature, aeration rates, and culture velocity. Closed PBR cultivation systems have better temperature control, less water loss due to evaporation, and reduced risk of contamination relative to other cultivation systems. They also provide higher areal productivity. A closed tubular PBR system was chosen for cyanobacterial biomass production. Areal productivity values for closed tubular photobioreactors are provided in Table 7-2 Sizing of polyethylene tubular photobioreactor was done based on the volume and surface required to produce the amount of biomass calculated in Section 8.3.1 using the equations from 1-3.

Table 7-2. Biomass productivity reported in literature for tubular PBR systems.

Location	Reactor orientation	Latidue	Areal productivity (g $m^{-2}day^{-1}$)	Reference
Netherlands	Horizontal	51.9812° N	12.6	(Slegers et al., 2013)
France	Horizontal	46.2276° N	19.5	(Slegers et al., 2013)
Algeria	Horizontal	28.0339° N	26.5	(Slegers et al., 2013)
Netherlands	Vertical	51.9812° N	19.4	(De Vree et al., 2015)
Netherlands	Horizontal	51.9812° N	12.1	(De Vree et al., 2015)
Alberta	Horizontal	51.0447° N	5.6	(Haines et al., 2022)

(Eq.7.1) $$Surface\ area = 2\pi L$$

(Eq.7.2) $$Volume = \pi r^2 L$$

(Eq.7.3) $$Number\ of\ tubes = \frac{100\ m}{Tube\ length}$$

Assumptions:

1. Required volume (V): 400 m^3

2. Length of the tube (L): 0.5
3. Diameter of the tube (D): 0.05 m
4. Surface area (A): 0.08 m^2
5. Number of tubes: 654545
6. Areal productivity: 0.012 $kg/m^2/day$

7.4.2. Settling tank

A lamella clarifier or inclined tube settler is a type of high efficient setter designed to remove particulates from liquids. Compared with conventional clarifier, treatment capacity of lamella clarifier is increased 7-10 times with inclined tube set up. a carbon steel with PVC inclined tube lamella clarifier with a 30 m^3 (5.6×2.2×2.5 cm) volume was chosen. To harvest 400 m^3 culture, 14 pieces of carbon steel, inclined tube lamella clarifier is needed.

7.4.3. Centrifuge

A disc stack centrifuge is chosen as it can provide quick and efficient separation of solids and liquids. Although disc stack centrifuges require high centrifugation force and power to operate, the removal of up to 90% of the cultivation media in the settling phase, reduces the energy required for further harvesting. Power calculations were done based on the equations from 4 to 12 (Saglam, 2020).

Specifications of the disc stack centrifuge and assumptions:

1. Operating speed (ω): 5800 rpm = 607.06 rad/s
2. The outer radius of the bowl: 0.34 m
3. Coefficient of friction (c_f): 0.006
4. The density of air (ρ_{air}): 1.127 kg/m^3
5. The minimum radius of the water layer ion the centripetal pump chamber (r_c): 0.0714 m

6. The density of water (ρ_{water}): 992.1 kg/m^3
7. Flow rate: 0.0005 m^3/ sec

Total power needed for centrifugation:

(Eq.7.4) $$P_{total} = P_{air\ friction} + P_{Mechanical} + P_{flow} + P_{electrical}$$

Power loss due to friction:

(Eq.7.5) $$P_{air\ friction} = \frac{2\times\pi\times\rho\times\omega^3\times R^5\times c_f}{5}$$

Power loss due to flow:

(Eq.7.6) $$P_{flow} = \rho \times Q \times \omega^2 \times {r_c}^2$$

Mechanical losses:

(Eq.7.7) $$P_{idle} = P_{air\ friction} + P_{Mechanical}$$

(Eq.7.8) $$P_{mechanical} = P_{idle} - P_{air\ friction} - P_{electrical,idle}$$

Electrical losses:

(Eq.7.9) $$\eta_{\ electrical} = \eta_{\ VDF} \times \eta_{\ motor}$$

(Eq.7.10) $$\eta_{\ electrical,total} = 0.91\ (motor\ efficiency\ is\ chosen\ for\ 75\%\ load)$$

(Eq.7.11) $$\eta_{\ electrical,idle} = 0.90\ (motor\ efficiency\ is\ chosen\ for\ 50\%\ load)$$

(Eq.7.12) $$P_{electrical} = P_{total} \times \frac{1-\eta_{\ electrical}}{\eta_{\ electrical}}$$

7.4.4. Fermentation tank

After centrifugation, the volume of the biomass slurry is reduced to 12 m^3. A stainless steel, conical bottom tank with a total volume of 16 m^3 is chosen for the batch autofermentation stage. Autofermentation can take up to 4 days to release phycocyanin and reach the highest titer for organic acid under these conditions. To accommodate the 12 m^3/day flow, 5 conical bottom tanks are needed.

7.4.5. Extraction/filtration

After extraction, biomass and extract were assumed to be separated with a rotary drum filter system. Rotary vacuum drum filter is one of the oldest filters used in the industrial liquid-solids separation. It offers a wide range of industrial processing with a continuous and automatic operation, low cost, easy modification for different applications, and easy cleanin procedures. Specification of the rotary drum filter is given below. The energy requirement of the rotary drum filtration system was done based on equations from 13 to 18 (Shao et al., 2015).

Specifications of the disc stack centrifuge and assumptions:

1. Drum diameter: 0.9 m
2. Drum length: 0.6 m
3. Working area: 1.69 m2
4. Vacuum pressure ranges fom10 kPa
5. Filter rotation cycle time: 10 to 120 s

Total energy requirement:

(Eq.7.13) $$W_{total} = W_{water\ pump} + W_{vacuum} + W_{rotation}$$

Energy consumed by water pump:

(Eq.7.14) $$W_{Water\ pump} = F_{Feed}(1-\emptyset)(p_{ambient} - p_{vacuum\ receiver})\frac{1}{\eta}$$

(Eq.7.15) $$p_{vacuum\ receiver} = p_{filtration} - \rho_{water} gR - \Delta p_{resistance}$$

(Eq.7.16) $$\Delta p_{resistance} = 0.5\rho_{water} gR$$

where R is the radius of the filter drum, and g is the energy efficiency of the water pump.

Energy consumed by vacuum:

(Eq.7.17) $$W_{vacuum} = \frac{kN_{air}RT}{k-1}\left[\left(\frac{p_0}{p_{dewatering}}\right)^{\frac{k-1}{k}} - 1\right]\frac{n}{\eta}$$

where k is the ratio of heat capacities of air at constant pressure and constant volume, N_{air} is the air flow rate, and p_0 is the atmospheric pressure.

Energy consumed by rotation:

(Eq.7.18) $$W_{rotation} = \left(\frac{2A\mu\omega^2 R}{3} . \frac{1}{1-\gamma^2} . \frac{MgR\omega}{16}\right)\frac{n}{\eta}$$

where ω is the angular velocity of the rotating drum filter, γ is the ratio of the radius of the drum filter to that of the feed tank, the first term is the drag force experienced by the rotating filter in the feed tank, and the second term is the torque resistance.

7.4.6. Anaerobic digestion

A stainless steel continuously stirred reactor (CSTR) design was chosen for AD process. Compared to other configurations, the CSTR provides greater uniformity of system parameters, such as temperature, mixing, chemical concentration, and substrate concentration. Based on this assumption, the total digester volume becomes 391 m^3. Ten digesters with a volume of 39.1 m^3 each were designed for the anaerobic digestion of waste biomass after the recovery of phycocyanin. Based on the volume and sizing equations, the diameter of the digester was found to be 3.2 m, while the height was 4.8 m. The required impeller size was calculated as 1.4 m with a speed of 200 rpm. For energy calculation, ambient temperature and the operational temperature of digesters were assumed as 21°C.

Digester volume:

(Eq.7.19) $$Volume: \pi r^2 h$$

(Eq.7.20) $$\frac{Digester\ height}{digester\ diameter} = 1.5$$

The energy required for pumping:

(Eq.7.21) $$Pressure\ loss(Pa) = \rho g d h$$

(Eq.7.22) $$Powet\ usage\ (J) = dpQ$$

The energy required for mixing:

(Eq.7.23) $$P = N_p \rho N^3 d^5$$

where ρ is the fluid density, N_p is the power number, d is the impeller diameter, and N is the impeller speed.

The energy required for heating:

(Eq.7.24) $$Heat\ loss = -kA\frac{dT}{dx}$$

(Eq.7.25) $$Energy\ required\ to\ heat\ influent: dQ = mCdT$$

where C is the heat capacity of water, k is the thermal conductivity, dx is the digester wall thickness, dT is the temperature difference, A is the surface area of the digester.

7.4.7. CO_2 absorption column

For CO_2 absorption column, packed absorption contactor was used to provide increased surface area for liquid and gas stream to interact. PVC was chosen as materials. Interaction between alkaline media and CO_2 rich stream allow absorption of CO2 and replenish carbon content in the media. This CO_2 absorption column was designed by Caceres Falla, (2020), who was a master's degree student in this research team. The column design, the cost and energy were done for both flue gas and direct air capture. The cost and energy required for direct air capture were found 52 and 36 times higher than the flue gas operated column. Because of this reason, a flue gas operated system was chosen to enrich alkaline media with CO_2.

7.5 Energy requirements

Energy requirements for each unit were calculated based on the assumptions and equations provided in section 7.4. The energy requirement for each unit is given in table 7-3. The energy return on energy investment (EROI), defined as the ratio between the energy output and the energy input of the system. A positive EROI value of 14.7 was calculated for integrated high alkalinity

and high pH cultivation system with anaerobic digestion by previous researcher in the team (Canon-Rubio et al., 2016).

Table 7-3. Energy requirements to operate each unit.

Equipment	Energy (kWh)
Pumping from CO_2 scrubber to cultivation	151.2
Pumping from settling to fermentation	4.6
Pumping from settling to air/flue gas unit	31.2
Pumping from fermentation to rotary drum separator	4.2
Mixing of anaerobic digestion	46.0
Blower	288.7
Pumping from air/flu to CO_2 scrubber	74.4
Centrifugation	480.0
Rotary drum separator	5.6
Total	1085.9

7.6 Capital and operation cost estimation

Capital cost calculations were estimated based on the cost to purchase each piece of equipment, and the cost for installations, piping, and construction. Equipment investment cost was calculated based on costs previously reported for similar equipment and using the Matches platform. For reported equipment cost, the currency was converted into US dollars using the exchange rates of the reported year. Then, the conversion of the price at the reported volume into the price at the volume calculated for the equipment was made based on Equation 26.

Eq 26. $$Cost_{\ 1} = Cost_2 \left(\frac{Volume_{\ 1}}{Volume_2}\right)^n$$

where n is the scale-up factor and is usually reported as 0.6.

Second, the Matches platform provides conceptual process equipment cost estimates based on the type, material, and dimension of a given piece of equipment. It provides cost estimation based on the Chemical Engineering Plant Cost Index (CEPCI) for 2014 (556.8) in USD. The cost estimation was corrected for the CEPCI for 2022 (824.5). Economic evaluation of integrated alkaline

cyanobacterial cultivation system with autofermentation and anaerobic digestion is given in Table 7.4. Capital investment was done based on each equipment purchase cost estimation of capital investment by percentage of delivered equipment method. Operational cost estimation was done based on total energy and raw material required to run the proposed cyanobacterial biorefinery. Liquid processing estimation was done as most of the processes are in liquid phase (cultivation system, harvesting, separation, anaerobic digestion, CO_2 absorption column). Salary of one operator per shift for three shifts was also included. Estimations were done based on 10-year depreciation and internal rate of return of 15% (Peters and Timmerhaous, 1991).

Table 7-4. Economic summary of integrated biorefinery. Numbers are reported in Thousands of US$ in 2022 (Peters and Timmerhaous, 1991).

Cost year basis	2023 $
Total phycocyanin production	100.92 tones/year
Phycocyanin price	$ 120
Internal rate of return	15 %
Return on investment	35.6 % per year
Payback period	2
Net return	3530 Thousands in $US
Net present worth	15830 Thousands in $US
Discounted cash flow rate of return	15.2 % per year

Estimation of capital investment by percentage of delivered equipment method

Equipment	Purchasing Cost
PBR	822
Settling	173
Centrifuge	21
Fermentation	265
Rotary drum separator	81
Anaerobic digestion	493
CO_2 capture unit	113
Total	2,564

Operation cost

Item	Cost
Chemicals	11
Labour	294
Electricity	41
Water	1.6
Total	348

Item	%	Cost
Purchased equipment		2,564
Delivery	0.1	256
Subtotal: delivered equipment		2820
Purchased equipment installation	0.47	1326
Instrumentation and Controls(installed)	0.36	1015
Piping (installed)	0.68	1918
Electrical systems (installed)	0.11	310
Buildings (including services)	0.18	508
Yard improvements	0.1	282
Service facilities (installed)	0.7	1,974
Total direct costs	2.6	10,153
Indirect Costs		
Engineering and supervision	0.33	931
Construction expenses	0.41	1,156
Legal expenses	0.04	113
Contractor's fee	0.22	620
Contingency	0.44	1,241
Total indirect costs	1.44	4,061
Fixed capital investment (FCI)		14,215
Working capital (WC)	0.89	2510
Total capital investment (TCI)		16,725

7.7. Yearly production of value added products

Based on the monthly biomass production determined in section 7.3.1, the production amount of phycocyanin, oxygen, hydrogen, and methane were determined (Table 7-7). Phycocyanin was determined as the main product of the process with a price range of $120 per kg to $251 per mg for different applications. Oxygen and methane are other major products in terms of production amount. Recovery of these products can further improve the economics of the process. The estimated methane production can supply low carbon neutral energy to 52 homes in Calgary. Although hydrogen production was much lower compared to other products, hydrogen price is higher at $13 per kg compared to methane and oxygen with a price of $3.35 and $1.45 per kg, respectively. Recovery of hydrogen further can be beneficial to obtain an economically feasible biorefinery approach.

Table 7-5. Total annual production per year per ha.

Product	Amount	Unit	Price	Annual value of product, thousands of US$
Biomass	49,274	kg/day		
Phycocyanin	3,364	kg/day	120 $US/kg	12,110
O_2	35,867	m^3/day	1.35 $US/ m^3	2,076
H_2	296	m^3/day	13 $US/ m^3	9.4
CH_4	17,738	m^3/day	3.35 $US/ m^3	1,087

Based on the capital, operational cost and annual value of production, yearly return on the investment, payback period, net return, net present value and discounted cash flow rate of return was estimated (Table 7.5). This alkaline cyanobacterial biorefinery process to produce phycocyanin as main products and O_2, H_2 and CH_4 as side products can become profitable after 2 years of operation.

7.8 Conclusion

In this chapter, pre-feasibility of an alkaline cyanobacteria-based biorefinery was evaluated to produce four different valuable products, phycocyanin, O_2, H_2 and CH_4 . Phycocyanin was determined as the primary product with 79% revenue, followed by O_2, CH_4, and H_2 with 13%, 7%, and 0.06%, respectively. Technoeconomic analysis showed this proposed cyanobacteria-based biorefinery can become profitable after 2 years of operation if phycocyanin price set to be $120/kg. The lowest phycocyanin price was found to be $70/kg to be still profitable with 10 years of depreciation plan.

7.9 References

De Vree JH, Bosma R, Janssen M, Barbosa MJ, Wijffels RH (2015) Comparison of four outdoor pilot-scale photobioreactors. Biotechnol. Biofuels, *8*(1): 1–12.

Engineering Climate Datasets - Environment and Climate Change Canada (2022) Retrieved December 20, 2022, from https://climate.weather.gc.ca/prods_servs/engineering_e.html

Saglam E (2020) Power consumption reduction studies and analysis for centrifugal. Master's thesis, Adnan Menderes University, Aydin, Turkey.

Caceres Falla MC (2020) Integrating direct dir carbon capture and microalgae-based bioenergy production. Master's degree thesis, University of Calgary, Calgary, Canada.

Canon-Rubio KA (2016) Strategies for improving the productivity and cost-effectiveness of microalgal production systems. Master's degree thesis, University of Calgary, Calgary, Canada.

Haines M, Vadlamani A, Daniel Loty Richardson W, Strous M (2022) Pilot-scale outdoor trial of a cyanobacterial consortium at pH 11 in a photobioreactor at high latitude. Bioresour. Technol. 354.

Shao P, Darcovich K, McCracken T, Ordorica-Garcia G, Reith M, O'Leary S (2015) Algae-dewatering using rotary drum vacuum filters: Process modeling, simulation and techno-economics. Chem. Eng. J. 268: 67–75.

Slegers PM, Beveren PJM, Wijffels RH, Van Straten G, Van Boxtel AJB (2013) Scenario analysis of large scale algae production in tubular photobioreactors. Appl. Energy. 105: 395–406.

Thevarajah B, Nishshanka GKSH, Premaratne M, Nimarshana PHV, Nagarajan D, Chang JS, Ariyadasa TU (2022) Large-scale production of *Spirulina*-based proteins and c-phycocyanin: A biorefinery approach. Biochem. Eng. J. 185: 108541.

Zorz J, Paquette AJ, Gillis T, Kouris A, Demirkaya C, De H, Siegler LH, Strous M, Vadlamani A (2022) A naturally occurring lytic bioprocess improves sustainability of phycocyanin production from cyanobacteria. BioRxiv, https://doi.org/10.1101/2022.10.17.512555

CHAPTER 8

Conclusion and Recommendations

8.1 Conclusion

This thesis developed a novel way for converting alkaline cyanobacterial biomass into biofuels and valuable bioproducts for the circular bioeconomy by integrating autofermentation and anerobic digestion operated at low temperature for maximum production with minimal energy input. This is the first report of a successfully strategy to enable the anaerobic digestion of alkaline biomass.

Autofermentation was shown to be a cost effective and energy efficient pretreatment to convert cyanobacterial biomass into hydrogen and organic acids by using cyanobacteria's own fermentative pathways. Up to 60 % of the initial carbon was converted into organic acids. This novel pretreatment path also results in the cost-effective production of pure hydrogen, with a yield of 326.1 µmol/g AFDM without the need for separation and purification steps as the alkaline conditions maintain the CO_2 in solution, thus reducing CO_2 emissions. In addition to pure hydrogen production, the highest ever-achieved organic acid yield of 10.28 ± 0.80 mmol/ AFDM was achieved from the fermentation of cyanobacteria using the natural settling capability of the cyanobacterial biomass, which further reduces the downstream processing cost.

Reducing the energy input of the anaerobic digestion process by operating lower temperature (21°C) provides a positive energy balance. Investigation of a suitable anaerobic inoculum that is capable of converting cyanobacterial biomass into methane at low temperature (21°C) was conducted. Soda lake sediment was found to be the only inoculum capable of performing anaerobic digestion at 21°C with a 42 mL CH_4/gVS, while the other inoculums failed to produce methane. Ammonium inhibition test showed a significant decrease of 74 % in the methane yield at 60 mM of NH_4^+. The accumulation of organic acid during anaerobic digestion is an indicator that further corroborates the inhibition of methanogenesis under high pH. COD and pH changes are important

process parameters to determine the volume, organic loading rates, and feeding strategies needed to obtain a successful semi-continuous anaerobic digestion of autofermented cyanobacterial biomass.

Semi-continuous anaerobic digestion of the autofermented cyanobacterial biomass, inoculated with soda lake sediment, resulted in continuous methane production with an average yield of 471 mL/gVS. This result is comparable to that obtained during the anaerobic digestion of biomasses that have a low risk of ammonium inhibition. The continuous feeding and removing of the digester contents stabilized ammonium concentration at 50-60 mM. Although initially this ammonium concentration was found to be inhibitory, continuous exposure to this high ammonium concentration resulted in the adaptation of the methanogenic community in the digester, leading to a satisfactory performance with 62% conversion. The non-heated digestion system has a high net energy production at 17 MJ/kgVS, which is higher than previously reported cyanobacterial digestion systems. The energy balance analysis showed that the digester can be operated at a temperature as low as 12°C.

Technoeconomical analysis of an integrated cyanobacterial biorefinery showed that the proposed processes are a promising pathway to produce valuable bioproducts and energy from cyanobacterial biomass. Phycocyanin, a valuable protein-based pigment was found to be an important contributor to the economic value of this biorefinery. A commercial alkaline cyanobacterial biorefinery process was found to turn profitable after 2 years of operation.

8.2 Recommendations for future work

This research brings out some new strategies to develop economically feasible alkaline cyanobacterial based biorefinery with minimum energy input for maximal value generation. Still, some unanswered questions need attention in the field of autofermentation and anaerobic digestion at low temperatures.

- The effect of different parameters on organic acid yield and product distribution was investigated in Chapter 4 with one-factor-at-a-time (OFAT) design. As there was no prior study that had established reasonable operating points around which to develop a full factorial design, the OFAT approach served to identify major effects and to test several hypotheses regarding the effect of key operating variables on overall process performance. The results from the OFAT design can be used to support the design of a factorial design or surface response design. A factorial experimental design will help to identify optimal operating conditions and to study the interaction between different operational factors.
- Both autofermentation and anaerobic digestion experiments were done at 21°C to demonstrate that the operation of autofermentation and anaerobic digestion is feasible at room temperature with minimal energy input. However, operation at temperatures lower than 21°C should be investigated to further improve the energy balance. Anaerobic digestion is known to be possible at psychrophilic temperatures.
- Batch anaerobic digestion tests were done to investigate the inoculums that are effective in digesting autofermented cyanobacterial biomass at temperatures lower than those typically used in commercial anaerobic digestion systems. This thesis showed that soda lake sediment is a successful inoculum for digesting the autofermented cyanobacterial biomass at low temperatures; however, no further investigations were not done. Some parameters

such as inoculum/substrate ratio, pH, and mixing rate were predetermined from previous studies. Further investigations are needed to determine the optimal operational conditions for the anaerobic digestion using soda lake sediment as inoculum.

- Batch and semi-continuous anaerobic digestion experiments were performed without actually separating the protein-based phycocyanin pigment. In actual commercial operation, the phycocyanin will be recovered prior to anaerobic digestion. Although phycocyanin only represents about 10% of the total protein in the autofermented biomass, it is necessary to conduct additional experiments to determine the effect that the separation of phycocyanin will have on the anaerobic digestion performance. It is expected that the lower protein content in the feed will be helpful to reduce ammonium accumulation.
- A life cycle inventory and impact assessment should be conducted to further evaluate the feasibility of the proposed alkaline cyanobacterial biorefinery.

Appendix I

Basic Experimental Details

OPA Colorimetric analysis of ammonia (NH_4^+) in aqueous media

Chemicals:

1. Sodium Sulfite (Na_2SO_3)
2. Sodium Tetraborate ($Na_2B_4O_7$)
3. OPA (*o*-phthaldiadehyde) ($C_8H_6O_2$) - Sigma P-1378 orthophthaldialdehyde
4. Milli-Q water

Preparation of Reagents:

1. Sodium sulfite solution – stable for ~1 month if in glass bottle at room temperature

   Add 1g of sodium sulfite to 125mL of DI water.

2. Borate buffer solution

   Add 20g of sodium tetraborate to 0.5L of DI water. Stir or shake thoroughly to dissolve.

3. OPA solution

   Add 1g of OPA to 25mL of ethanol. Be sure to use a high-grade ethanol. OPA is light sensitive, so it should be protected from light while dissolving in ethanol and stored in the dark.

4. Working Reagent – stable for ~3 months when stored in dark at room temperature

   In a 1L brown polyethylene bottle, mix 2.5mL sodium sulfite solution, 0.5L of borate buffer solution, and 25mL OPA solution. Allow the working reagent to "age" for 1 day or more prior to use because its blank will decrease over time.

Procedure:

1. In small glass test tubes, add 4mL working reagent to each tube.
2. Add 1.0mL of standard or sample, vortex.
3. Allow tubes to incubate for at least 2-3 hours.

4. After incubating, read absorbance of each sample at 410nm on spectrophotometer.
5. Use an absorbance v. concentration regression curve for standards to calculate concentrations for samples measured.

Determination of Protein Content

Chemicals

- Trichloroacetic acid 24%(w/v)
- Na_2CO_3 (anhydrous)
- NaOH
- NaK Tartrate tetrahydrate 1%(w/v)
- $CuSO_4.5H_2O$
- 2 N Folin-Ciocalteu phenol reagent

Stock Solutions: Prepare all stock solutions before proceeding with the protein extraction.

Note: Stocks A, B, and C can be stored indefinitely at room temperature. Stocks D and E should be prepared daily.

a. Lowry Reagent A: 2%(w/v) Na_2CO_3 (anhydrous) in 0.1 N NaOH
b. Lowry Reagent B: 1% (w/v) NaK Tartrate tetrahydrate
c. Lowry Reagent C: 0.5% (w/v) $CuSO_4.5H_2O$ in H_2O
d. Lowry Reagent D: Mix reagents A, B, and C in the ratio 48:1:1 (Volume basis)
e. Folin-Ciocalteu phenol reagent: Prepare stock mixing a 1:1 ratio of 2 N Folin-Ciocalteu phenol reagent and ultra-pure water

Procedure

<u>Sample collection and storage</u>

1. Freeze-dry samples prior to analysis.

2. To avoid degradation, store dried sample in the dark, at -80°C, under nitrogen atmosphere.

Protein Extraction

1. Weigh out 5 mg (+/- 10%) of dried sample.
2. Vortex the 5 mg DW in 200 µL 24% (w/v) trichloroacetic acid (TCA).
3. Incubate for 15 min at 95°C in a screw-capped micro-centrifuge tubes, then allow them to cool to room temperature (RT).
4. Add 600 µL of water
5. Centrifuge at 15000 g for 20 min at 4°C.
6. Discard supernatant.
7. Re-suspend the pellet in 0.5mL of Lowry Reagent D.
8. Vortex and incubate for 3 h at 55°C and allow sample to cool to RT.
9. Centrifuge at 15000 g for 20 min at RT.
10. Keep supernatant and discard pellet.
11. At this point extracted samples might be frozen at -20°C.

Protein Quantification

1. Add 50µL of the protein extract to 1.5mL microfuge tubes
2. Add 950µL of the Lowry Reagent D to each tube and mix immediately by inversion.
3. Incubate for 10min at RT.
4. Add 0.1 mL of diluted Folin-Ciocalteu phenol reagent and vortex.
5. Allow to sit for 30 min at RT.
6. Check absorbance at 600nm.

Note: for proper data analysis perform each extraction and quantification in triplicate.

Chemical Oxygen Demand (COD) Analysis

Chemicals

- Potassium hydrogen phthalate (KHP) standard, $HOOCC_6H_4COOK$
- COD vials (0-1500 ppm)
- DI water

Procedure

Standard preparation

Potassium hydrogen phthalate (KHP) standard

1. Lightly crush and then dry KHP to constant weight at 110°C.
2. Dissolve 425 mg in distilled water and dilute to 1000 mL. KHP has a theoretical COD of 1.176 mg O_2/mg and this solution has a theoretical COD of 500 µg O_2/ mL.
3. Prepare weekly fresh solution and store solution under sterile conditions.

COD analysis

1. Dilute samples to the range of COD vials (0-1500 ppm)
2. Open the cap of COD vials in fume hood.
3. Add 5 mL of sample and standard solution into each vial.
4. Close caps and vortex gently.
5. Incubate at 150°C in a dry bath for 2 hours.
6. Read the absorbance by using tue reading apparatus of UV/Vis spectrometer at 600 nm.

Total Carbohydrate Analysis (Sulfuric acid/Phenol Method)

Chemicals

- Glucose
- DI water
- Phenol
- 96% Sulfuric acid

Procedure

Solution and standard preparation

1. Weight 0.1 g 99.9% glucose and dissolve in 100 ml DI water
2. Weigh 5 g of phenol and dissolve in 100 ml DI water

Total Carbohydrate analysis in biomass

1. Weigh out 5 mg (+/- 10%) of dried sample in glass tube.
2. Dissolve dry biomass in 1 ml DI water. If needed incubate in sonication bath to dissolve completely.
3. Apply appropriate dilution to be in the range of standard curve.
4. Take 200 µL sample and mix with 200 µL of 5% phenol solution.
5. Add 1 ml of 96% sulfuric acid.
6. Gently mix and incubate for 30 at room temperature.
7. After 30 min, incubate in cold water to cool down solution
8. Transfer 200 µL of sample into 96 well plate and read the absorbance at 450 nm

Total Carbohydrate analysis in superatant

1. Transfer 1 ml sample into microcentrifuge tube
2. Centrifuge at 5000 rpm for 5 min at room temperature.

3. Separate liquid phase and discard the solids.
4. Apply appropriate dilution to be in the range of standard curve.
5. Take 200 µL sample and mix with 200 µL of 5% phenol solution
6. Add 1 ml of 96% sulfuric acid.
7. Gently mix and incubate for 30 at room temperature.
8. After 30 min, incubate in cold water to cool down solution
9. Transfer 200 µL of sample into 96 well plate and read the absorbance at 450 nm

Appendix II

Statistical Analysis

In Appendix II, raw data of organic acid yield obtained from autofermentation experiments and raw data of methane yield obtained from anaerobic digestion of autofermented biomass with different inoculums are provided. The detailed two-way Anova test result that were done to examine the influence of independent variables, effect of biomass concentration, temperature, and oxygen presence on organic acid yield and different inoculum sources on methane yield are included. Statistical analysis were done using Graph pad Prism Software with using significance level (α) of 0.05.

Chapter 4 Error Analysis

Figure 4.4: Autofermentation – Temperature Experiments

Succinate raw data

Day	21°C (%C mol/ C mol biomass)		30°C (%C mol/ C mol biomass)		37°C (%C mol/ C mol biomass)	
0	0.00	0.00	0.11	0.14	0.11	0.13
2	0.65	0.47	0.00	0.55	0.00	0.00
4	0.73	1.03	1.14	1.16	1.37	1.24
6	0.24	0.31	1.44	1.10	1.69	1.63
8	1.04	1.29	1.43	0.00	5.38	3.73
10	0.31	1.26	2.37	0.00	3.10	2.86

Succinate two-way Anova Analysis

Table Analyzed	Succinate				
Two-way ANOVA	Ordinary				
Alpha	0.05				
Source of Variation	% of total variation	P value	Significant?		
Interaction	32.48	0.0017	Yes		
Row Factor	36.98	<0.0001	Yes		
Column Factor	18.66	0.0002	Yes		
ANOVA table	SS	DF	MS	F (DFn, DFd)	P value
Interaction	16.31	10	1.631	F (10, 18) = 4.920	P=0.0017
Row Factor	18.57	5	3.714	F (5, 18) = 11.20	P<0.0001
Column Factor	9.371	2	4.686	F (2, 18) = 14.13	P=0.0002
Residual	5.969	18	0.3316		

Lactate raw data

Day	21°C (%C mol/ C mol biomass)		30°C (%C mol/ C mol biomass)		37°C (%C mol/ C mol biomass)	
0	0.00	0.00	0.00	0.00	0.00	0.00
2	0.00	0.00	0.88	1.00	1.00	0.90
4	0.00	0.00	1.46	2.39	2.39	2.58
6	1.38	0.67	1.84	1.66	8.90	8.90
8	0.98	1.66	1.59	1.03	2.99	2.17
10	1.88	2.08	2.76	1.86	1.88	3.43

Lactate two-way Anova Analysis

Table Analyzed	Lactate				
Two-way ANOVA	Ordinary				
Alpha	0.05				
Source of Variation	% of total variation	P value	Significant?		
Interaction	38.25	<0.0001	Yes		
Row Factor	38.34	<0.0001	Yes		
Column Factor	21.29	<0.0001	Yes		
ANOVA table	SS	DF	MS	F (DFn, DFd)	P value
Interaction	55.51	10	5.551	F (10, 18) = 32.39	P<0.0001
Row Factor	55.64	5	11.13	F (5, 18) = 64.93	P<0.0001
Column Factor	30.9	2	15.45	F (2, 18) = 90.15	P<0.0001
Residual	3.085	18	0.1714		

Acetate raw data

Day	21°C (%C mol/ C mol biomass)		30°C (%C mol/ C mol biomass)		37°C (%C mol/ C mol biomass)	
0	0.00	0.00	0.20	0.20	0.14	0.18
2	0.25	0.19	3.40	5.38	4.56	3.29
4	0.47	0.32	4.40	4.27	2.27	2.47
6	1.00	0.59	4.46	4.16	2.46	2.58
8	0.75	0.71	3.96	4.60	2.73	2.37
10	0.35	0.81	6.78	4.75	2.12	2.25

Acetate two-way Anova Analysis

Table Analyzed	Acetate				
Two-way ANOVA	Ordinary				
Alpha	0.05				
Source of Variation	% of total variation	P value	Significant?		
Interaction	14.97	0.0004	Yes		
Row Factor	25.49	<0.0001	Yes		
Column Factor	55.32	<0.0001	Yes		
ANOVA table	SS	DF	MS	F (DFn, DFd)	P value
Interaction	19.07	10	1.907	F (10, 18) = 6.382	P=0.0004
Row Factor	32.48	5	6.496	F (5, 18) = 21.74	P<0.0001
Column Factor	70.5	2	35.25	F (2, 18) = 118.0	P<0.0001
Residual	5.379	18	0.2988		

Propionate raw data

Day	21°C (%C mol/ C mol biomass)		30°C (%C mol/ C mol biomass)		37°C (%C mol/ C mol biomass)	
0	0.00	0.00	0.00	0.00	0.00	0.00
2	0.00	0.00	0.00	0.00	0.00	0.00
4	0.00	0.00	4.49	6.34	7.36	7.31
6	1.26	1.15	8.68	8.86	4.10	0.00
8	1.93	2.76	13.18	13.18	2.36	0.00
10	2.35	2.67	13.18	13.00	1.38	3.21

Propionate two-way Anova Analysis

Table Analyzed	Propionate				
Two-way ANOVA	Ordinary				
Alpha	0.05				
Source of Variation	% of total variation	P value	Significant?		
Interaction	34.17	<0.0001	Yes		
Row Factor	31.18	<0.0001	Yes		
Column Factor	32.45	<0.0001	Yes		
ANOVA table	SS	DF	MS	F (DFn, DFd)	P value
Interaction	232.9	10	23.29	F (10, 18) = 27.96	P<0.0001
Row Factor	212.6	5	42.52	F (5, 18) = 51.03	P<0.0001
Column Factor	221.2	2	110.6	F (2, 18) = 132.8	P<0.0001
Residual	15	18	0.8331		

Figure 4.6. Autofermentation – Biomass Concentration Experiments

Succinate raw data

Day	High speed centrifugation (%C mol/ C mol biomass)			Low speed centrifugation (%C mol/ C mol biomass)			Secondary settling (%C mol/ C mol biomass)			Primary settling (%C mol/ C mol biomass)		
0	0.00	0.00	0.00	0.00	0.00	0.00	0.00	0.00	0.00	0.00	0.00	0.00
2	0.65	0.36	0.47	0.73	0.35	0.34	0.13	0.15	0.29	0.00	0.00	0.00
4	0.73	0.86	1.03	0.00	1.85	1.96	1.60	0.51	2.12	0.00	0.00	0.00
6	0.24	0.26	0.31	1.47	0.52	0.70	0.95	0.40	0.48	0.93	0.96	0.78
8	1.04	0.26	1.29	0.57	0.76	0.73	0.62	0.71	0.71	5.50	5.83	6.75
10	0.31	0.41	1.26	1.00	0.84	1.18	1.35	0.70	0.54	4.44	6.04	3.67

Succinate two-way Anova Analysis

Table Analyzed	Succinate				
Two-way ANOVA	Ordinary				
Alpha	0.05				
Source of Variation	% of total variation	P value	Significant?		
Interaction	51.17	<0.0001	Yes		
Row Factor	26.79	<0.0001	Yes		
Column Factor	15.48	<0.0001	Yes		
ANOVA table	SS	DF	MS	F (DFn, DFd)	P value
Interaction	78.12	15	5.208	F (15, 48) = 24.96	P<0.0001
Row Factor	40.89	5	8.177	F (5, 48) = 39.19	P<0.0001
Column Factor	23.63	3	7.876	F (3, 48) = 37.75	P<0.0001
Residual	10.02	48	0.2086		

Lactate raw data

Day	High speed centrifugation (%C mol/ C mol biomass)			Low speed centrifugation (%C mol/ C mol biomass)			Secondary settling (%C mol/ C mol biomass)			Primary settling (%C mol/ C mol biomass)		
0	0.00	0.00	0.00	0.00	0.00	0.00	0.00	0.00	0.00	0.00	0.00	0.00
2	0.26	0.00	0.00	0.04	0.26	0.00	0.00	0.04	0.26	0.00	0.00	0.04
4	0.29	0.00	0.00	0.00	0.29	0.00	0.00	0.00	0.29	0.00	0.00	0.00
6	0.23	0.66	0.20	0.27	0.23	0.66	0.20	0.27	0.23	0.66	0.20	0.27
8	0.60	0.20	0.30	0.34	0.60	0.20	0.30	0.34	0.60	0.20	0.30	0.34
10	0.55	0.36	0.25	0.39	0.55	0.36	0.25	0.39	0.55	0.36	0.25	0.39

Lactate two-way Anova Analysis

Table Analyzed	Lactate				
Two-way ANOVA	Ordinary				
Alpha	0.05				
Source of Variation	% of total variation	P value	Significant?		
Interaction	44.75	<0.0001	Yes		
Row Factor	24.14	<0.0001	Yes		
Column Factor	13.78	<0.0001	Yes		
ANOVA table	SS	DF	MS	F (DFn, DFd)	P value
Interaction	9.11	15	0.6073	F (15, 48) = 8.262	P<0.0001
Row Factor	4.915	5	0.9829	F (5, 48) = 13.37	P<0.0001
Column Factor	2.805	3	0.9349	F (3, 48) = 12.72	P<0.0001
Residual	3.528	48	0.07351		

Formate raw data

Day	High speed centrifugation (%C mol/ C mol biomass)			Low speed centrifugation (%C mol/ C mol biomass)			Secondary settling (%C mol/ C mol biomass)			Primary settling (%C mol/ C mol biomass)		
0	0.00	0.00	0.00	0.00	0.00	0.00	0.00	0.00	0.00	0.00	0.00	0.00
2	0.00	0.00	0.00	0.00	0.00	0.01	0.05	0.00	0.05	0.00	0.00	0.00
4	0.19	0.23	0.17	0.08	0.06	0.13	0.19	0.12	0.33	0.00	0.00	0.16
6	0.23	0.19	0.22	0.21	0.36	0.20	0.29	0.00	0.00	0.19	0.20	0.00
8	0.25	0.23	0.22	0.38	0.31	0.26	0.44	0.43	0.40	1.17	1.45	1.54
10	0.24	0.32	0.18	0.19	0.28	0.20	0.54	0.44	0.45	0.67	1.37	0.40

Formate two-way Anova Analysis

Table Analyzed	Formate				
Two-way ANOVA	Ordinary				
Alpha	0.05				
Source of Variation	% of total variation	P value	Significant?		
Interaction	34.78	<0.0001	Yes		
Row Factor	45.32	<0.0001	Yes		
Column Factor	9.976	<0.0001	Yes		
ANOVA table	SS	DF	MS	F (DFn, DFd)	P value
Interaction	2.628	15	0.1752	F (15, 48) = 11.22	P<0.0001
Row Factor	3.425	5	0.685	F (5, 48) = 43.86	P<0.0001
Column Factor	0.7539	3	0.2513	F (3, 48) = 16.09	P<0.0001
Residual	0.7497	48	0.01562		

Acetate raw data

Day	High speed centrifugation (%C mol/ C mol biomass)			Low speed centrifugation (%C mol/ C mol biomass)			Secondary settling (%C mol/ C mol biomass)			Primary settling (%C mol/ C mol biomass)		
0	0	0.00	0.00	0.00	0.00	0.00	0.00	0.00	0.00	0.00	0.00	0.00
2	0.97	0.67	0.78	1.25	1.16	0.99	1.18	0.62	1.13	0.72	0.71	0.81
4	0.63	0.78	0.91	2.50	2.61	2.74	5.49	5.28	5.56	4.16	1.23	3.04
6	1.26	0.93	1.22	4.31	3.28	3.40	8.51	7.86	7.39	9.98	10.56	6.71
8	1.85	2.14	1.87	3.42	4.26	4.64	10.09	9.35	9.40	32.78	33.96	32.01
10	2.54	2.22	1.69	5.89	4.22	4.99	10.37	9.91	10.50	29.31	32.33	30.74

Acetate two-way Anova Analysis

Table Analyzed	Acetate				
Two-way ANOVA	Ordinary				
Alpha	0.05				
Source of Variation	% of total variation	P value	Significant?		
Interaction	39.32	<0.0001	Yes		
Row Factor	33.2	<0.0001	Yes		
Column Factor	27.02	<0.0001	Yes		
ANOVA table	SS	DF	MS	F (DFn, DFd)	P value
Interaction	2063	15	137.5	F (15, 48) = 271.3	P<0.0001
Row Factor	1742	5	348.4	F (5, 48) = 687.2	P<0.0001
Column Factor	1418	3	472.6	F (3, 48) = 932.3	P<0.0001
Residual	24.33	48	0.5069		

Propionate raw data

Day	High speed centrifugation (%C mol/ C mol biomass)			Low speed centrifugation (%C mol/ C mol biomass)			Secondary settling (%C mol/ C mol biomass)			Primary settling (%C mol/ C mol biomass)		
0	0.00	0.00	0.00	0.00	0.00	0.00	0.00	0.00	0.00	0.00	0.00	0.00
2	0.11	0.01	0.03	0.13	0.11	0.04	0.00	0.00	0.00	0.00	0.00	0.00
4	0.00	0.06	0.18	0.25	0.24	0.23	0.57	0.57	0.76	0.00	0.00	0.00
6	0.13	0.15	0.22	1.93	1.61	0.74	0.86	0.00	0.00	0.90	2.45	0.00
8	0.78	0.86	1.01	0.92	0.74	1.17	1.10	1.14	1.26	7.78	8.97	9.47
10	1.27	0.35	0.88	1.28	0.77	1.19	0.78	0.27	0.33	4.86	8.25	2.23

Propionate two-way Anova Analysis

Table Analyzed	Propionate				
Two-way ANOVA	Ordinary				
Alpha	0.05				
Source of Variation	% of total variation	P value	Significant?		
Interaction	42.99	<0.0001	Yes		
Row Factor	29.07	<0.0001	Yes		
Column Factor	19.39	<0.0001	Yes		
ANOVA table	SS	DF	MS	F (DFn, DFd)	P value
Interaction	125.4	15	8.359	F (15, 48) = 16.08	P<0.0001
Row Factor	84.79	5	16.96	F (5, 48) = 32.62	P<0.0001
Column Factor	56.57	3	18.86	F (3, 48) = 36.27	P<0.0001
Residual	24.96	48	0.5199		

Butyrate raw data

Day	High speed centrifugation (%C mol/ C mol biomass)			Low speed centrifugation (%C mol/ C mol biomass)			Secondary settling (%C mol/ C mol biomass)			Primary settling (%C mol/ C mol biomass)		
0	0.00	0.00	0.00	0.00	0.00	0.00	0.00	0.00	0.00	0.00	0.00	0.00
2	0.12	0.06	0.00	0.00	0.00	0.07	0.00	0.00	0.00	0.00	0.00	0.00
4	0.81	1.18	0.97	0.00	0.00	0.00	0.00	0.00	0.00	0.00	0.00	0.00
6	1.28	1.01	1.37	0.22	0.42	0.64	0.47	0.00	0.00	0.00	0.00	0.00
8	1.52	1.61	1.34	0.29	0.50	0.79	0.00	0.00	0.00	8.23	8.25	10.51
10	1.92	2.25	1.32	0.80	0.45	1.11	0.00	0.00	0.00	7.84	8.83	1.15

Butyrate two-way Anova Analysis

Table Analyzed	Butyrate				
Two-way ANOVA	Ordinary				
Alpha	0.05				
Source of Variation	% of total variation	P value	Significant?		
Interaction	45.72	<0.0001	Yes		
Row Factor	24.41	<0.0001	Yes		
Column Factor	18.65	<0.0001	Yes		
ANOVA table	SS	DF	MS	F (DFn, DFd)	P value
Interaction	161.3	15	10.75	F (15, 48) = 13.04	P<0.0001
Row Factor	86.09	5	17.22	F (5, 48) = 20.89	P<0.0001
Column Factor	65.76	3	21.92	F (3, 48) = 26.60	P<0.0001
Residual	39.56	48	0.8242		

Figure 4.9: Autofermentation – Oxygen Presence Analysis

Succinate raw data

Day	Anoxic (%C mol/ C mol biomass)			Hypoxic (%C mol/ C mol biomass)		
0	0.00	0.00	0.00	0.24	0.19	0.29
2	0.65	0.36	0.47	0.53	0.40	0.39
4	0.73	0.86	1.03	1.05	0.89	0.68
6	0.24	0.26	0.31	0.19	0.43	0.66
8	1.04	0.26	1.29	0.61	0.26	0.26
10	0.31	0.41	1.26	0.00	0.00	0.00

Succinate two-way Anova Analysis

Table Analyzed	Succinate				
Two-way ANOVA	Ordinary				
Alpha	0.05				
Source of Variation	% of total variation	P value	Significant?		
Interaction	20.87	0.0249	Yes		
Row Factor	43.94	0.0005	Yes		
Column Factor	3.452	0.1192	No		
ANOVA table	SS	DF	MS	F (DFn, DFd)	P value
Interaction	0.976	5	0.1952	F (5, 24) = 3.157	P=0.0249
Row Factor	2.054	5	0.4109	F (5, 24) = 6.645	P=0.0005
Column Factor	0.1614	1	0.1614	F (1, 24) = 2.610	P=0.1192
Residual	1.484	24	0.06183		

Lactate raw data

Day	Anoxic (%C mol/ C mol biomass)			Hypoxic (%C mol/ C mol biomass)		
0	0.00	0.00	0.00	0.01	0.01	0.00
2	0.28	0.28	0.26	0.00	0.00	0.00
4	0.23	0.24	0.29	0.00	0.00	0.00
6	0.10	0.19	0.23	0.00	0.00	0.00
8	0.49	0.16	0.60	0.00	0.00	0.00
10	0.20	0.13	0.55	0.74	0.00	0.49

Lactate two-way Anova Analysis

Table Analyzed	Lactate				
Two-way ANOVA	Ordinary				
Alpha	0.05				
Source of Variation	% of total variation	P value	Significant?		
Interaction	19.87	0.0415	Yes		
Row Factor	28.76	0.0088	Yes		
Column Factor	16.85	0.0022	Yes		
ANOVA table	SS	DF	MS	F (DFn, DFd)	P value
Interaction	0.288	5	0.05761	F (5, 24) = 2.763	P=0.0415
Row Factor	0.4169	5	0.08338	F (5, 24) = 3.999	P=0.0088
Column Factor	0.2442	1	0.2442	F (1, 24) = 11.71	P=0.0022
Residual	0.5004	24	0.02085		

Formate raw data

Day	Anoxic (%C mol/ C mol biomass)			Hypoxic (%C mol/ C mol biomass)		
0	0.00	0.00	0.00	0.05	0.06	0.06
2	0.00	0.00	0.00	0.26	0.27	0.24
4	0.19	0.23	0.17	0.43	0.21	0.22
6	0.23	0.19	0.22	0.14	0.12	0.11
8	0.25	0.23	0.22	0.10	0.10	0.10
10	0.24	0.32	0.18	0.11	0.09	0.10

Formate two-way Anova Analysis

Table Analyzed	Formate				
Two-way ANOVA	Ordinary				
Alpha	0.05				
Source of Variation	% of total variation	P value	Significant?		
Interaction	49.2	<0.0001	Yes		
Row Factor	39.01	<0.0001	Yes		
Column Factor	0.04343	0.7684	No		
ANOVA table	SS	DF	MS	F (DFn, DFd)	P value
Interaction	0.1871	5	0.03741	F (5, 24) = 20.11	P<0.0001
Row Factor	0.1483	5	0.02966	F (5, 24) = 15.94	P<0.0001
Column Factor	0.0001651	1	0.0001651	F (1, 24) = 0.08873	P=0.7684
Residual	0.04466	24	0.001861		

Acetate raw data

Day	Anoxic (%C mol/ C mol biomass)			Hypoxic (%C mol/ C mol biomass)		
0	0.00	0.00	0.00	0.10	0.10	0.11
2	0.97	0.67	0.78	2.29	4.07	3.13
4	0.63	0.78	0.91	4.89	4.84	4.12
6	1.26	0.93	1.22	1.94	1.08	1.05
8	1.85	2.14	1.87	1.05	1.12	1.12
10	2.54	2.22	1.69	1.05	1.14	1.27

Acetate two-way Anova Analysis

Table Analyzed	Acetate				
Two-way ANOVA	Ordinary				
Alpha	0.05				
Source of Variation	% of total variation	P value	Significant?		
Interaction	46.77	<0.0001	Yes		
Row Factor	38.85	<0.0001	Yes		
Column Factor	9.213	<0.0001	Yes		
ANOVA table	SS	DF	MS	F (DFn, DFd)	P value
Interaction	27.74	5	5.547	F (5, 24) = 43.45	P<0.0001
Row Factor	23.05	5	4.609	F (5, 24) = 36.10	P<0.0001
Column Factor	5.465	1	5.465	F (1, 24) = 42.80	P<0.0001
Residual	3.064	24	0.1277		

Propionate raw data

Day	Anoxic (%C mol/ C mol biomass)			Hypoxic (%C mol/ C mol biomass)		
0	0.00	0.00	0.00	0.00	0.00	0.00
2	0.11	0.01	0.03	0.15	0.11	0.14
4	0.00	0.06	0.18	0.21	0.20	0.07
6	0.13	0.15	0.22	0.00	0.00	0.00
8	0.78	0.86	1.01	0.00	0.00	0.00
10	1.27	0.35	0.88	0.00	0.00	0.00

Propionate two-way Anova Analysis

Table Analyzed	Propionate				
Two-way ANOVA	Ordinary				
Alpha	0.05				
Source of Variation	% of total variation	P value	Significant?		
Interaction	39.91	<0.0001	Yes		
Row Factor	27.69	<0.0001	Yes		
Column Factor	19.38	<0.0001	Yes		
ANOVA table	SS	DF	MS	F (DFn, DFd)	P value
Interaction	1.526	5	0.3052	F (5, 24) = 14.72	P<0.0001
Row Factor	1.059	5	0.2117	F (5, 24) = 10.21	P<0.0001
Column Factor	0.741	1	0.741	F (1, 24) = 35.73	P<0.0001
Residual	0.4978	24	0.02074		

Butyrate raw data

Day	Anoxic (%C mol/ C mol biomass)			Hypoxic (%C mol/ C mol biomass)		
0	0.00	0.00	0.00	0.06	0.00	0.01
2	0.12	0.06	0.00	0.41	1.01	0.82
4	0.81	1.18	0.97	0.00	0.00	0.00
6	1.28	1.01	1.37	0.00	0.00	0.28
8	1.52	1.61	1.34	0.19	0.12	0.16
10	1.92	2.25	1.32	0.14	0.00	0.00

Butyrate two-way Anova Analysis

Table Analyzed	Butyrate				
Two-way ANOVA	Ordinary				
Alpha	0.05				
Source of Variation	% of total variation	P value	Significant?		
Interaction	40.68	<0.0001	Yes		
Row Factor	21.17	<0.0001	Yes		
Column Factor	32.48	<0.0001	Yes		
ANOVA table	SS	DF	MS	F (DFn, DFd)	P value
Interaction	6.387	5	1.277	F (5, 24) = 34.48	P<0.0001
Row Factor	3.324	5	0.6648	F (5, 24) = 17.95	P<0.0001
Column Factor	5.099	1	5.099	F (1, 24) = 137.6	P<0.0001
Residual	0.889	24	0.03704		

Chapter 5 Error Analysis

Figure 5.1: Batch Anaerobic Digestion Test – Methane Yield

Methane yield from fresh biomass AD at 21°C – Raw data

Day	Digested Sewage Sludge (mL/ gVS)			Digested Manure (mL/ gVS)			Soda Lake Sediment (mL/ gVS)		
0	0.00	0.00	0.00	0.00	0.00	0.00	0.00	0.00	0.00
5	0.64	3.11	0.59	0.00	0.00	0.00	12.20	11.61	11.59
10	0.44	4.13	0.42	0.00	0.00	0.00	13.69	12.89	12.91
15	0.52	4.22	0.47	0.00	0.00	0.00	22.08	20.57	20.67
20	0.71	4.58	0.71	0.00	0.00	0.00	19.13	23.07	23.25
25	0.48	4.34	0.45	0.00	0.00	0.00	20.97	25.23	25.57
30	0.09	3.95	0.14	0.00	0.00	0.00	20.59	25.47	25.93
35	0.48	4.34	0.45	0.00	0.00	0.00	20.59	25.47	25.93
40	0.09	3.95	0.14	0.00	0.00	0.00	20.59	25.47	25.93

Methane yield from fresh biomass AD at 21°C – Two-way Anova Test

Table Analyzed	Fresh Biomass - 21°C				
Two-way ANOVA	Ordinary				
Alpha	0.05				
Source of Variation	% of total variation	P value	Significant?		
Interaction	14.29	<0.0001	Yes		
Row Factor	8.413	<0.0001	Yes		
Column Factor	75.24	<0.0001	Yes		
ANOVA table	SS	DF	MS	F (DFn, DFd)	P value
Interaction	1049	16	65.55	F (16, 54) = 23.48	P<0.0001
Row Factor	617.5	8	77.19	F (8, 54) = 27.65	P<0.0001
Column Factor	5523	2	2761	F (2, 54) = 989.3	P<0.0001
Residual	150.7	54	2.791		

Methane yield from fresh biomass AD at 35°C – Raw data

Day	Digested Sewage Sludge (mL/ gVS)			Digested Manure (mL/ gVS)			Soda Lake Sediment (mL/ gVS)		
0	0.00	0.00	0.00	0.00	0.00	0.00	0.00	0.00	0.00
5	0.72	0.54	0.56	0.00	0.00	0.00	14.04	12.80	12.83
10	-0.15	-0.45	-0.42	0.00	0.00	0.00	14.64	13.19	13.26
15	0.24	0.04	0.12	0.00	0.00	0.00	21.03	18.19	19.03
20	-0.03	0.14	-0.14	0.00	0.00	0.00	20.76	17.46	19.00
25	1.00	0.94	1.02	0.00	0.00	0.00	16.05	16.76	18.62
30	0.97	0.97	0.88	0.00	0.00	0.00	15.80	16.56	18.52
35	1.00	0.94	1.02	0.00	0.00	0.00	14.46	13.20	13.16
40	0.97	0.97	0.88	0.00	0.00	0.00	15.92	16.72	18.59

Methane yield from fresh biomass AD at 35°C - Two-way Anova Test

Table Analyzed	Fresh Biomass - 35°C				
Two-way ANOVA	Ordinary				
Alpha	0.05				
Source of Variation	% of total variation	P value	Significant?		
Interaction	12.13	<0.0001	Yes		
Row Factor	6.508	<0.0001	Yes		
Column Factor	80.82	<0.0001	Yes		
ANOVA table	SS	DF	MS	F (DFn, DFd)	P value
Interaction	547.3	16	34.21	F (16, 54) = 75.39	P<0.0001
Row Factor	293.7	8	36.72	F (8, 54) = 80.93	P<0.0001
Column Factor	3648	2	1824	F (2, 54) = 4020	P<0.0001
Residual	24.5	54	0.4537		

Methane yield from autofermented biomass AD at 21°C – Raw data

Day	Digested Sewage Sludge (mL/ gVS)			Digested Manure (mL/ gVS)			Soda Lake Sediment (mL/ gVS)		
0	0.00	0.00	0.00	0.00	0.00	0.00	0.00	0.00	0.00
5	19.73	21.94	19.84	0.67	0.59	0.54	-0.42	-0.09	-0.18
10	18.15	21.21	20.77	2.14	1.82	1.77	-4.35	-3.28	-3.50
15	21.54	23.13	23.45	2.25	2.00	1.93	11.84	19.56	17.80
20	12.10	14.81	15.06	2.34	2.02	1.97	12.87	23.92	20.61
25	12.71	14.39	14.55	17.53	14.38	14.15	22.18	41.53	34.51
30	12.90	11.17	11.02	17.33	14.21	13.98	27.25	56.22	44.94
35	12.41	0.88	-0.11	13.75	17.10	13.94	26.30	52.39	42.06
40	23.20	21.91	20.61	13.75	17.10	13.94	26.71	54.33	43.47

Methane yield from autofermented biomass AD at 21°C - Two-way Anova Test

Table Analyzed	Autofermented Biomass - 21°C				
Two-way ANOVA	Ordinary				
Alpha	0.05				
Source of Variation	% of total variation	P value	Significant?		
Interaction	38.21	<0.0001	Yes		
Row Factor	35.8	<0.0001	Yes		
Column Factor	15.79	<0.0001	Yes		
ANOVA table	SS	DF	MS	F (DFn, DFd)	P value
Interaction	5986	16	374.2	F (16, 54) = 12.64	P<0.0001
Row Factor	5610	8	701.2	F (8, 54) = 23.70	P<0.0001
Column Factor	2474	2	1237	F (2, 54) = 41.80	P<0.0001
Residual	1598	54	29.59		

Methane yield from autofermented biomass AD at 35°C – Raw data

Day	Digested Sewage Sludge (mL/ gVS)			Digested Manure (mL/ gVS)			Soda Lake Sediment (mL/ gVS)		
0	0.00	0.00	0.00	0.00	0.00	0.00	0.00	0.00	0.00
5	0.86	-0.11	0.29	0.46	0.48	0.45	0.91	1.06	0.77
10	23.78	16.16	21.51	17.96	18.70	20.95	-0.54	-0.07	-0.75
15	47.37	52.93	35.06	34.39	28.15	44.52	48.53	49.60	43.10
20	142.67	117.89	165.39	43.48	37.73	57.92	105.12	88.90	86.09
25	225.38	199.81	214.82	161.67	176.13	145.19	123.86	125.13	125.13
30	325.27	278.60	330.98	223.11	225.36	177.61	157.79	140.17	141.47
35	320.99	272.75	329.35	302.10	312.88	248.05	157.79	140.17	141.47
40	328.00	273.94	340.51	291.04	310.62	244.43	154.89	139.32	140.62

Methane yield from autofermented biomass AD at 35°C - Two-way Anova Test

Table Analyzed	Autofermented Biomass - 35°C				
Two-way ANOVA	Ordinary				
Alpha	0.05				
Source of Variation	% of total variation	P value	Significant?		
Interaction	9.231	<0.0001	Yes		
Row Factor	82.17	<0.0001	Yes		
Column Factor	7.058	<0.0001	Yes		
ANOVA table	SS	DF	MS	F (DFn, DFd)	P value
Interaction	92478	16	5780	F (16, 54) = 20.18	P<0.0001
Row Factor	823170	8	102896	F (8, 54) = 359.3	P<0.0001
Column Factor	70713	2	35356	F (2, 54) = 123.5	P<0.0001
Residual	15466	54	286.4		